Detailed report of the effect of PCSs on air quality in the future CC (2050) in the target cities

D6.5

July 2019

This project has received funding from the European Union's Horizon 2020 research and innovation programme under grant agreement No 689954.

Project Acronym and Name	iSCAPE - Improving the Smart Control of Air Pollution in Europe	
Grant Agreement Number	689954	
Document Type	Report	
Document version & WP No.	V. 04	WP6
Document Title	Detailed report of the effect of PCSs on air quality in the future CC (2050) in the target cities	
Main authors	Silvana Di Sabatino (UNIBO), Erika Brattich (UNIBO), Francesca Di Nicola (UNIBO), Kirsti Jylhä (FMI), Carl Fortelius (FMI), Olli Saranko (FMI), Bidroha Basu (UCD), John Gallagher (TCD), Aonghus MNabola (TCD), Francesco Pilla (UCD)	
Partner in charge	University of Bologna (UNIBO)	
Contributing partners	University of Bologna (UNIBO), Finnish Meteorological Institute (FMI), University College Dublin (UCD), Trinity College Dublin (TCD)	
Release date	29/07/2019	

Document Control Page			
Short Description	*This report is the output of the work carried out in Task 6.4.2 of the iSCAPE project, which focuses on the evaluation of the effectiveness of Passive Control Systems (PCS) on air quality under future climate change scenarios in the target cities. The evaluation of the efficacy of PCSs has been conducted by reconstructing detailed air quality maps in three iSCAPE cities, namely Bologna, Dublin and Vantaa, chosen as representative of south, western and north Europe respectively. Following a thorough validation of all numerical models used in present scenarios, simulations have been conducted using downscaled climate projections for the three cities. Changes in air quality in future climate scenarios and in the presence or absence of selected PCSs are documented allowing to extract recommendations for the selected cities and easily extendable to other European cities.*		
Review status	**Action**	**Person**	**Date**
	Quality Check	*Coordination Team*	06/08/2019
	Internal Review	*Bidroha Basu*	01/08/2019
	Internal Review	*Felix Othmer*	01/08/2019
Distribution	Public		

Revision history			
Version	**Date**	**Modified by**	**Comments**
V0.1	10/06/2019	Silvana Di Sabatino, Erika Brattich, Francesca Di Nicola, Kirsti Jylhä, Carl Fortelius, Olli Saranko	The first draft.
V0.2	19/06/2019	Silvana Di Sabatino, Erika Brattich, Francesca Di Nicola, Kirsti Jylhä, Carl Fortelius, Olli Saranko	Revision after receiving the internal reviewers' comments
V0.3	27/06/2019	Silvana Di Sabatino, Beatrice Pulvirenti, Sara Baldazzi, Erika Brattich	Added CFD simulations for Bologna
V0.4	27/07/2019	Silvana Di Sabatino, Erika Brattich, Bidroha Basu, John Gallagher, Aonghus Mc Nabola, Francesco Pilla	Added CFD simulations for Dublin and revisions to check consistency
V0.5			
V0.6			
V0.7			
V0.8			
V0.9			

Table of Contents

List of Tables

List of Figures

List of Abbreviations

ADMS:	Atmospheric Dispersion Modeling System
ADMS-TH:	ADMS-Temperature and Humidity
AQ:	Air Quality
ARPAE:	Emilia Romagna Environmental Protection Agency (new acronym replacing ARPA-ER)
CC:	Climate Change
CERC:	Cambridge Environmental Research Consultants
CESM:	Community Earth System Model
CLRTAP:	Convention on Long-Range Transboundary Air Pollution
CMIP5:	Coupled Model Intercomparison Project, Phase 5
D:	Deliverable
EU:	Europe
FA2:	Factor of two
FB:	Fractional Bias
FMI:	Finnish Meteorological Institute
GCM:	Global Climate Model
GHG:	GreenHouse Gas
GI:	Green Infrastructure
GIS:	Geographic Information System
HSY:	Helsinki Region Environmental Services Authority
LAI:	Leaf Area Index
LBW:	Low Boundary Wall
LCZ:	Local Climate Zone
NCAR:	National Center for Atmospheric Research
NMSE:	Normalized Mean Square Error
NO_x:	Nitrogen Oxides
NO_2:	Nitrogen Dioxide
O_3:	Ozone
PCS:	Passive Control System

PM:	Particulate Matter
$PM_{2.5}$:	Particulate Matter with aerodynamic diameter less or equal to 2.5 μm
PM_{10}:	Particulate Matter with aerodynamic diameter less or equal to 10 μm
r:	Pearson's correlation coefficient
R^2:	coefficient of determination
RCP:	Representative Concentration Pathway
SCATS:	Sydney Coordinated Adaptive Traffic System
SCLP:	Short-Lived Climate Pollutant
SD:	Standard Deviation
TEB:	Town Energy Balance
UH:	University of Hasselt
UHI:	Urban Heat Island
UK:	United Kingdom
UNECE:	United Nations Economic Commission for Europe
WMO:	World Meteorological Organization
WP:	Work Package
WRF:	Weather Research and Forecasting

1 Executive Summary

This report addresses the efficacy of Passive Control Systems (PCSs) to improve air quality and urban thermal comfort in present and future climate conditions The evaluation of the efficacy of the PCSs is conducted with two methodologies, i.e.: 1) by reconstructing pollutant concentration maps using a well-validated dispersion model in two iSCAPE cities, namely Bologna and Vantaa, representative of two different latitudinal bands in Europe (southern and northern Europe, respectively), 2) and with high resolution CFD (Computational Fluid Dynamics) simulations for a neighborhood of Bologna and Dublin, again representative of two different latitudinal bands in Europe (southern and western Europe, respectively), whose setup was previously verified in D6.2 ("*Microscale CFD evaluation of PCS impacts on air quality*"[1]) against observations gathered within the intensive experimental campaigns conducted as part of WP5.

Besides representing different climate bands differently impacted by climate change, the choice of the three cities was also based on the methodology adopted to assess the efficacy of PCSs. In fact, in Bologna and Vantaa a detailed urban emission inventory of the pollutant sources was already developed previously within the iSCAPE project to evaluate the efficacy of different policy options in WP4 ('*Report on policy options for AQ and CC*'[2]). In this work, similar to what previously done in D4.5, those emission inventories were used as input to dispersion modeling simulations conducted in the present and in future conditions as evaluated by future climate projections. In Dublin, instead, an emission inventory was developed precisely for the purpose of this Task.

In the three cities, we analysed the impact of a slightly different interventions. Specifically, while in Bologna we examined the impact of an intervention consisting in planting trees in an originally tree-free street canyon, in Vantaa we focused on the impact of an intervention where the urban layout was modified replacing all relatively dense commercial and industrial areas with a suburban type, characterized by both lower and less dense buildings and a larger fraction of vegetated spaces, whereas in Dublin intervention of low boundary walls (LBWs) as passive control structure inside a street canyon were explored. The three interventions were therefore parameterized in a similar but not equal way in the three cities. To this aim, the simulation setup originally developed for the two cities in D4.5 was modified ad-hoc to be capable to represent modifications in pollutant dispersion induced by the presence of Green Infrastructure (GI) or by modifications of the urban layout. Therefore, here, we do not present again thoroughly the methodology used to construct the emission inventories and conduct the dispersion modeling simulations, while we present the methodologies used to represent GI and/or modifications of the urban layout in those simulations. In Bologna and Vantaa, the setup in the real current conditions is validated against observations available from monitoring stations, available as open data in the case of Vantaa or gathered within the experimental field campaigns conducted as part of the planning and evaluation of the iSCAPE Passive Control System solutions for Bologna, whose results were reported in the '*Air pollution and meteorology monitoring report*[3]' (D5.2). In both cities, the simulated concentrations are in good agreement with the observations, indicating that the setup adopted is indeed capable of correctly representing the current situation.

[1] The Report will be available on the iSCAPE reports webpage
[2] The Report will be available on the iSCAPE reports webpage
[3] The Report will be available on the iSCAPE reports webpage

A different methodology was also used in the cities to evaluate the impact of climate change, and to conduct simulations for the variations of air temperature in the different scenarios analysed. While the methodology and the results obtained with downscaled climate projections conducted with a large ensemble of state-of-the-art global climate model simulations for all the iSCAPE cities are reported in the parallel '*Detailed report on local meteorological conditions*' (D6.4)[4], here we present the methods and the results obtained with high-resolution simulations for the three cities.

In all the three cities, simulations were conducted in two different periods, representative of cold and warm seasons, in order to assess the impact of the interventions under the winter and summer periods, which in general present a different trend in meteorological variables in the iSCAPE cities as reported in D6.4.

The results of the simulations indicate different impacts of the interventions in the three cities. In fact, while the planting trees intervention demonstrated capable of improving air quality in Bologna in both current and future climate conditions, the alteration of the urban layout did not cause major changes in air pollution in Vantaa, while a slight overall improvement in air quality were noted for Dublin.

Conversely, in both Bologna and Vantaa the interventions result to improve urban thermal comfort in present and future conditions and reduce the temperature increase which will affect both cities under future climate conditions as indicated by projections, even though in this case the effectiveness of PCSs seems to be higher in Vantaa than in Bologna.

[4] The Report will be available on the iSCAPE reports webpage

2 Introduction

Air pollution and climate change are tightly linked. Besides being connected through their main anthropogenic source, i.e. the extraction and burning of fossil fuels which is a major source of CO_2 emissions and air pollutants, many air pollutants also contribute to climate change by impacting on the amount of energy that is reflected or absorbed by the atmosphere. In fact, some air pollutants such as O_3 and black carbon, a component of fine particulate matter deriving from combustion processes, are known as short-lived climate pollutants (SCLPs) because of their ability to absorb long-wave radiation; the deposition of black carbon on ice and snow greatly increases albedo causing local warming and melting. Conversely, other aerosol components like sulphates are able to scatter solar radiation thus leading to reductions in air temperature. CH_4, besides being itself a strong GHG (greenhouse gas), is a precursor to ground-level O_3, which causes asthma and other respiratory diseases and is a GHG. In addition, while both air pollution and climate change are environmental phenomena, they also have profound social and economic consequences, with serious impacts on health and related health costs. Moreover, climate and weather affect deeply the spatial and temporal distribution of air pollution concentrations, influencing the reaction rates and the movement and dispersion of air pollutants (Kinney, 2018).

Because of their strong interconnections, the mitigation of air pollution and climate change is increasingly being approached in an integrated way. For instance, UNECE (United Nations Economic Commission for Europe) is contributing to climate change mitigation through the CLRTAP (Convention on Long-Range Transboundary Air Pollution) which sets emission targets for a number of key air pollutants[5].

The iSCAPE project aims to integrate and advance the control of air quality and carbon emissions in European cities in the context of climate change. iSCAPE focuses on the use of “Passive Control Systems” (PCSs) in urban spaces, on policy intervention and behavioural changes of citizens lifestyle. The target cities are Bologna in Italy, Bottrop in Germany, Dublin in Ireland, Guilford in United Kingdom, Hasselt in Belgium and Vantaa in Finland. Infrastructural PCSs in the iSCAPE cities include low boundary walls (Dublin), photocatalytic coatings (Lazzaretto in the outskirts of Bologna), urban design and planning (Bottrop) and various green infrastructures: hedge-rows (Guilford), trees (Bologna) and green urban spaces (Vantaa).

In particular, WP6 of the iSCAPE project focuses on the assessment of the impacts of the infrastructural PCSs with respect to air pollutants levels and their linkages to climate changes in the urban environment in order to evaluate their effectiveness both in the current and in the future scenarios (2050).

After the assessment of the air pollution levels and microclimate in the target cities (D6.1, *‘Detailed report for the assessment of air quality and UHI in EU selected cities pre-infrastructural solutions’*), this WP involved the development of numerical simulations aimed to determine the impact of PCSs on air pollution and thermal comfort at different spatial scales. As such, high resolution Computational Fluid Dynamics simulations were used to assess the effect of PCSs on air pollution levels at neighbourhood

[5] https://www.unece.org/unece-and-the-sdgs/climate-change/sustainable-developmentclimate-change/improving-air-quality-while-fighting-climate-change.htm

scale (D6.2 '*Microscale CFD evaluation of PCSs impacts on air quality*'[6]), while D6.3 ('*Detailed report based on numerical simulations of the effect of PCS at the urban level*'[7]) focused on the effects of PCSs on air quality and thermal comfort at urban scale.

This report completes the series of Deliverables of WP6 and aims to extend the analysis of the impacts of PCSs to future climate conditions. In particular, this report is the output of Task 6.4.2, 'Evaluation of the effectiveness of PCSs implementation for both air quality and CC in future scenarios'), which focuses on the future projections of air quality in the selected cities in the presence of PCSs. In the parallel D6.4 *('Detailed report on local meteorological conditions'*[8]), results obtained by means of regional scale climate projections based on a large number of climate model simulations were presented for all the iSCAPE cities. After that, an atmosphere-surface interaction model was used to derive information on the impact of green infrastructure in the current and future climate in the city of Vantaa.

In this report, the impact of PCSs on air quality and thermal comfort is analysed for three iSCAPE cities under present and future climate conditions, Bologna, Dublin and Vantaa, as representative of different latitudinal bands impacted differently by climate change. A complete emission inventory including all major pollutant emission sources was previously developed for the two cities of Bologna and Vantaa in WP4 (D4.5 '*Report on policy options for AQ and CC*'[9]). As previously done in D4.5, the developed emission inventories were used as input to atmospheric dispersion model. However, the setup originally developed for D4.5 was modified here to be capable to represent the introduction of PCSs in the base case reference scenario. In addition, in Bologna, while D4.5 focused on the whole urban scale, here we considered just the neighbourhood of one particular free-street canyon where the experimental field campaigns described in D5.2 *('Air pollution and meteorology monitoring report'*[10]) were carried out. Before application to scenarios considering the introduction of PCSs in the current reference scenario, both simulation setups herein used for the two cities were verified against air quality observations, available as open data in the case of Vantaa and gathered within the experimental field campaigns in the case of Bologna.

After verification, the impacts of the introduction of PCSs and future climate on air quality and air temperature are evaluated considering successive modifications of the base reference case, including modifications of the setup and/or of the meteorological input data.

High resolution CFD simulations were also conducted to evaluate the efficacy of PCSs at neighbourhood level under future climate conditions for the city of Bologna and Dublin. In particular, in both cases, here we used the CFD simulations previously presented in D6.2 and well validated against observations obtained within the experimental campaigns described in D5.2 to evaluate the efficacy of trees and LBws (Low-Boundary Walls) in improving air quality in the neighborhoods of two street canyons.

Table 1 presents an overview of all the simulations which were performed and will be described in this Deliverable to analyse the effects of PCSs on air quality and thermal comfort under present and future climate conditions in the three cities.

[6] The Report will be available on the iSCAPE reports webpage

[7] The Report will be available on the iSCAPE reports webpage

[8] The Report is available on the iSCAPE reports webpage

[9] The Report will be available on the iSCAPE reports webpage

[10] The Report will be available on the iSCAPE reports webpage

City	Scenario	Intervention	Research purpose
Bologna	Current (baseline) 2017-2018	None	Verification of the simulation setup; analysis of concentration maps and air pollution hotspots in the current (baseline) case for the warm and cold period
Bologna	Current (baseline) 2017-2018	None	Verification of the simulation setup; analysis of air temperature maps and UHI in the current (baseline) case for the warm period
Bologna	Current 2017 with trees	Planting trees in a tree-free street canyon	Analysis of the effects of trees on air pollution in the vicinity of the identified street canyon under present climate conditions
Bologna	Current 2017 with modification of the urban layout	Planting trees in a tree-free street canyon	Analysis of the effects of changing the urban layout type on air temperature in the vicinity of the identified street canyon under present climate conditions
Bologna	Future CC (2050)	None	Analysis of the effects of climate change on air pollution in the vicinity of the identified street canyon
Bologna	Future CC (2050)	None	Analysis of the effects of climate change on air temperature in the vicinity of the identified street canyon
Bologna	Future CC (2050) with trees	Planting trees in a tree-free street canyon	Analysis of the effects of trees on air pollution in the vicinity of the identified street canyon under future climate conditions
Bologna	Future CC (2050) with modification of the urban layout	Planting trees in a tree-free street canyon	Analysis of the effects of trees on air temperature in the vicinity of the identified street canyon under future climate conditions
Dublin	Current baseline period	None	Analysis of concentrations for two periods, summer and winter; comparison with those obtained in the intervention scenario
Dublin	Current baseline period with LBWs	Inserting LBWs in a street canyon	Analysis of the effects of LBWs on air pollution in the vicinity of the identified street canyon under present climate conditions
Dublin	Future CC (2050)	None	Analysis of concentrations for two periods, summer and winter; comparison with those obtained in the intervention scenario
Dublin	Future CC (2050) with LBWs	Inserting LBWs in a street canyon	Analysis of the effects of LBWs on air pollution in the vicinity of the identified street canyon under fuutre climate conditions
Vantaa	Current (baseline) 2017	None	Verification of the simulation setup; analysis of concentration maps and air pollution hotspots in the current (baseline) case for the warm and cold period
Vantaa	Current (baseline) 2017	None	Verification of the simulation setup; analysis of air temperature maps and UHI in the current (baseline) case for the warm and cold period
Vantaa	Current 2017 with modification of the urban layout	Modifying the urban layout type of dense built-up area	Analysis of the effects of altering the urban layout on air pollution under present climate conditions
Vantaa	Current 2017 with trees	Modifying the urban layout type of dense built-up area	Analysis of the effects of changing the urban layout type on air temperature under present climate conditions
Vantaa	Future CC (2050)	None	Analysis of the effects of climate change on air pollution
Vantaa	Future CC (2050)	None	Analysis of the effects of climate change on air temperature

Vantaa	Future CC (2050) with modification of the urban layout	Modifying the urban layout type of dense built-up area	Analysis of the effects of changing the urban layout type on air pollution under future climate conditions
Vantaa	Future CC (2050) with a modification of the urban layout	Modifying the urban layout type of dense built-up area	Analysis of the effects of changing the urban layout type on air temperature in the vicinity of the identified street canyon under future climate conditions

Table 1. Overview and main purpose of the numerical simulations conducted in this Deliverable for the three iSCAPE cities

As such, this report fulfils the objective of providing high resolution maps of air quality post-intervention of PCSs in future climate. The results of this report, together with those of other Deliverables in this WP, provide the science-based assessments of the PCSs and will be used as input for WP7 and WP8 to formulate solid policy options for future interventions in EU cities for the reduction of carbon footprint.

3 Methodology

In this section, we provide an overview of the methodologies adopted to analyse the effect of PCSs on air quality and thermal comfort in the present and future climate conditions in the three selected cities. In both cases of Bologna and Vantaa, the simulation setup of the reference case was validated in the present climate conditions against available observations. After that, the effectiveness of the PCSs was evaluated comparing the results obtained in a scenario considering the implementation of some interventions with that obtained in the reference case. In the case of Dublin, here we provide some details of the meteorological conditions and the emission inventory used as input to the CFD simulations.

3.1 Bologna

Among the various types of PCSs interventions carried out in the iSCAPE project, Bologna is focusing on the impact of the Green Infrastructure (GI) on air quality and urban thermal comfort. In particular, Bologna carried out two experimental field campaigns and ad hoc high-resolution numerical simulations with the purpose to verify the impact of trees in modifying ventilation pollution levels in street canyons and at urban level (see D5.2 for a description of the results of the experimental field campaigns, and D6.2, D6.3, and D5.3 for a description of the setup and the results obtained by numerical simulations). In this work, in Bologna, we tested the effectiveness of a greening policy in an ad-hoc identified tree-free street canyon on air quality. For this purpose, the reference base case simulations were conducted in a tree-free street canyon, Marconi St., one of the two street canyons where the intensive experimental field campaigns were carried out. Simulations in this street canyon were conducted in a real base case (Base Case - Actual Trees scenario) and in a scenario of tree planting (Base Case - Added Trees scenario). The two scenarios created were compared to evaluate the impact of planting trees in a neighborhood in the vicinity of the street canyon. Furthermore, the impact of the intervention under the influence of climate change is also tested, for which purpose two additional scenarios are created: Future Case - Actual Trees scenario to assess the impact of climate change only and Future Case -

Added Trees scenario to evaluate the effectiveness of trees in mitigating air pollution in the future climate conditions.

3.1.1 Dispersion modelling

In this work, the ADMS-Urban model (version 4.1.1.0) developed by Cambridge Environmental Research Consultants (CERC) was used (CERC, 2011) to carry out atmospheric dispersion simulations through which to evaluate the concentration of pollutants emitted from the sources considered in the emission inventory into the atmosphere. A detailed description of the model and the methodology for creating the emission inventory, as well as information on the study domain is reported in deliverables D4.5 and D6.3.

The simulations were conducted in two different ways:

- Short term - any gridded concentration output files will contain output for the first 24 lines of meteorological data only. If specified point output is selected will contain a set of concentrations for every line of meteorological data. This simulation type in particular was used for the verification and comparison of model outputs with measured values.
- Long term - the concentration output files will contain a single set of concentration data, averaged over all the lines of meteorological data. However, a file containing data at all output points for each meteorological line can be created for the long-term output. This simulation type in particular was used for evaluating the dispersion producing concentration maps in the actual scenario (base reference case) and in the simulations to be compared to it (policies, and climate change to be presented in the next section).

Output concentrations of short-term simulation are post-processed to calculate long-term averages as required for the validation. Output concentrations of long-term simulation are used to obtain the concentration maps for each pollutant in the various scenarios.

In order to evaluate the effectiveness of PCSs in Bologna, the simulations were conducted at the neighborhood scale. In particular, Marconi St., one of the two street canyons where the two intensive field campaigns were carried out (see D5.2 for further details) is considered as study site. In summary, Marconi St. is a tree-free street canyon located in the city center of Bologna. Emissions covering the Bologna area were considered, using the same emission inventory used in D4.5 (for more details see D4.5). Briefly, the road network of Bologna was divided into major and minor roads. Major road is a source type, providing emissions from traffic on a road that is represented explicitly as a line source. Minor road is a source type, providing emissions from traffic on small roads which are not represented explicitly but their emissions are combined (aggregated) over one or more grid squares. In order to get down to the street canyons scale, the whole graph is split into major and minor roads. For the purpose of this work, it has been assumed that all the main roads around Marconi street canyon are major roads (Figure 1), while all the other roads are considered minor roads. Input traffic counts to calculate pollutant emissions were provided by the Municipality of Bologna.

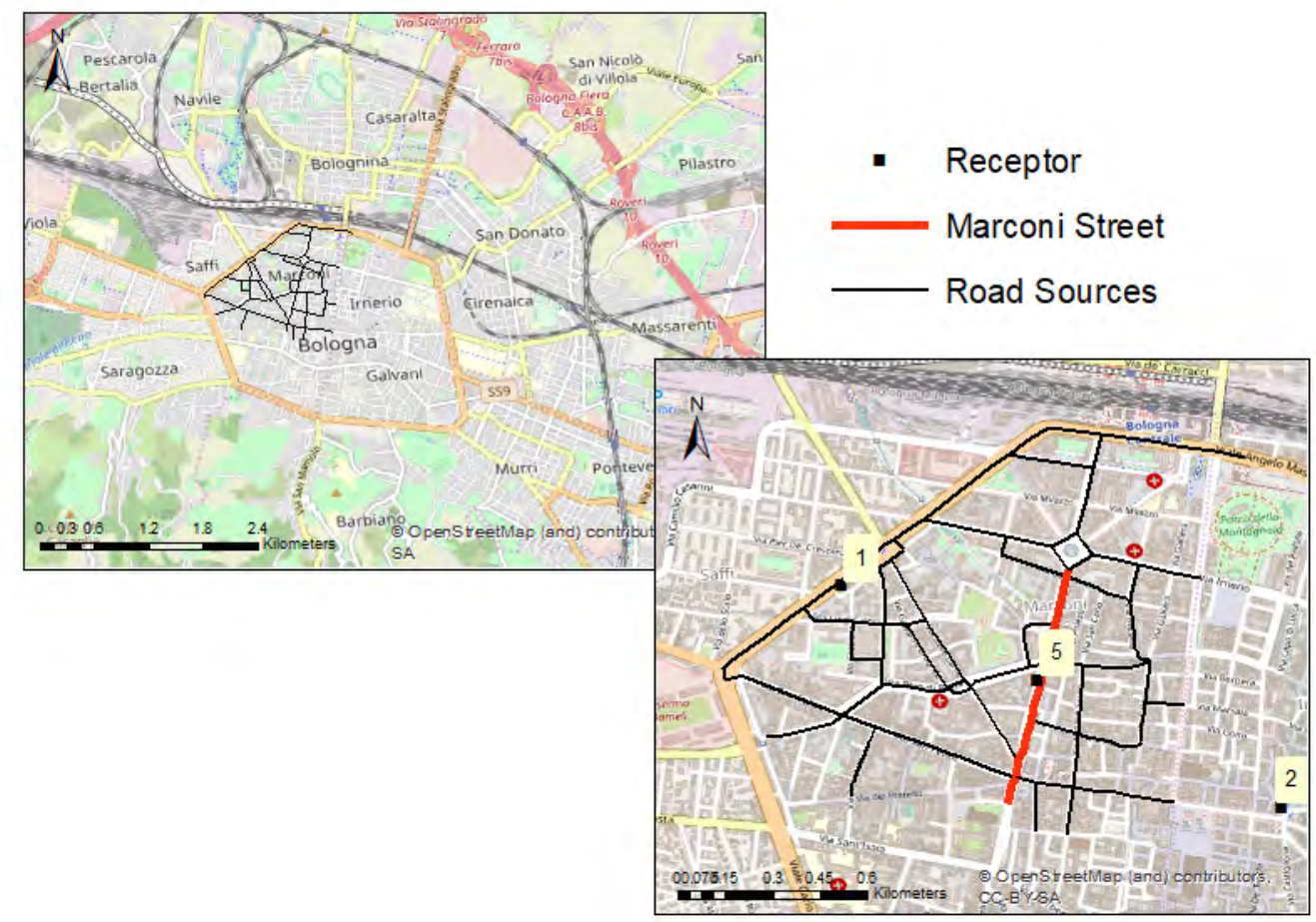

Figure 1. Roads inside the area around Marconi street and location of the receptor sites (points corresponding to the ARPAE air quality stations): 1) Porta S. Felice Receptor; 5) ARPAE van receptor; 2) Asinelli Receptor.

Since the pilot in Bologna is focused on trees, in this study the effects of trees on air quality are considered. Considering Marconi St., a tree-free street canyon in the base current scenario, we considered a scenario in which trees will be planted in the center of the road (Figure 2). In particular, the scenario was developed considering the planting of deciduous trees, to include also the seasonal effects due to the fall of foliage and of trees having all the same dimensions (crown diameter = 7 m, tree height = 10 m, distance between two crowns = 3 m, Figure 3). In the model, the trees are modeled as elements of roughness (porous bodies), which, together with the buildings, contribute to modify the wind field.

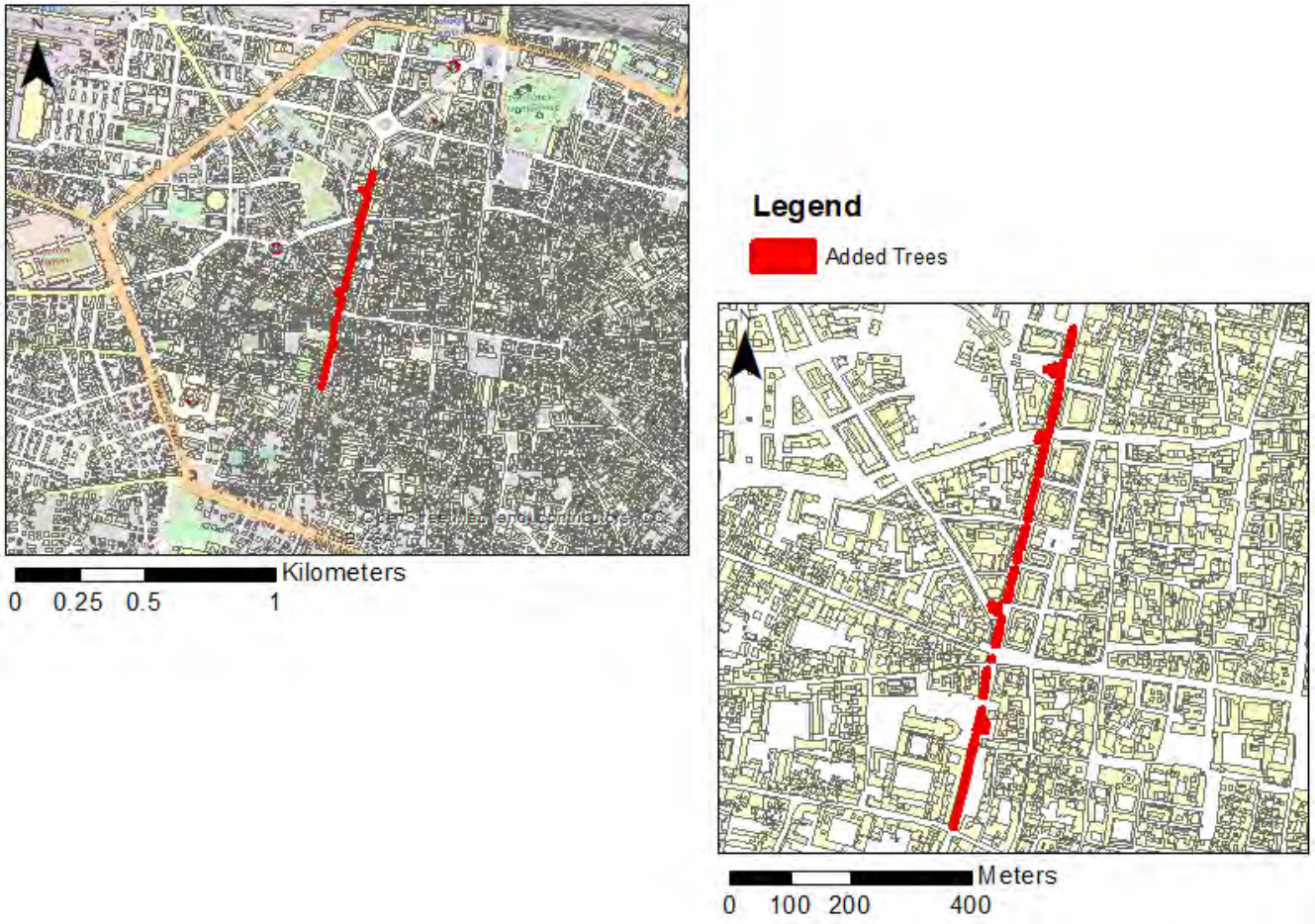

Figure 2. Location of the intervention of GI, trees added in Marconi St. for the Added Trees scenario

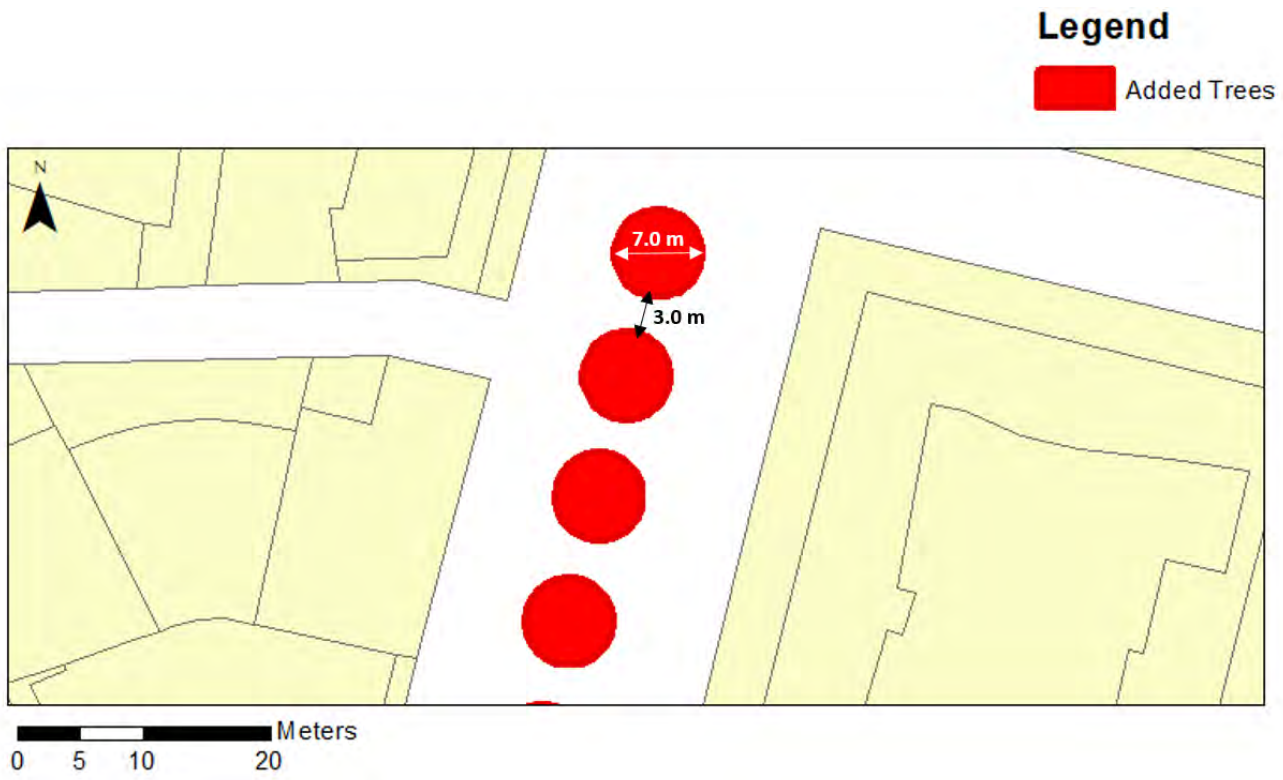

Figure 3. Detail of the location of trees added in Marconi and relative crown diameter and distance between two crowns

In order to consider the effects of climate change, the simulations carried out are divided into current and future cases, as shown in Table 2.

Case	Street	Year	Season	Trees	Scenario
Validation	Marconi	2017	summer	current trees	-
Validation	Marconi	2018	winter	current trees	-
Base Case	Marconi	2017	summer	current trees	Base Case –Actual Trees
Base Case	Marconi	2017	summer	added trees	Base Case –Added Trees
Base Case	Marconi	2018	winter	actual trees	Base Case –Actual Trees
Base Case	Marconi	2018	winter	added trees	Base Case –Added Trees
Future Case	Marconi	2050	summer	actual trees	Future Case –Actual Trees
Future Case	Marconi	2050	summer	added trees	Future Case –Added Trees
Future Case	Marconi	2050	winter	actual trees	Future Case –Actual Trees
Future Case	Marconi	2050	winter	added trees	Future Case –Added Trees

Table 2. Scheme of the simulations carried out on Bologna

3.1.1.1 Parameterization of trees

The exact geometry of vegetation (i.e. leaves and branches) is not explicitly modelled in the ADMS Urban dispersion model, but the presence of trees can be represented by introducing their geometry in the roughness calculation. In this work, the morphometric method presented by Kent et al. (2017) is used to calculate the aerodynamic roughness length on the urban area of Bologna (Italy).

Specifically, the zero-plane displacement (z_d), defined as the height at which the mean velocity is zero due to large obstacles such as buildings/canopy, is calculated as:

$$z_d = \left[1 + \alpha^{-\lambda_p}\left(\lambda_p - 1\right)\right] \cdot z$$

Where:

α is z_d correction coefficient = 4.43 (Macdonald et al., 1998)

λ_p is plan area index of roughness elements

z is the average height of roughness-elements

The aerodynamic roughness length (z_0), i.e. the height above the displacement plane at which the mean wind becomes zero when extrapolating the logarithmic wind- speed profile downward through the surface layer, is calculated as

$$z_0 = \left(\left(1 - \frac{z_d}{z}\right) exp^{\left[-\left(\frac{1}{k^2} 0.5 \beta C_{Db} \left(1 - \frac{z_d}{z}\right) \lambda_f\right)^{-0.5}\right]} \right) \cdot z$$

Where:

k is von Karman's constant = 0.4 (Hogstrom, 1996)

β is Drag correction coefficient = 0.55 (Macdonald et al., 1998)

C_{Db} is Drag coefficient for buildings = 1.2 (Macdonald et al., 1998)

λ_f *is* frontal area index of roughness elements of both solid and porous elements, considering the volumetric/aerodynamic porosity (P) as descriptor of the internal structure:

$$\lambda_f = \frac{\{A_{fb} + (A_{fT} \cdot P)\}}{A_{Tot}}$$

According to Yuan et al. (2017), since the leaf area index is a good estimator of tree porosity, the frontal area index is calculated using the LAI values:

$$\lambda_f = \frac{\{A_{fb} + (A_{fT} \cdot LAI)\}}{A_{Tot}}$$

Where:

A_{fb} is Frontal area of buildings

A_{fT} is Frontal area of trees

LAI is Leaf Area Index (Bewer et al., 2003)

A_{Tot} is Total area under consideration

The aerodynamic roughness length values were calculated using georeferenced data from buildings and trees. Height data, planar area and perimeter are associated with each roughness elements, while all the other parameters necessary for the calculation of z_0 have been calculated in a GIS (Geographic Information System) environment. The illustrated methodology, allowed to create spatial maps of z_0 considering the differences between winter and summer (leaf-on and leaf-off) (Figure 4 and Figure 5).

The Leaf Area Index (LAI) was used to parameterize the trees in the morphometric method. In particular, the LAI values reported in Breuer et al. (2003) have been used, subdividing all tree species into 4 broad

categories (Table 3). The values shown in the Table 3 have been assigned to each tree in the domain considered, differentiating between winter and summer.

Tree type	LAI mean	LAI leaf-off (winter)	LAI leaf-on (summer)
Evergreen tree	6.3	6.3	6.3
Deciduous tree	5.4	3.7	7.1
Evergreen shrub	6.2	6.2	6.2
Deciduous shrub	6.2	2.4	10

Table 3. Leaf Area Index (LAI) values used for evergreen and deciduous trees and shrubs (source: Breuer et al., 2003)

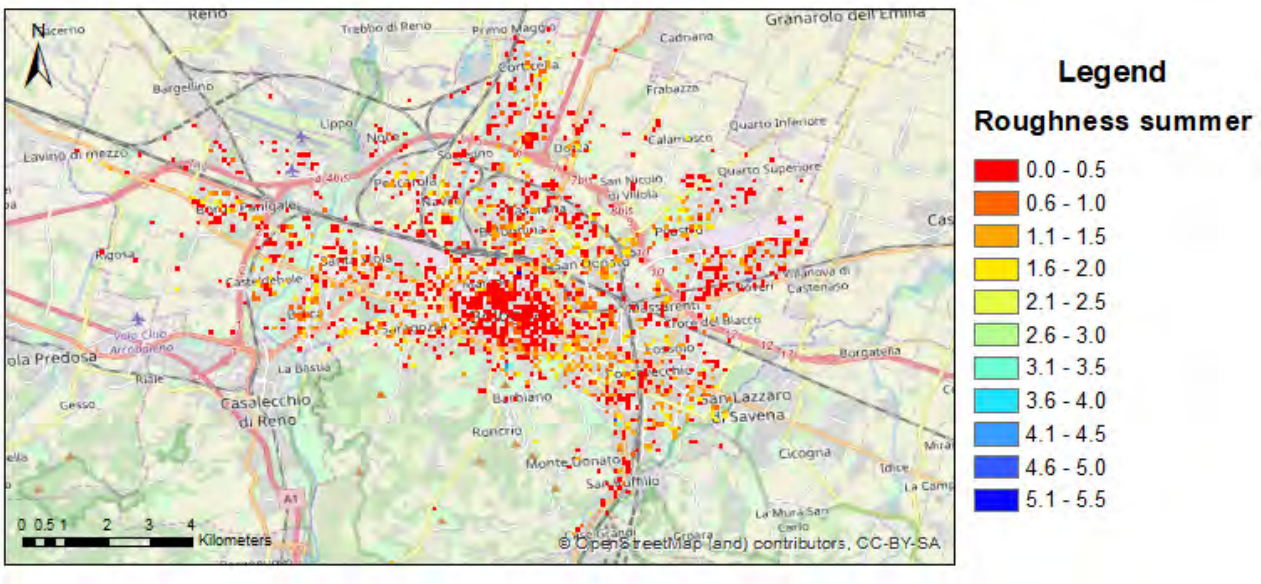

Figure 4. Map of aerodynamic roughness length in the summer period.

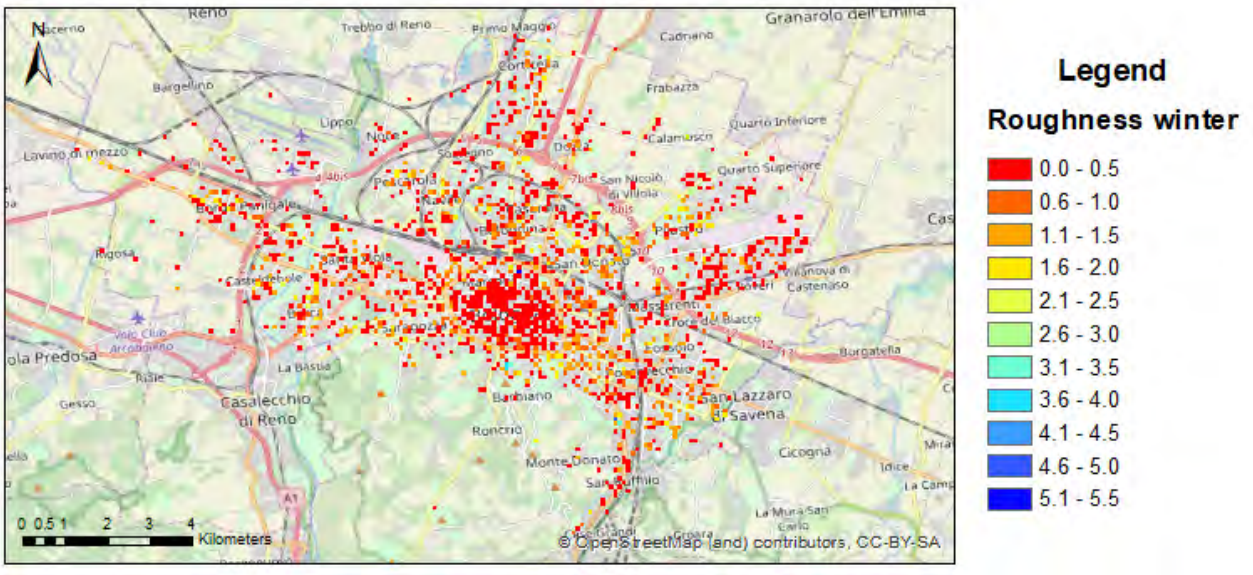

Figure 5. Map of aerodynamic roughness length in the winter period.

3.1.1.2 Base Case

In the base case, the dispersion of pollutants in the neighborhood of the street canyon has been modeled considering the months of August in 2017 and February 2018 as representative of both the summer and winter seasons. The meteorological dataset contained hourly sequential data measured at the Bologna airport weather station, considered as representative of the meteorology impinging on the city of Bologna not influenced by the presence of buildings in the city itself:

- Name: Bologna/Borgo Panigale (Bologna airport);
- WMO number: 16140 and WMO code: LIPE;
- Latitude: 44.5308 and Longitude: 11.2969.

Data collected during the two intensive field campaigns in Bologna (one summer campaign in August-September 2017, one winter campaign in January-February 2018, thoroughly described in D3.3 and D5.2) were used in the analysis and in the evaluation of the simulations. In fact, as described in those Deliverables, within the two summer and winter experimental campaigns, two ARPAE mobile laboratories for the measurement of atmospheric pollutants (NO_x, CO, SO_2, O_3, PM_{10} and $PM_{2.5}$) in addition to other instrumentation for the measurement of meteorological and turbulence variables were located along two parallel urban street canyons in Bologna, Marconi and Laura Bassi Veratti Sts.

3.1.1.3 Future Case

In the case of Bologna, the future scenario was derived running high resolution with the mesoscale numerical weather prediction model WRF (Weather Research and Forecasting). The WRF simulations were performed for two time periods, one in the warm period 20–26 August 2050, and one in the warm period 20-25 February 2050. The horizontal domain is composed of four two-way nested domains with

100x136, 88x124, 76x112, and 64x100 cells, and grid spacing of 13.5, 4.5, 1.5, and 0.5 km, respectively. For the vertical resolution, 51 levels were used, ten of which settled below 120m from the ground. We adopted a high-resolution topography data set with an original spatial resolution of 30" (~0.9Km). As regards the land use, the MODIS dataset with the present meteorological simulations was used.

The initial and boundary conditions were supplied by a new dataset including global bias-corrected climate model output data suitable for WRF. The new dataset deriving from version 1 of NCAR's (National Center for Atmospheric Research) Community Earth System Model allows estimating the weather under different future climatic scenarios. In this case, the WRF model has been driven by the Global 6-Hourly Bias-corrected Coupled Model Intercomparison Project, Phase 5 (CMIP5), Community Earth System Model (CESM) dataset over Europe under the RCP8.5 scenario (Monaghan et al., 2014).

Since the NCAR-CESM models participated in the CMIP5 Intercomparison and to the ensemble of GCM simulations used in D6.4 to downscale future climate projections for the six iSCAPE cities (28 for daily mean temperature, precipitation and solar radiation, 25 for daily minimum and maximum temperature and the diurnal temperature range and 24 for wind speed), in the following the simulations of the NCAR-CESM1-CAM5 and NCAR-CESM1-BGC were compared to the multi-model means for Bologna. In this framework, the multi-model means can be regarded as "best-estimates" for the future climate change, while the 90% uncertainty intervals for the change were calculated from inter-model standard deviations for the simulated changes, using the normality approximation.

In the following, we report the main results of the comparison for Bologna:

- the projected changes in mean, minimum and maximum temperatures based on NCAR-CESM1-CAM5, are close to the multi-model means in all calendar months (Figure 6a, c-d)
- The warming predicted by NCAR-CESMI-BGC presents an average rate in spring, but is weaker in the other seasons.
- For precipitation changes, the differences between the NCAR-CESM1 results and the multi-model means are largest in July and August, when even the sign of the projected changes deviates from the multi-model mean (Figure 6b).
- The NCAR simulations suggest somewhat larger increases in the monthly mean diurnal temperature range during the first half of the year than the multi-model means (Figure 2a).
- Solar radiation is generally projected to increase more strongly in the NCAR-CESM1-CAM5 simulation compared to the best estimate (except of July-September) (Figure 7b).
- Little differences between NCAR-CESM1 models and the multi-model means are found for wind speed (Figure 7c).
- The NCAR-CESM1 results mostly stay inside the 90 % uncertainty intervals, but are close to the upper limit for precipitation changes in August (Figure 6b).

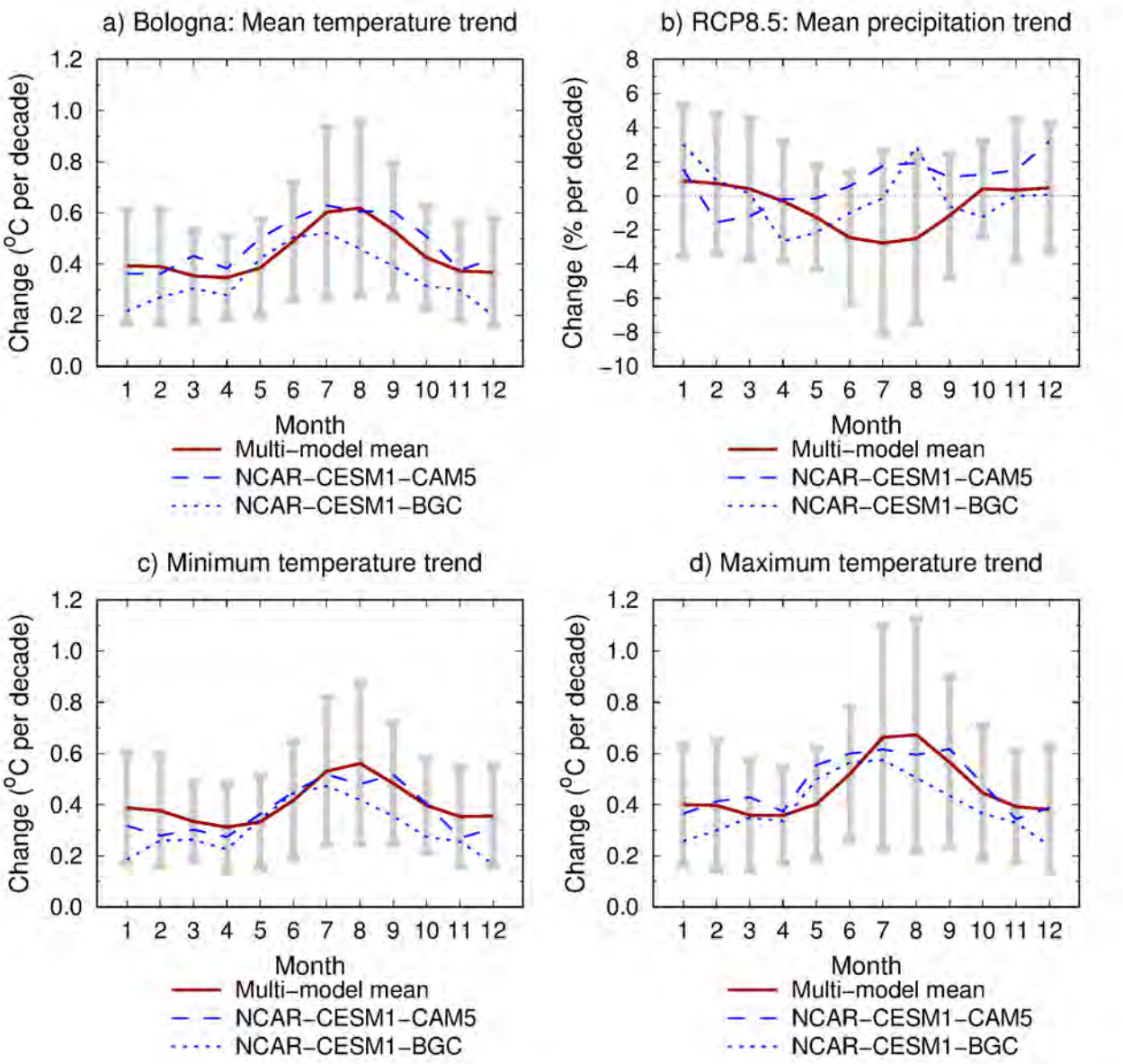

Figure 6. Projected trends in (a) monthly mean air temperature, (b) monthly precipitation total, (c) monthly mean of daily minimum temperature, and (d) monthly mean of daily maximum temperature between the periods 1981-2010 and 2040-2069 in Bologna under the RCP8.5 scenario. The multi-model mean projections for each calendar month (1 = January, 12 = December) are depicted by solid red curves. The grey bars indicate the 90 % uncertainty intervals for the change. The blue curves indicate outcomes from a simulation by NCAR-CESM1-CAM5 (dashed) and NCAR-CESM1-BGC (dotted).

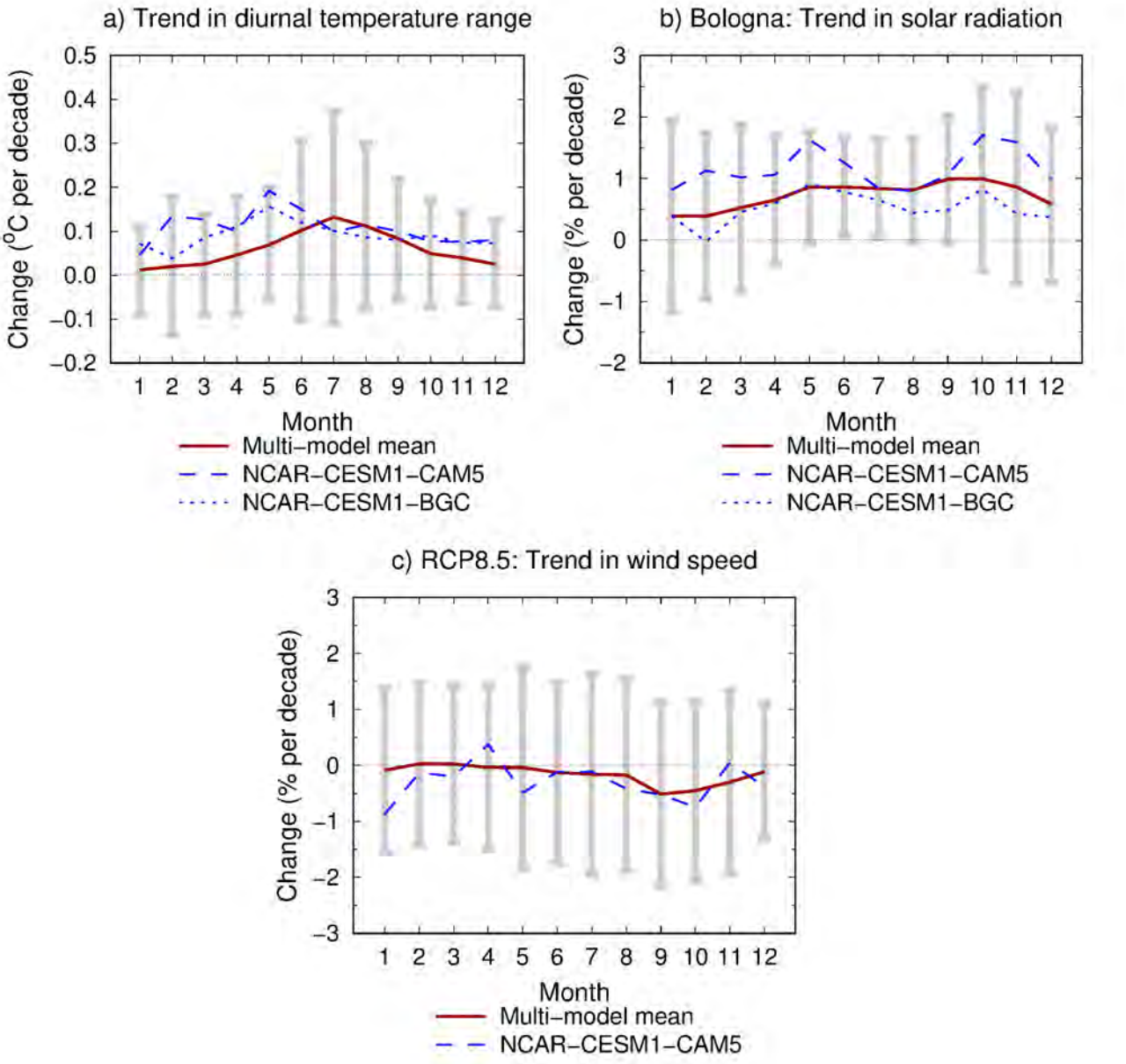

Figure 7. Projected trends in (a) monthly mean diurnal temperature range, (b) monthly mean incident solar radiation, and (c) monthly mean wind speed between the periods 1981-2010 and 2040-2069 in Bologna under the RCP8.5 scenario. For further information, see the caption for Figure 1. Note: NCAR-CESM1-BGC is missing from (c).

3.1.1.4 Validation

In order to evaluate the performance of the dispersion setup of the ADMS-Urban model, comparisons of measured and predicted concentrations carried out in the current base case were carried out by using the Model Evaluation Toolkit (CERC, 2015). In particular, the performance of the ADMS-Urban model was evaluated by calculating some basic statistical parameters, (mean and the standard deviation (SD)

of the mean), and other indicators with a methodology developed by Hanna (1993) and summarized by Chang and Hanna (2004). The indicators set, proposed by Carruthers et al. (2003), comprise: mean, standard deviation (SD), normalized mean square error (NMSE), Pearson's correlation coefficient (r), factor of two (FA2), fractional bias (FB), for more details see D.4.5 section 3. Ideally, a perfect model would have FB and NMSE tending to zero, while FA2 and r should be equal to 1.

3.1.2 UHI modelling

This section presents the model simulations carried out on an urban scale on the effects of PCSs and climate change on UHI. The site description and the domain information, as well as the complete methodology used for parameterization of the Bologna land use and for acquire meteorological variables, are in detail reported in D6.3. In particular, for the UHI analysis, the ADMS - Temperature and Humidity (ADMS-TH) Module is used (CERC; 2018). It belongs to the category of models that derives the resulting distributions as a perturbation of an existing field. In particular, ADMS-TH reports the spatial distribution of the temperature and humidity field generated by spatial variations in land use, city morphology and anthropogenic heat emissions with respect to the unperturbed upwind input values (ADMS-Urban, 2018). Land use type used for the analysis is derived from the Local Climate Zone (LCZ) classification adopted by Stewart and Oke (2012), which provides a useful framework for the UHI studies. The classification consists in 17 LCZs, subdivided in built types (1-10) related to structural features of the surface, and land cover types (A-G) accounting for seasonal and ephemeral properties (Stewart and Oke, 2012). Since the center of Bologna has been classified as "Compact Midrise" (from LCZ classification: Dense mix of midrise buildings. Few or no trees. Land cover mostly paved. Stone, brick, tile, and concrete construction materials), the effects that green infrastructures produce on the UHI effect at city scale were evaluated by modifying the LCZ classes. Considering Marconi St. as a typical representative street canyon in the Bologna city center (LCZ2), the presence of trees was simulated by modifying the surface parameter of the reference class with that used in the LCZ5 class. As described in section 3.1.1, considering Marconi St., a tree-free street canyon in the base current scenario, we considered a scenario in which trees will be planted in the center of the road. The trees are modeled as elements of roughness (like in dispersion model).

In the first part of the section, the UHI analysis performed to obtain more general and spatially detailed results on the increasing temperature inside the urban environment with respect to the countryside is summarized briefly in the current scenario (see reported in D6.3). In the second part of the section, a UHI analysis is performed in a future scenario for the city of Bologna. The results in present and future scenarios are compared to assess the effectiveness of GI intervention.

3.1.2.1 Base Case

Since one of the purposes of this deliverable is to highlight the effects of green infrastructure on urban-scale UHI effects, in Bologna the modeling of the current base case scenario was carried out over a period during which an intensive experimental field campaign carried out in two street canyons in Bologna (the summer experimental campaign in August-September 2017, thoroughly described in D3.3 and D5.2). During both campaigns, two days intensive thermographic campaigns involving measurements of the temperature of building facades and asphalt in the two canyons by means of thermographic IR cameras, were also carried out in the two canyons, with the purpose to evaluate the

UHI effect at neighborhood scale. For this reason, the simulations presented in D6.3 refer to the days 22 and 23 August 2017, when the summer thermographic campaign was carried out in Bologna. Since, the purpose of this deliverable is to compare the results in the present with the results in the future, here the results of the simulations are averaged over the entire period considered.

3.1.2.2 Future Case

In the future case, the analysis of the air temperature field on the city of Bologna was simulated running high-resolution numerical simulations with the WRF model for the year 2050, considering only the summer season. The meteorological dataset and the simulations were described in detail previously in Section 3.1.1.3

3.1.2.3 Validation

In order to evaluate the ADMS-TH model, comparisons of measured and predicted temperatures were carried out by using the Model Evaluation Toolkit (CERC, 2015). The performance of the ADMS-TH model was evaluated by calculating the same indicators set, proposed by Carruthers et al. (2003), of ADMS-Urban evaluation, (mean, standard deviation (SD), normalized mean square error (NMSE), Pearson's correlation coefficient (r), factor of two (FA2), fractional bias (FB)), for more details see D.4.5 section 3.

3.2 Vantaa

In Vantaa, the impact of an intervention consisting in a modification of the urban layout, previously described in D6.4, was evaluated. In the following, we summarize the simulation setup adopted to carry out the simulations for air pollution and air temperature in the present and future climate conditions.

3.2.1 Air pollution dispersion modeling

Here we report a brief synthesis of the main information on the air pollution dispersion simulations setup for Vantaa, reported thoroughly in D4.5.

Vantaa is a Finnish city and municipality part of the inner core of the Finnish Capital region together with Helsinki, Espoo and Kauniainen. Most of the main roads (Ring Road III, Tuusulanvaylä, Hämeenlinna motorway), run through Vantaa. In particular, four freeways out of Helsinki go to Vantaa and the main east-western road is the third ring road (Kehä III). In Finland, in general, highways radiate from the capital Helsinki or from Turku in the south-western coast of Finland. Out of the seven highways radiating from Helsinki, one highway connects Vantaa with Tampere and Ylöjärvi.

As such, Vantaa contains 162.3km of state-managed roads, 13.4km of railways and 1,264km of municipal roads, with a total length of about 1440km (Vantaan kaupunki, 2012).

The major local pollutant emissions in Vantaa derive from road traffic and energy production, in particular by power plants and fireplaces used in residential areas of the city (City of Vantaa, 2012; Soares et al., 2014, D6.1).

The climate of Vantaa is typically cold and temperate, with significant rainfall also during the driest months (D4.5). Wind direction distribution is quite homogeneous all over the cardinal rose, with a slight

prevalence of SW direction, accounting for winds flowing along the coast or coming from the western part of the Baltic Sea which provide the main contribution to the ventilation of the Helsinki Metropolitan Area (D6.1). Wind speeds are generally included between 2 m s^{-1} and 10m s^{-1} in every sector, accounting prevalently in the range 2-7 m s^{-1}. The wind intensity spread over all the wind cardinal directions provides an efficient mechanism for cleaning air pollutants and mitigate the cold climate compared to countries located at similar latitudes.

The emission inventory developed in D4.5 for Vantaa consists of two major emission sources, namely road traffic and residential heating; all the emissions were calculated using the EMIT toolkit by CERC (CERC, 2015). In particular, emissions from road traffic sources are calculated starting from traffic counts estimated by the light-activity based model developed by UH for cities other than Hasselt, and dividing the road links between major and minor roads on the base of the traffic counts and their length, with a final inventory of 3000 major roads. Urban UK NAEI 2014 emission factors, including emission data from the COPERT 4 version 10 (Katsis et al., 2012) were considered. Diurnal and monthly time varying emission factors were also considered to adjust for the variability of the road sources during the day and month.

Figure 8 represents estimated NO_x emissions for the 3000 road sources (major roads) considered in the emission inventory for Vantaa.

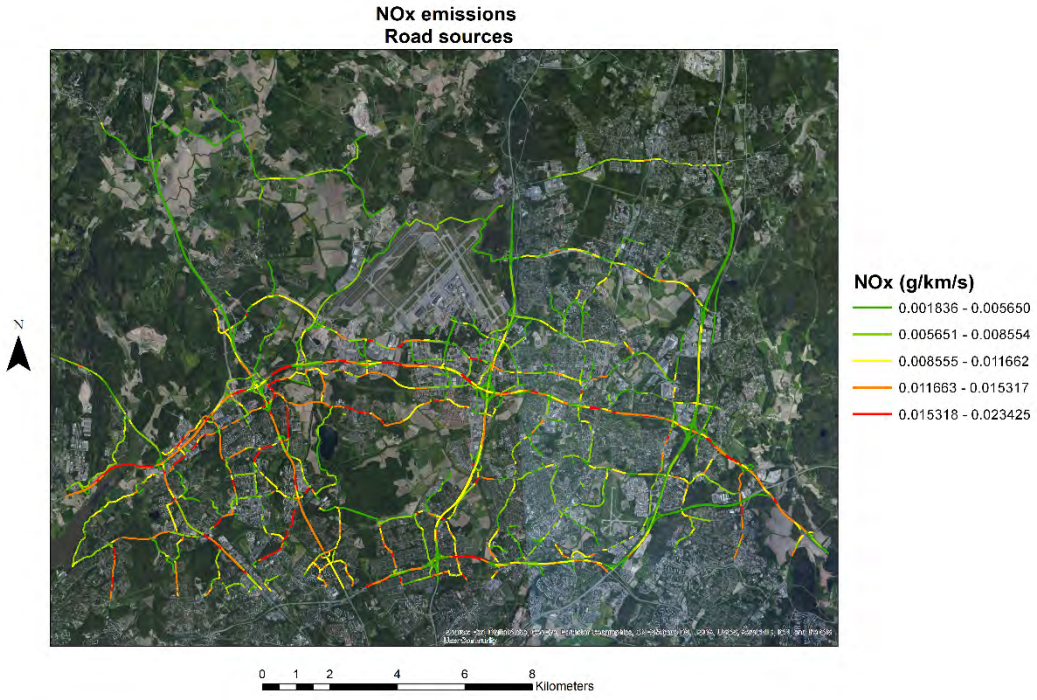

Figure 8. NO_x emissions (in g/km/s) for road sources considered as major roads in the emission inventory developed for dispersion modeling simulations in Vantaa (source: D4.5).

Figure 8 shows that the main emissions of air pollutants are located in vicinity of the major arteries such as ring roads and highways, even though emissions seem to be quite spread over the simulation domain.

Emissions from domestic sources were modeled as area sources, in particular utilizing a scaling of the national emissions from residential heating in Finland with respect to the population (i.e., deriving a scaling factor from the ratio of the population in Vantaa with the whole Finnish population). Information on population and emissions for the whole Finland was derived from Statistics Finland[11], while Helsinki population data are available as open-source data from avoindata.fi

Monthly and diurnal variation of residential heating sources were estimated considering the normal operating hours and operating periods (October to April) of residential heating sources in households in Finland from the Finnish Energy company[12].

Figure 9 shows the estimated NOx emissions from residential heating over the Helsinki Metropolitan Area. Even in the case of residential heating, emissions appear as largely spread over the simulation domain, even though with larger values over the more populated city centre.

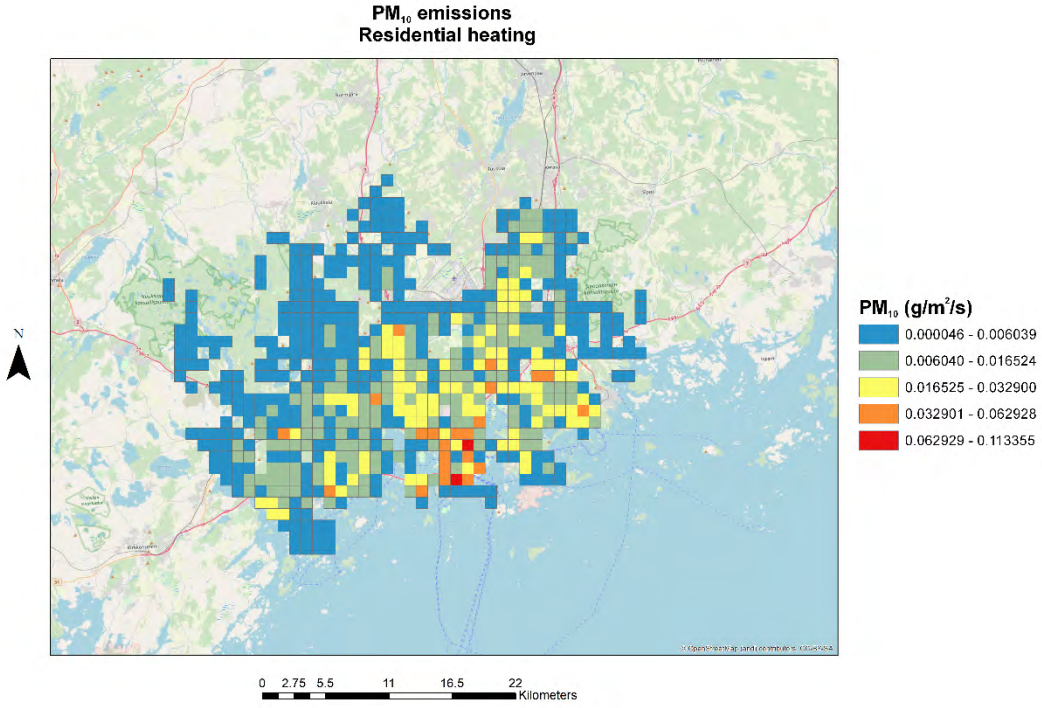

Figure 9. PM_{10} emissions ($g/m^2/s$) from residential heating in Helsinki Metropolitan Area in the base case (present) scenario (source: D4.5).

The source emission inventory was then used as input to the dispersion model simulations carried on under present and future climate scenarios. Similar to what done in D4.5, the ADMS-Urban model

[11] https://www.stat.fi/til/tilma/index_en.html

[12] https://energia.fi/en/news_and_publications/statistics/district_heating_statistics

(version 4.1.1.0) developed by Cambridge Environmental Research Consultants (CERC) was used (CERC, 2011) to calculate the concentration of pollutants emitted from the sources considered in the emission inventory. The ADMS-Urban model is a quasi-Gaussian plume air dispersion model able to simulate a wide range of passive and buoyant releases to the atmosphere. The dispersion of pollutants has been simulated with the Atmospheric Dispersion Modelling System (ADMS; CERC, 2017). This model has been already extensively verified within a large number of studies and its performance has been compared with other EU and US EPA models, such as CALPUFF, AERMOD for instance (e.g., Carruthers et al., 2000; Di Sabatino et al., 2008; Stocker et al., 2012).

Being a local dispersion model, ADMS is able to resolve concentration gradients occurring close to various emission source types, including point, jet, line, area and volume sources. Minimum input data for the modeling setup and for the representation of the modeled domain consists in the emission sources including emission rates and time varying emission factors, meteorological data (at least: air temperature, wind speed, wind direction, and either cloud cover either sensible heat flux either Monin-Obukhov length for estimating boundary layer height), and background concentrations. Within the model, the dispersion calculations are driven by hourly meteorological profiles of wind speed and direction, characterized through Monin-Obukhov length similarity theory. As such, input meteorological data are among the most important input parameters for modeling air pollution dispersion. Further details of the meteorological input parameters used for dispersion model simulations are provided in the following sections.

The setup of the dispersion model simulations for Vantaa takes into account into account emissions of all the main sources within the domain, either explicitly with detailed with detailed time-varying profiles, such as major roads and industrial sources, or as grid-averaged emissions with simpler time variations, normally representing diffuse sources (for instance, heating and minor roads). In this case, road traffic and residential heating emissions covering the whole Vantaa area were taken into account, with time varying emission factors (i.e., weekday-Saturday-Sunday and monthly) derived from the traffic simulations and from the operating hours of households for residential heating in Finland in the winter-spring season (from October to April).

Background hourly concentrations for NO_x, NO_2, O_3, PM_{10} and $PM_{2.5}$ were obtained from the rural background air quality station of Espoo Luuki through an open data service offered by FMI[13].

It is important to note that ADMS treats all NO_x data as "NO_x as NO_2", i.e., assuming that 100% of the NO_x is NO_2, which generally results in an overestimation of the true situation (CERC, 2011), since the molecular mass of NO_2 (46 g mol^{-1}) is greater than the molecular mass of NO (30 g mol^{-1}).

3.2.2Present scenario

In D6.4, high-resolution simulations were conducted with the regional scale surface interaction module SURFEX (Masson et al., 2013) to analyse the effects of altering urban characteristics in the city of Vantaa on local meteorological conditions in the present and in the future climate. In particular, SURFEX was deployed over a roughly square domain, with size 38 x 42 km, located in the southern coast of Finland, with the city of Vantaa in the middle of the domain.

[13] https://ilmatieteenlaitos.fi/avoin-data

In D6.4, the baseline period of the study was constructed as an artificial test reference year representing the recent past climate, choosing 12 historical months out from the 1980-2009 period in such a way that the monthly cumulative frequency distributions of daily mean air temperature, relative humidity, solar radiation and wind speed to be as close as possible to their respective climatological, i.e. 30-year average, cumulative frequency distributions. Hourly time series of meteorological data (forcing data to run SURFEX) were generated by the HARMONIE-AROME configuration of the ALADIN-HIRLAM numerical weather prediction system (Bengtsson et al., 2017).

In this work, instead, the setup of the present scenario utilized the 2017 hourly meteorological observations of wind speed, wind direction, surface temperature, solar radiation, precipitation, and cloud cover at the Vantaa Helsinki airport (WMO number 02974; 60.33 N, 24.96 E), retrieved from the open data service offered by FMI previously cited. The use of the meteorological observations taken at the airport for the baseline present period, instead that of the artificially constructed test reference year utilized in D6.4 to represent the recent past climate was aimed to verify the model setup comparing the results with air quality observations from reference stations in the Vantaa region (Figure 10)

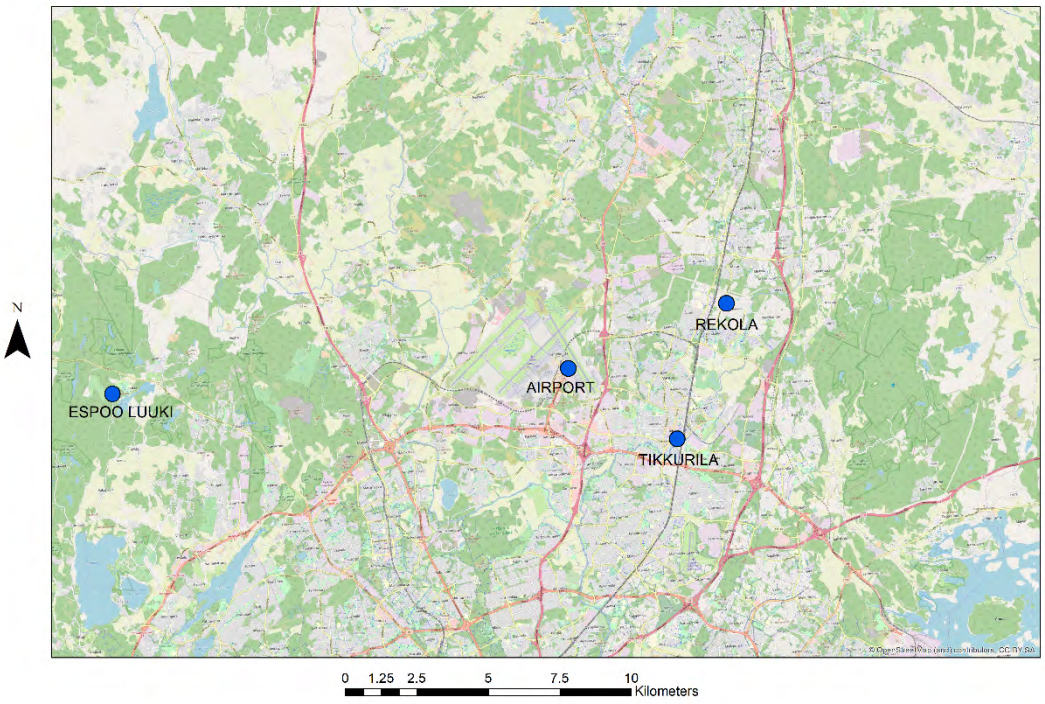

Figure 10. Map of permanent and mobile air quality stations in Vantaa (2017) (source: D4.5).

In addition, the use of the meteorological observations gathered at the airport served to derive a meteorology representative of the whole Vantaa area, not affected by the presence of buildings or other structures perturbing the flow in the urban city centre.

However, as we will see later, information on the surface roughness as retrieved by the SURFEX simulations at the meteorological and dispersion sites were included in the dispersion model setup. The surface roughness retrieved by the SURFEX model at the dispersion site presented important variations when considering modifications of the urban layout in Vantaa city centre, in proximity of Tikkurila: therefore, the changes in surface roughness enabled to consider different scenarios to analyse the effect of changing the urban layout on pollutant concentrations.

Having included in the simulations solar radiation, time and hour of the day, and background concentration data for the critical pollutants NO_X, NO_2, O_3 and SO_2, it was possible also to consider the NOx photolytic chemistry module, which accounts for fast, near-road oxidation of NO by O_3 to form NO_2 (Smith et al., 2017) and the oxidation of sulfur dioxide (SO_2) leading to the formation of ammonium sulfate particles, i.e. particulate matter (PM).

NAEI 2014 emission factors for the 2017 year were used in the model for road traffic sources.

In the present scenario, simulations were conducted in two different ways, i.e. considering short-term and long-term simulations, for two months, one in the winter (January 2017) and one in the summer (July 2017). In particular, short term simulations containing a set of pollutant concentrations were utilized for the comparison of model outputs with observations from reference stations for the verification of the model setup, while long-term simulations were used to produce pollutant concentration maps in the considered scenarios.

3.2.3Future climate scenario

As described in D6.4, the meteorological dataset used as input for dispersion modeling simulations was generated modifying the present baseline artificial year previously described with morphing adjustment methodologies (Belcher et al., 2005). Full details of the methods used to derive temperature, wind speed and direction, total precipitation and shortwave radiation are available elsewhere (Jylhä et al., 2015a, 2015b; Lehtonen et al., 2014). The climate change scenario considered global GHG emissions following the Representative Concentration Pathway RCP8.5. In D.6.4, a detailed comparison between the reference test year and the altered climate at the Vantaa airport is presented, showing that the parameter most seriously affected was temperature, while other parameters show more modest, but still systematic, changes.

Even in the future climate scenario, the meteorological input was derived for the airport meteorological station, while modifications of the urban layout were simulated through changes in the surface roughness at the dispersion site, as retrieved by the SURFEX module. In this case, as cloud cover is not an output from GCMs and the SURFEX model, it was substituted by the sensible heat flux to calculate the boundary layer height in the dispersion model simulations.

3.2.4Validation of dispersion model simulations

Similar to what done in D4.5, the verification of the dispersion model simulations was conducted comparing hourly simulated pollutant concentrations in the present baseline scenario with measured concentrations at the air quality stations in the Vantaa region (see Figure 10), focusing in particular over the Tikkurila station where the intervention consisting in an alteration of the urban layout was considered

in the scenarios. The performance was evaluated for one winter (January 2017) and one summer (July 2017) month.

The performance of the dispersion model simulations was evaluated using the Model Evaluation Toolkit (CERC, 2015) and calculating a set of basic statistical parameters and other statistical indicators following ta methodology by Hanna (1993)) recently summarized by Chang and Hanna (2004). In particular, we considered a set of indicators proposed by Carruthers et al. (2000) to evaluate the performance of the dispersion model:

- the fractional bias (FB), a measure of the mean difference between the modelled and observed concentrations
- the normalized mean square error (NMSE), a measure of the mean difference between matched pairs of modelled and observed concentrations
- the factor of two (FA2), i.e. the fraction of modelled concentrations within a factor of 2 of observations
- the Pearson's correlation coefficient (r), a measure of the extent of a linear relationship between the modelled and observed concentrations,
- and the coefficient of determination (R^2), the proportion of the variance in the dependent variable that is predictable from the independent variable(s).

Following equations describe the calculations of those statistical parameters:

$$FB = \frac{(\overline{C_o} - \overline{C_m})}{0.5(\overline{C_o} + \overline{C_m})}$$

$$NMSE = \frac{\overline{(M-O)^2}}{\overline{MO}}$$

FA2 = the fraction of data for which $0.5 < C_m/C_o < 2$

$$r = \frac{\sum_{i=1}^{n}(C_{o.i} - \overline{C_o})(C_{m.i} - \overline{C_m})}{\sqrt{\sum_{i=1}^{n}(C_{o,i} - \overline{C_o})^2 \sum_{i=1}^{n}(C_{m,i} - \overline{C_m})^2}}$$

$$R^2 = \frac{[\sum_{i=1}^{n}(C_{o.i} - \overline{C_o})(C_{m.i} - \overline{C_m})]^2}{\sum_{i=1}^{n}(C_{o,i} - \overline{C_o})^2 \sum_{i=1}^{n}(C_{m,i} - \overline{C_m})^2}$$

Where C_o denotes observations, C_m denotes model simulations, and the overbar denotes the average over the dataset.

Ideally, a perfect model would have FB and NMSE tending to zero, while FA2, r and R^2 should be equal to 1.

In addition, comparison of the simulated and measured diurnal and weekly patterns was also considered to analyse the performance of the model setup in correctly predicting airborne pollutant concentrations.

3.2.5 Effect of vegetation on air quality

As previously outlined, the meteorological observations at the Vantaa airport station used as input to the ADMS-Urban dispersion were gathered though an online service offered by FMI in the baseline scenario and retrieved by the SURFEX model for the future climate scenario. In addition, in this work, observations were complemented with the surface roughness at the meteorological and dispersion sites retrieved as an output of the SURFEX surface interaction model, capable of clearly separating buildings, air within urban canyons, roads, trees, green areas (parks, gardens). As such, the alterations of the urban layout considered in the intervention were modeled through a modification of the surface roughness (m) at the dispersion site as retrieved by the SURFEX module when forced with an alteration of the urban layout. In particular, the intervention consisted in an alteration of the urban layout for the 500 m by 500 m grid cell representing the Tikkurila area in central Vantaa (see D6.4 for further details on the intervention) (Figure 11).

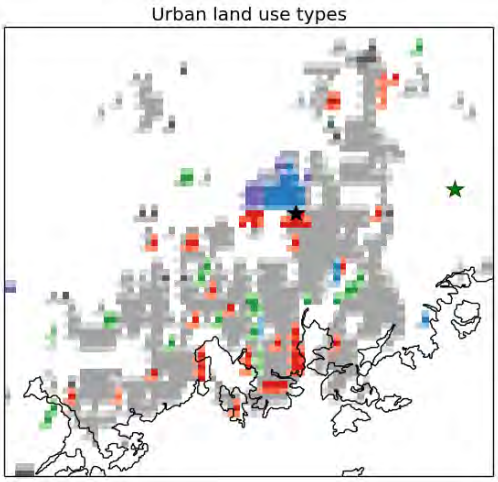

Figure 11. Urban land use types over the domain of SURFEX. Suburban types are shown in grey, commercial and industrial areas in red, parks and sports facilities in green, and airports and ports in blue color. The commercial area of Vantaa Tikkurila and the forest of the Sipoonkorpi National Park are shown by black and green stars, respectively (source: D6.4).

In particular, the intervention consisted in increasing the share of green areas substituting all relatively dense commercial and industrial areas (red color in Figure 11) with a suburban type, characterized by lower and less dense buildings and a larger fraction of vegetated spaces (Table 4). In addition, during the warm period when the ground is expected to be snow-free, albedo was increased from the value of 0.23 representative of not snow-covered surfaces (Oke, 1987) to 0.4 when substituting buildings with vegetation, to consider the effect of the larger reflection of solar radiation by green areas with respect to urbanized areas. Both values are comparatively high with respect to typical albedo ranges for human-made surfaces and vegetated surfaces (Ramírez and Muñoz, 2012), however the precise values would depend on the precise kind of surfaces considered (asphalt, concrete, bricks, roofs, grass, trees). In addition, the strongest impacts deriving from changing the albedo of the surfaces are predicted on global

warming, whereas pollutant concentrations, apart from ozone, will not be much affected by this change. In winter, instead, the albedo was set in both cases to 0.6 as representative of snow-covered ground surfaces (not changing when altering the urban layout). Since the changes in urban characteristics are not extreme and take place only in limited areas, they are not expected to impact over the whole urban boundary layer, and the SURFEX module was forced with the same atmospheric forcing in the base reference case ("baseline") and in the altered ("intervention") scenario.

	Building fraction	Building height (m)	Vegetated fraction	wall surface ratio	Albedo (summer case)
baseline	0.45	20	0.1	0.45	0.23
intervention	0.28	10	0.44	0.28	0.4

Table 4. Urban characteristics at Vantaa Tikkurila in the baseline case and in the intervention scenario with lower and less dense buildings and more widespread green space.

3.2.6 Effects of vegetation on UHI in current and future climate

As described in D6.4 and as detailed above, the SURFEX model was run in the current and future climate with an atmospheric forcing consisting in an artificially constructed test reference year representing the recent past climate and a modified test-year forcing generated by morphing adjustment for the 2050 climate. As detailed in D6.4, the simulated test-year weather data used as atmospheric forcing to the SURFEX model in the current scenario were verified against observations from Helsinki-Vantaa airport.

The Urban Heat Island effect, and the effect of vegetated areas over urban thermal comfort, was analysed by constructing maps of air temperature retrieved as an output of the SURFEX model in the various simulations conducted. As such, it is possible to analyse the differences in air temperature in the surroundings of Tikkurila in the present scenario, in a climate change scenario (RCP8.5), and in scenarios considering alterations of the urban layout when substituting buildings with vegetated areas in the current and future climate.

3.3 Dublin

Effectiveness of low boundary walls (LBWs) as passive control structure to reduce air pollution for the current (baseline) period and for future scenarios due to climate change were investigated by using computational fluid dynamics (CFD) based simulation studies. The air pollution considered for the comparative study is particulate matter 2.5 ($PM_{2.5}$). The study area considered for the analysis is the Pearse Street located at proximity to the Dublin city center. Details of the study area is provided in D6.2. To perform the comparative analysis, one CFD model were developed without any boundary walls and the pollution concentration inside the canyon were estimated. Subsequently, after installing the

boundary walls, change in air pollution were estimated at the same locations inside the canyon by considering the boundary conditions to be the same as before. Differences between the air pollution at the selected locations with and without the presence of LBWs were estimated. In order to understand the changes in air pollution in the future scenario, projections of the meteorological variables were considered as the boundary conditions and the differences in pollution concentration inside the canyon were estimated for both with and without the presence of passive control structures.

3.3.1 Meteorological conditions for the present and future scenario

The air pollution inside the canyon is dependent on the wind velocity and the wind direction. As reported in D5.2, the wind pattern was found to vary considerably in Dublin during the winter and summer months. For this purpose, two different models were developed in the study, in particular using the first model to simulate the air pollution from 20th August till 25th August as representative of the summer season and the second model for the simulations from 6th February till 11th February representative winter season. Wind velocity and wind direction data for the baseline (current) period were obtained from Dublin airport (WHO number: 03969, latitude 53.4333 N, longitude: 6.25 W). For the summer season of the baseline period, data were collected for August 2018, while for the winter season data were collected for February 2019. In order to evaluate the changes in air pollution for the future, wind velocity and wind direction data were simulated for Dublin airport using the WRF model for the year 2050, choosing again two time periods in the warm (20–26 August 2050) and in the cold (20-25 February 2050) season.

As previously done for Bologna, here we present the main results of the comparison between the NCAR-CESM models and the ensemble of GCM simulations used in D6.4 to downscale future climate projections for Dublin:

- The projected changes in mean, minimum and maximum temperatures (Figure 12a, c-d): based on NCAR-CESM1-CAM5, are close to the multi-model means in all calendar months. The warming based on NCAR-CESMI-BGC is of an average rate in spring, but weaker in the other seasons.
- The precipitation decreases in August and increases in September, as projected by NCAR-CESM1-BGC, fall outside the 90 % uncertainty intervals (Figure 12c).
- The NCAR simulations suggest larger increases in the monthly mean diurnal temperature range throughout the year than the multi-model means do (Figure 13a).
- Solar radiation is projected to increase more strongly in the NCAR-CESM1-CAM5 simulation compared to the best estimate (Figure 13b).
- Some differences can be observed in the projected changes in wind speed, but within the 90 % uncertainty intervals (Figure 13c).

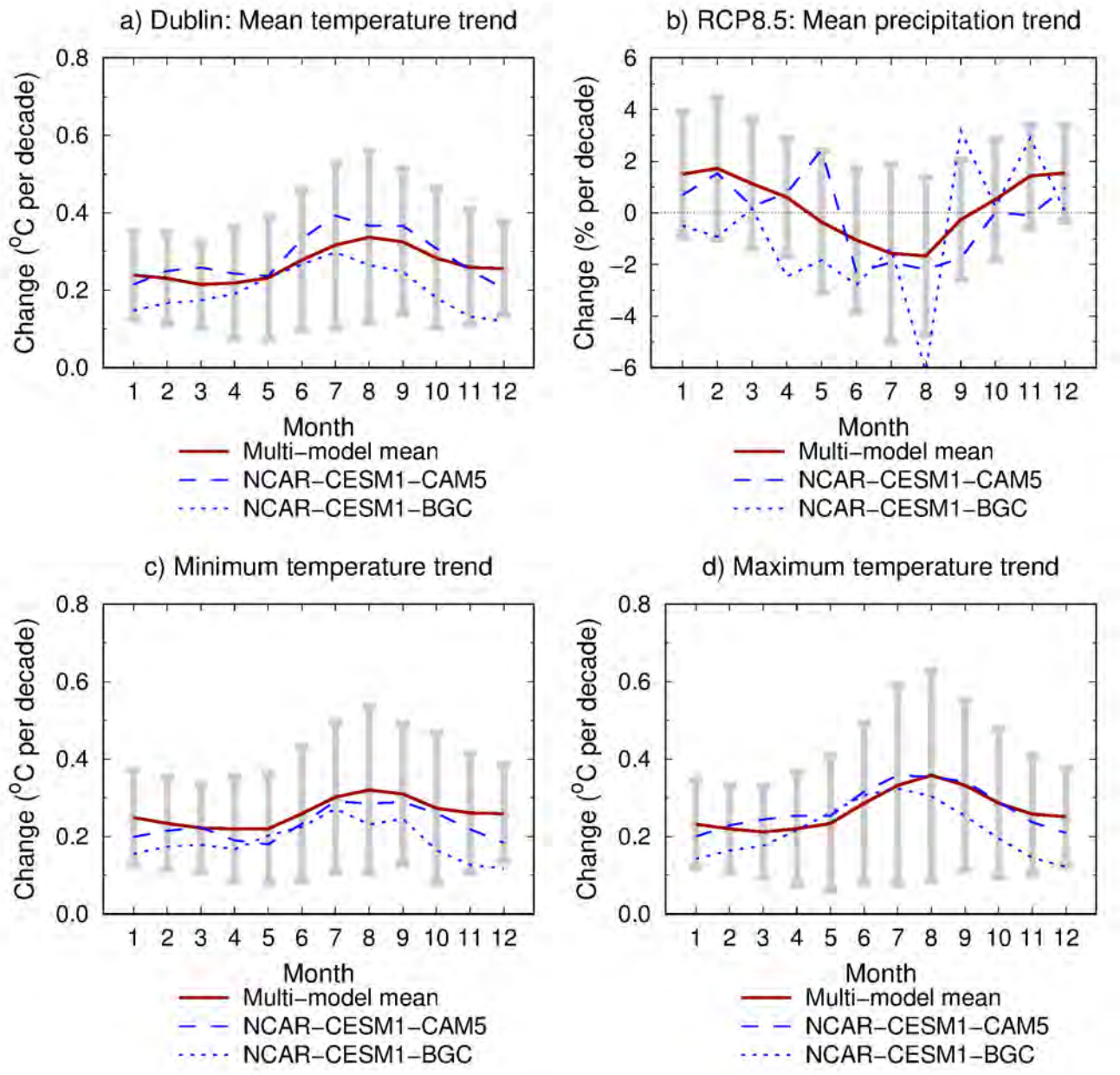

Figure 12: Projected trends in (a) monthly mean air temperature, (b) monthly precipitation total, (c) monthly mean of daily minimum temperature, and (d) monthly mean of daily maximum temperature between the periods 1981-2010 and 2040-2069 in Dublin under the RCP8.5 scenario. The multi-model mean projections for each calendar month (1 = January, 12 = December) are depicted by solid red curves. The grey bars indicate the 90 % uncertainty intervals for the change. The blue curves indicate outcomes from a simulation by NCAR-CESM1-CAM5 (dashed) and NCAR-CESM1-BGC (dotted).

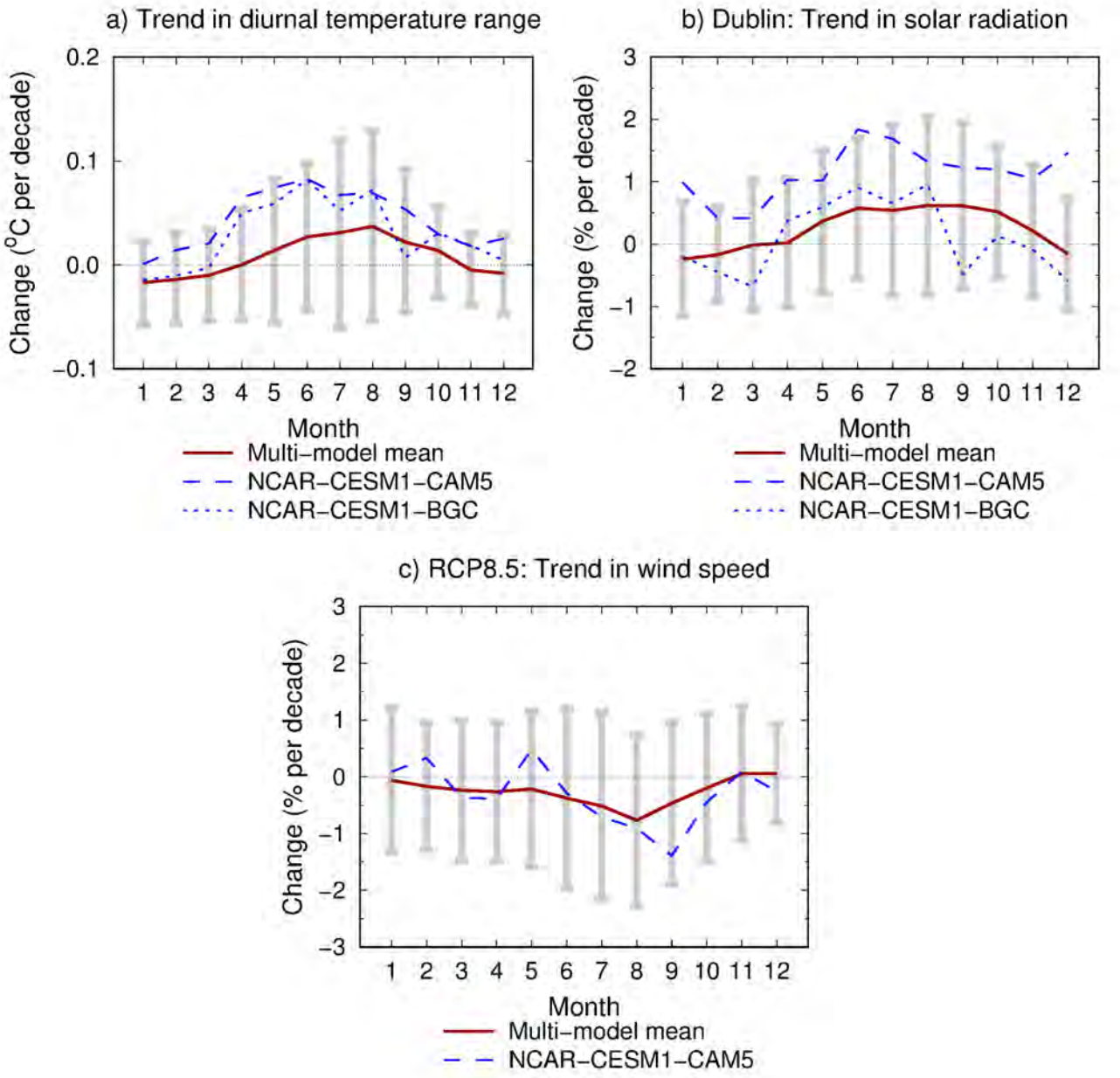

Figure 13. Projected trends in (a) monthly mean diurnal temperature range, (b) monthly mean incident solar radiation, and (c) monthly mean wind speed between the periods 1981-2010 and 2040-2069 in Bologna under the RCP8.5 scenario. For further information, see the caption for Figure 1. Note: NCAR-CESM1-BGC is missing from (c).

3.3.2 Emission inventory and CFD model

Once the meteorological boundary conditions (wind speed and velocity) were selected, the $PM_{2.5}$ pollutant emissions inside the canyon were estimated. For this purpose, the traffic count data were obtained from Dublin City Council's intelligent transport system, which is known as Sydney Coordinated Adaptive Traffic System (SCATS) that continuously monitors traffic flows in Dublin (NRA, 2010). The types of vehicles considered for the analysis were categorized as follows: (i) light vehicles including motorcycles, (ii) medium and large vehicles, (iii) buses and (iv) cyclists. To estimate the emissions from each type of vehicles, the European Emission Model COPERT4 (Kakosimos et al., 2010) has been considered. Emissions from different vehicle category were estimated based on the hourly average speed of the vehicles. The fleet composition was derived from traffic count data and the Irish national fleet composition. Fleet proportions for each category (e.g., passenger cars as light vehicles, van and trucks as medium and large vehicles, and buses) were derived from the SCATS count data in Dublin city center. Within each category, the percentages for each vehicle sub-category (petrol and diesel) were assumed to be in proportion with the Irish national fleet composition (Duffy et al, 2015). Summarized fleet data are provided below:

Category	Fuel type	Baseline
Passenger car	Petrol	63%
	Diesel	37%
Van	Petrol	0.3%
	Diesel	99.7%
Truck	Petrol	0%
	Diesel	100%
Bus	Petrol	0%
	Diesel	100%

Table 5. Fleet data for each category and fuel type

Once the traffic emissions inside the canyon were estimated, a CFD based model was developed to estimate the $PM_{2.5}$ air pollution concentration at different locations inside the street canyon, by considering the wind velocity, wind direction and traffic emissions as input to the model. The average $PM_{2.5}$ concentration at 2 meter height inside the canyon were estimated from the CFD model outputs. Comparison of the $PM_{2.5}$ concentration with and without the low boundary walls were performed for both summer and winter season and for baseline as well as future scenarios. The CFD models were solved based on large eddy simulation (LES).

4 Results

In this section we present the results obtained in the two cities of Bologna and Vantaa from dispersion modeling simulations of pollutant concentrations, and of high-resolution simulations of air temperature, conducted both in the present and in the future scenario with the methodologies previously outlined. First, we verify the performance of the dispersion model simulations conducted in the present reference case in order to demonstrate that the chosen setup is capable to correctly predict air pollutant

concentrations. After that, we compare the outputs of the simulations conducted in the reference scenarios with those of the "PCSs interventions" scenarios. For the city of Bologna and Dublin, we also present the results obtained from high resolution CFD simulations conducted at neighborhood scale, with a methodology previously thoroughly presented in D6.2

4.1 Bologna

In this section, we describe the results obtained with the methodology previously outlined for Bologna, starting with the verification of the model setup and followed by the evaluation of the impact of the planting trees intervention on air quality and air temperature in the present and future climate conditions.

4.1.1 AQ simulations

As described in the methodology section, in the following we will present the evaluation of the performance of the ADMS-Urban model and the results of the dispersion conducted in the current and future scenarios. Results are presented in the form of concentration maps for considered pollutants obtained as output of long-term simulations of the ADMS-Urban 4 dispersion model.

4.1.1.1 Validation

The statistical evaluation of the performance of the ADMS-Urban model was carried out comparing graphically simulations for August 2017 and February 2018 with measured values in Marconi St. from the ARPAE van equipped for measurements of air pollutants during the summer and winter experimental field campaign in Bologna and calculating some statistical parameters. In particular, the assessment was carried out considering NO_x concentrations. The following figures (Figure 14 and Figure 15) represents the comparison of diurnal, weekly pattern and monthly patterns in the simulated and observed NO_x concentrations in Marconi St.

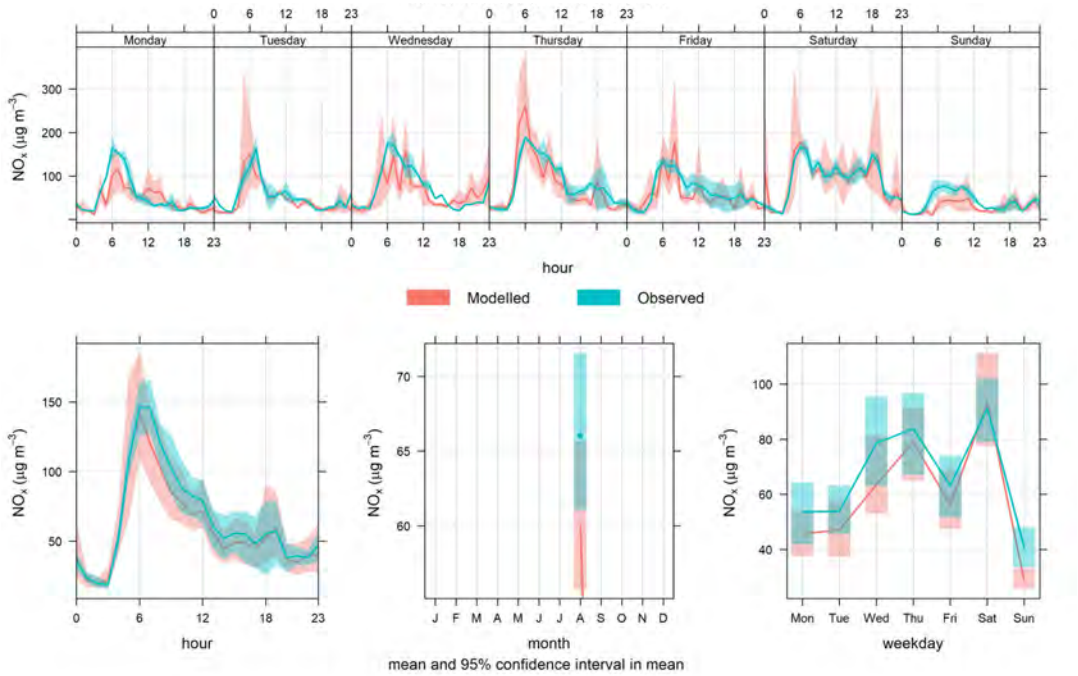

Figure 14. Time variation analysis for NO_x concentrations from 10 to 31 August 2017, representing diurnal, weekly and monthly pattern for the base case simulation for Marconi St., as compared to the measurements from the ARPAE van.

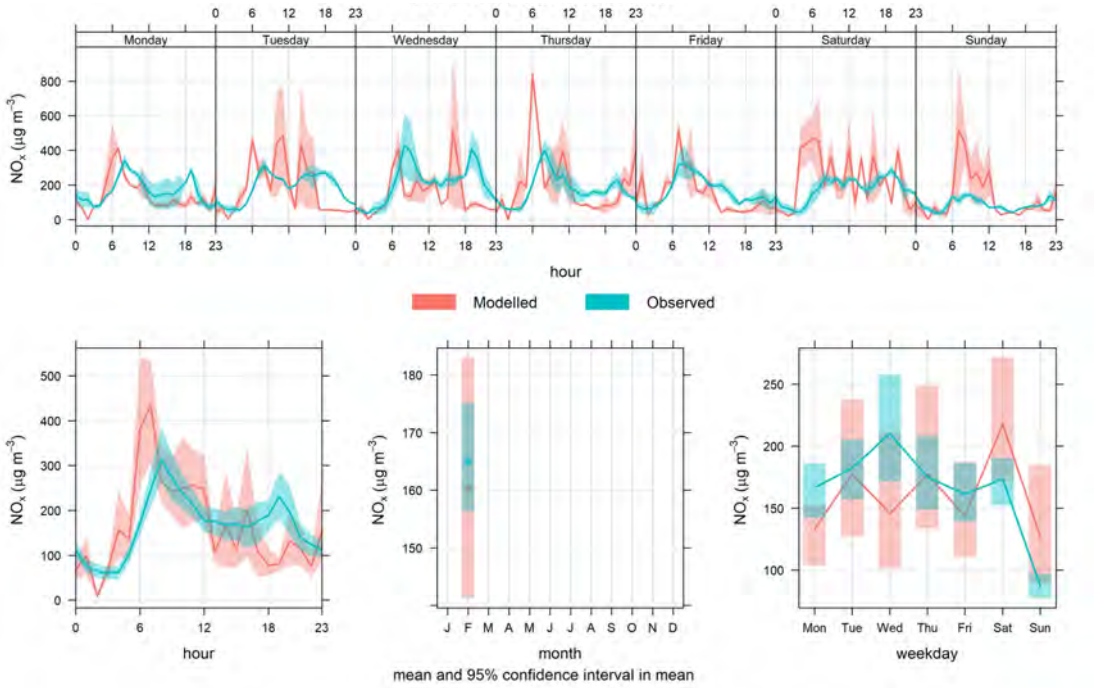

Figure 15. Time variation analysis for NO_x concentrations from 1 to 15 February 2018, representing diurnal, weekly and monthly pattern for the base case simulation for Marconi St., as compared to the measurements from the ARPAE van

The Figures shows that the model represents correctly the overall pattern of air quality pollutants, even though it tends to underestimate NO_x concentrations. In particular, snow events occurred during the winter period, besides affecting deeply wet deposition, might have impacted on the traffic flow, determining a non-optimal correspondence between simulated and measured data. However, as from Table 6, statistical parameters for the ADMS simulations are reasonably good.

Station	Season	$Mean_{OBS}$ ± SD	$Mean_{MOD}$ ± SD	NMSE	r	FA2	FB
Arpae van	Summer	65. ± 18.0	58.7 ± 26.1	0.05	0.91	1	-0.10
Arpae van	Winter	165.3 ± 41.0	160.8 ± 43.7	0.07	0.48	1	-0.03

Table 6. Statistical analyses for the considered periods: mean, standard deviation (SD), normalized mean square error (NMSE), Pearson's correlation coefficient (r), factor of two (FA2), fractional bias (FB). Reference station: ARPAE van located in Marconi street. Observed (OBS) and modelled (MOD) data for NO_x.

FA2 results show good agreement between observed and modelled concentrations, the normalized mean square error is low for all cases. The values of the fractional bias are very low, and in particular the low negative values exhibited by the simulations in both summer and winter period indicate the tendency for the model to show a slight underestimation of measured values.

4.1.1.2 Base Case

Since the concentrations of pollutants present significant variations during the seasons, and these variations are especially significant between summer and winter, simulations for the current scenario (base case) were conducted selecting two periods, one during summer (20 - 25 August 2017) and one during winter (6 - 11 February 2018). For each period, simulations were conducted both in a scenario of trees planting (added trees) and in the absence of trees (actual trees). The results are presented in the form of concentration maps averaged over the period considered and concentration difference maps (added trees map - actual trees map).

Base Case - Actual Trees scenario

The following figures show the spatial distribution of the concentration of pollutants in the base case for 2017, averaged over the period considered. The NO_x concentration maps (Figure 16) appear similar in the two seasons as for the spatial distribution, with higher values in the study area and a lower and more homogeneous background around; however, the winter case shows higher concentrations in a larger spatial area, in agreement with the more frequent stagnation regimes typical of the winter season.

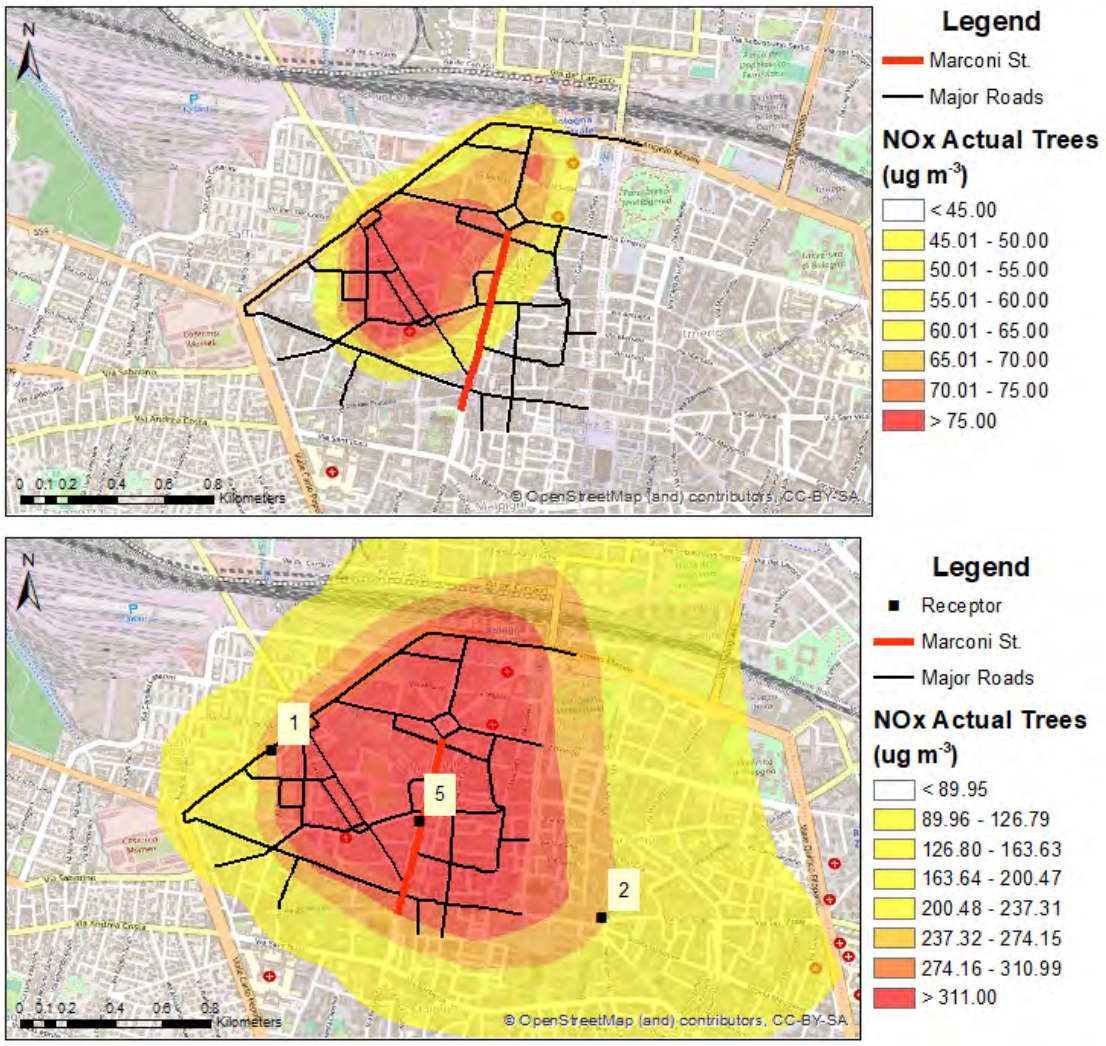

Figure 16. Concentration maps for NO_x (top: summer 2017, bottom: winter 2018) in the current reference case (Base Case - Actual trees) for a neighborhood of Marconi St. in Bologna. The maps represent concentration values averaged over the period considered. The location of the receptor sites is indicated with a number: 1) Porta S. Felice Receptor; 5) ARPAE van receptor; 2) Asinelli Receptor.

The simulated concentration ranges are, as expected, very different in the two seasons. The comparison of the average values measured from the ARPAE van in Marconi St. and at Porta S. Felice receptor sites for the two periods (Table 7) highlight how winter represents a critical period.

Scenario	Receptor name	Season	NO_x (µg m^{-3})
Base Case – Actual Trees	ARPAE van	Summer	48.9
Base Case – Actual Trees	ARPAE van	Winter	457.5
Base Case – Actual Trees	Porta S. Felice	Summer	199.5
Base Case – Actual Trees	Porta S. Felice	Winter	619.8

Table 7. Average concentration values simulated at the two receptor sites of Marconi St. and Porta San Felice in the summer and winter reference case (Base Case - Actual Trees) in Bologna.

Base Case - Added Trees scenario

As reported in section 3, deciduous trees are added in Marconi St. to assess the effectiveness of PCs in Bologna. The comparison of the average values simulated at the two receptor sites between the Base Case - Added Trees scenario and the current reference case for the two periods (Table 8) shows that the winter is still a critical period. However, the average values are lower than in the current reference case (Base Case - Actual Trees scenario).

Scenario	Receptor name	Season	NO_x (µg m^{-3})
Base Case - Added Trees	ARPAE van	Summer	63.1
Base Case - Added Trees	ARPAE van	Winter	280.8
Base Case - Added Trees	Porta S. Felice	Summer	167.7
Base Case - Added Trees	Porta S. Felice	Winter	491.1

Table 8. Average concentration values simulated at the two receptor sites of Marconi St. and Porta San Felice in summer and winter for the scenario of planting trees in the current climate conditions (Base Case - Added Trees) in Bologna.

Figure 17 shows the concentration maps for NO_x in Base Case - Added Trees scenario to compare with that obtained for the Base Case - Actual Trees scenario. The comparison shows that the trees planting intervention does not impact neither on maximum values have not substantially changed compared to the base case, neither on the spatial pattern.

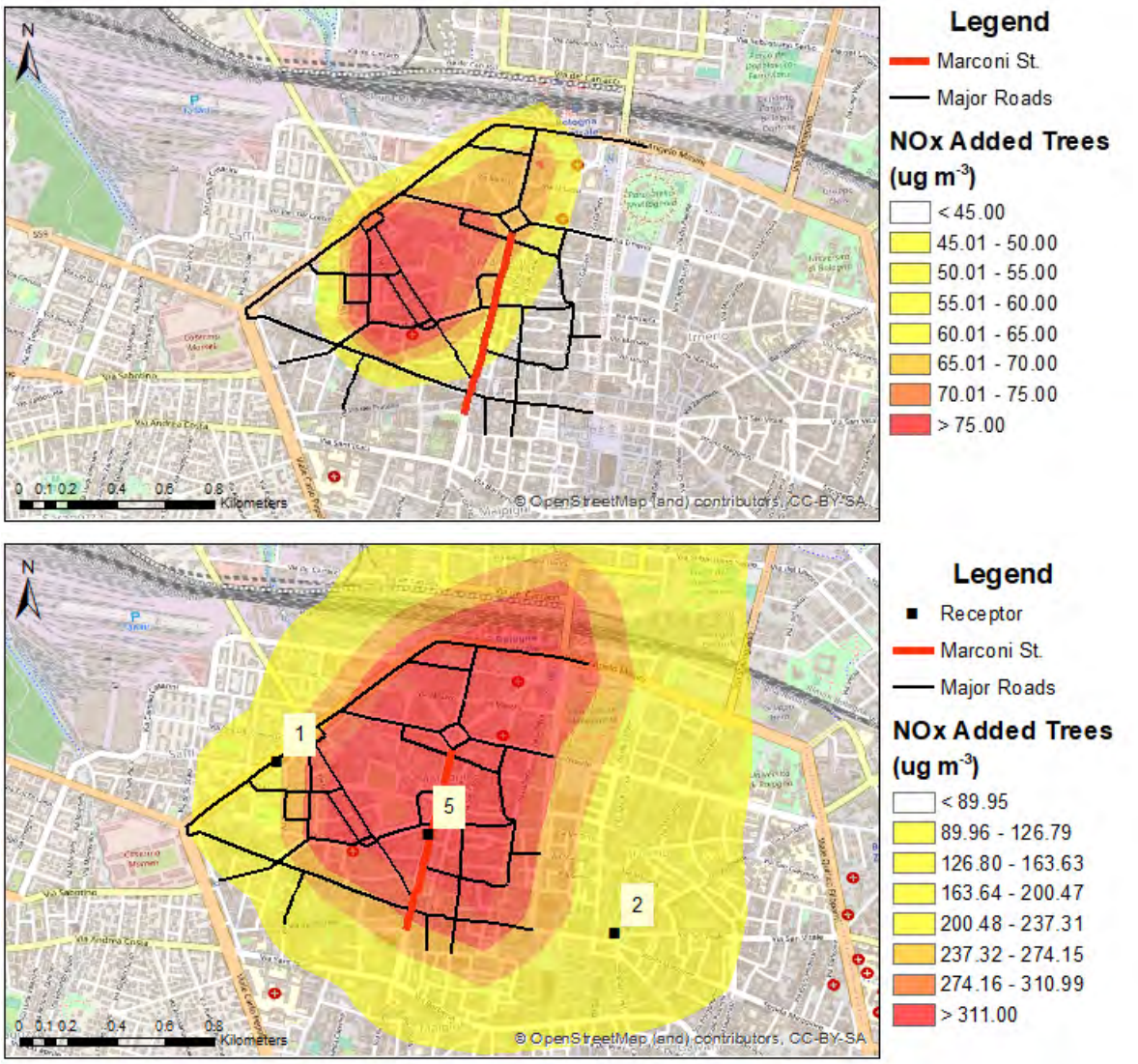

Figure 17. Concentration maps for NO_x (top: summer 2017, bottom: winter 2018) in the current climate conditions with a tree-planting scenario (Base Case - Added trees) for a neighborhood of Marconi St. in Bologna. The maps represent concentration values averaged over the period considered. The location of the receptor sites is indicated with a number: 1) Porta S. Felice Receptor; 5) ARPAE van receptor; 2) Asinelli Receptor.

The comparison between the two cases is presented in terms of maps of concentration differences, which highlight more clearly the presence of areas of reduced and increased NO_x concentrations. Below, the maps of NO_x are presented for both summer and winter period.

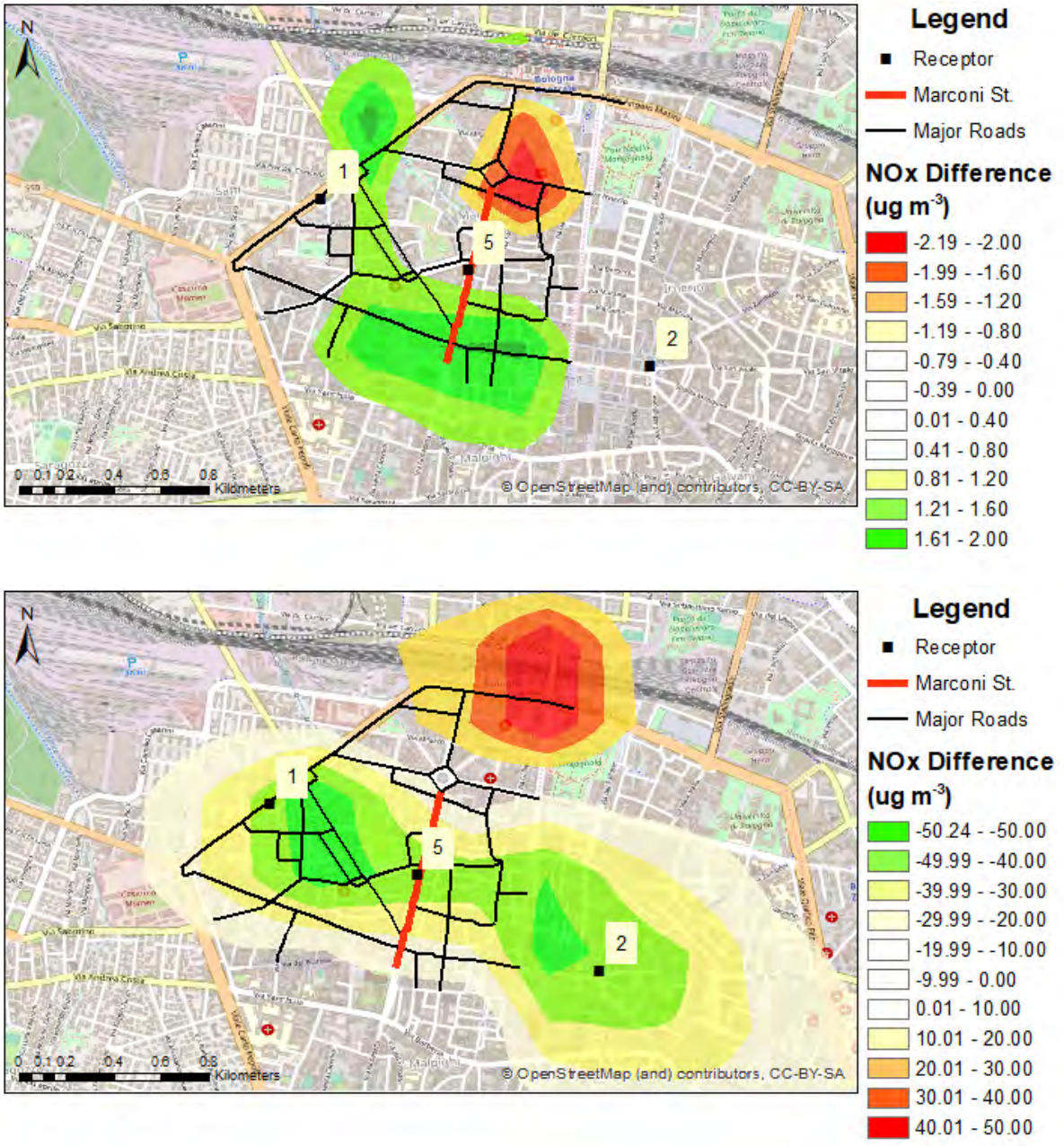

Figure 18. Maps of concentration differences for NO_x (top: summer 2017, bottom: winter 2018). The differences are calculated between the Base Case - Added Trees scenario and the Base Case - Actual Trees current reference case. The location of the receptor sites is indicated with a number: 1) Porta S. Felice Receptor; 5) ARPAE van receptor; 2) Asinelli Receptor.

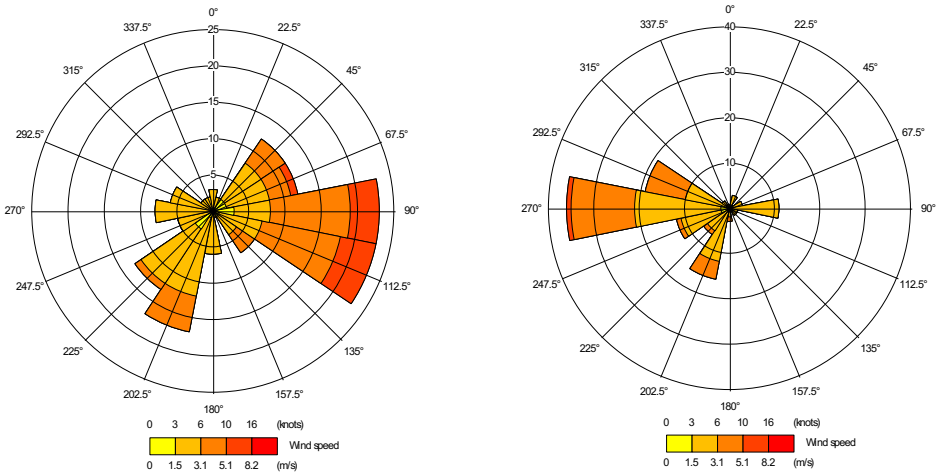

Figure 19. Wind rose for base reference case in Bologna, summer 2017 (left) and winter 2018 (right). Meteorological observations from Bologna airport meteorological station.

Maps of concentration differences (Figure 18) show how the planting of trees along Marconi St. has an impact on the dispersion of pollutants and therefore air pollutant levels in the neighborhood of the street canyon. In both summer and winter period, two distinct areas are highlighted: one in which concentration increases and one in which concentration decreases. While the decrease and increase in concentration present the same intensity in terms of maximum values, the spatial area affected by these variations is different, with a bigger area covered by reductions of NO_x concentrations. This could be due to the wind direction which was different for the two periods (Figure 19). Therefore, our results show that the tree planting in an area can lead to an improvement in air quality in its neighborhood, as shown by the percentages of reduction/increase in concentration (Table 9, calculated for ARPAE van and Porta S. Felice receptors), compared to the Base Case - Actual Trees.

Receptor name	Season	NO_x
ARPAE van	Summer	29%
ARPAE van	Winter	-39%
Porta S. Felice	Summer	-16%
Porta S. Felice	Winter	-21%

Table 9. Percentages of reduction/increase in concentration in the scenario of tree planting compared to the reference case (Base Case - Actual Trees scenario) (calculated for ARPAE van and Porta S. Felice receptor).

4.1.1.3 Future Case

This section shows the results of the simulations conducted in Bologna utilizing input meteorological data derived from the WRF high resolution numerical simulations for the winter and summer seasons under the RCP8.5 emission scenario. For the summer case, the month of August 2050 was considered, while for the winter case the month of February 2050 was chosen. As in the base case, the results of

the effect due to the presence (added trees) and the absence of trees (actual trees) are reported in both months. The results are presented in form of concentration maps averaged over the period considered and concentration difference maps (added trees map - actual trees map).

Future Case - Actual Trees scenario

The following figures show the spatial distribution of pollutant concentrations in the future case for 2050, averaged over the two periods considered. The NO_x concentration maps (Figure 20) appear similar in the two seasons with regard to the spatial distribution, with higher values in the study area and a lower and more homogeneous background around. Even here, as in the base case, the winter period shows higher concentrations in a wider spatial area.

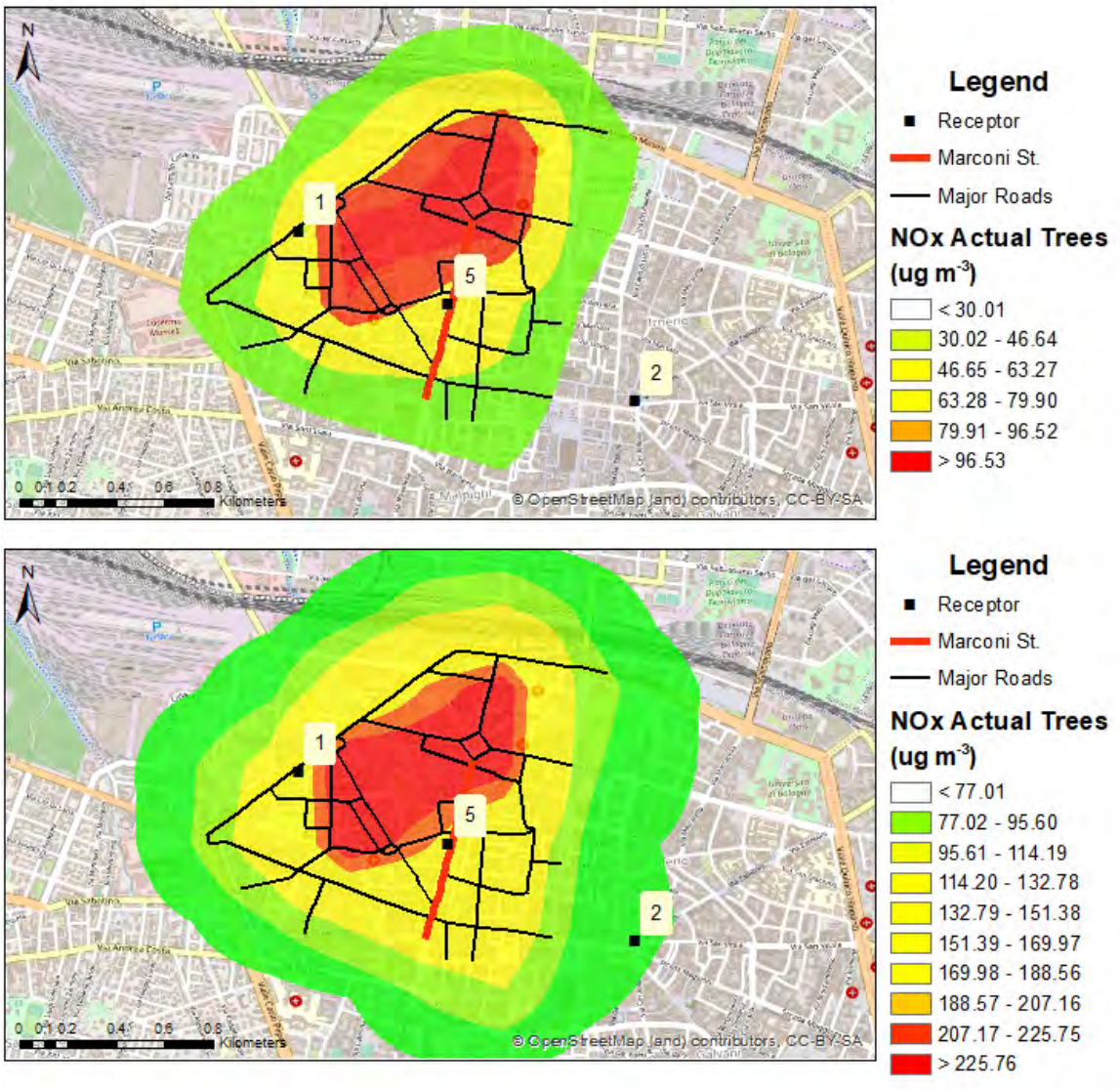

Figure 20. Concentration maps for NO_x (top: summer 2050, bottom: winter 2050) in a scenario considering the impact of future climate conditions (Future Case - Actual trees scenario) for a neighborhood of Marconi St. in

Bologna. The maps represent concentration values averaged over the period considered. The location of the receptor sites is indicated with a number: 1) Porta S. Felice Receptor; 5) ARPAE van receptor; 2) Asinelli Receptor.

The simulated concentration ranges are, as in the base case, very different in the two seasons. The comparison of the average values simulated at the ARPAE van and Porta S. Felice receptor sites for the two periods (Table 10) highlight again how winter represents a critical period also in the future.

Scenario	Receptor name	Season	NO_x (µg m^{-3})
Future Case - Actual trees	ARPAE van	Summer	95.8
Future Case - Actual trees	ARPAE van	Winter	227.7
Future Case - Actual trees	Porta S. Felice	Summer	283.2
Future Case - Actual trees	Porta S. Felice	Winter	597.8

Table 10. Average concentration values simulated at the two receptor sites of Marconi St. and Porta San Felice in future summer and winter for Future Case - Actual Trees scenario in Bologna, i.e. under the effect of climate change only.

Future Case - Added Trees scenario

Here we report the results of a future scenario considering the implementation of an intervention planting deciduous trees in Marconi St. The comparison of the average values obtained at the two receptor sites in the two scenarios with and without the intervention for the two periods (Table 11) shows results similar to those obtained in the present climate conditions scenario. However, the average concentrations are slightly lower than in the current reference case, only in the winter case.

Scenario	Receptor name	Season	NO_x (µg m^{-3})
Future Case - Added trees	ARPAE van	Summer	126.9
Future Case - Added trees	ARPAE van	Winter	176.0
Future Case - Added trees	Porta S. Felice	Summer	292.7
Future Case - Added trees	Porta S. Felice	Winter	450.3

Table 11. Average concentration values simulated at the two receptor sites of Marconi St. and Porta San Felice in the future with a scenario considering planting trees in Marconi St. (Future Case - Added Trees).

Figure 21 shows the NO_x concentration maps in the scenario when planting trees under future climate conditions (Future Case - Added Trees scenario) for comparison with the results obtained under climate change only (Future Case - Actual Trees scenario). The results indicate a similar spatial pattern in the two scenarios, but in the summer period concentration levels are more reduced than in the scenario without trees (Future Case - Actual Trees scenario).

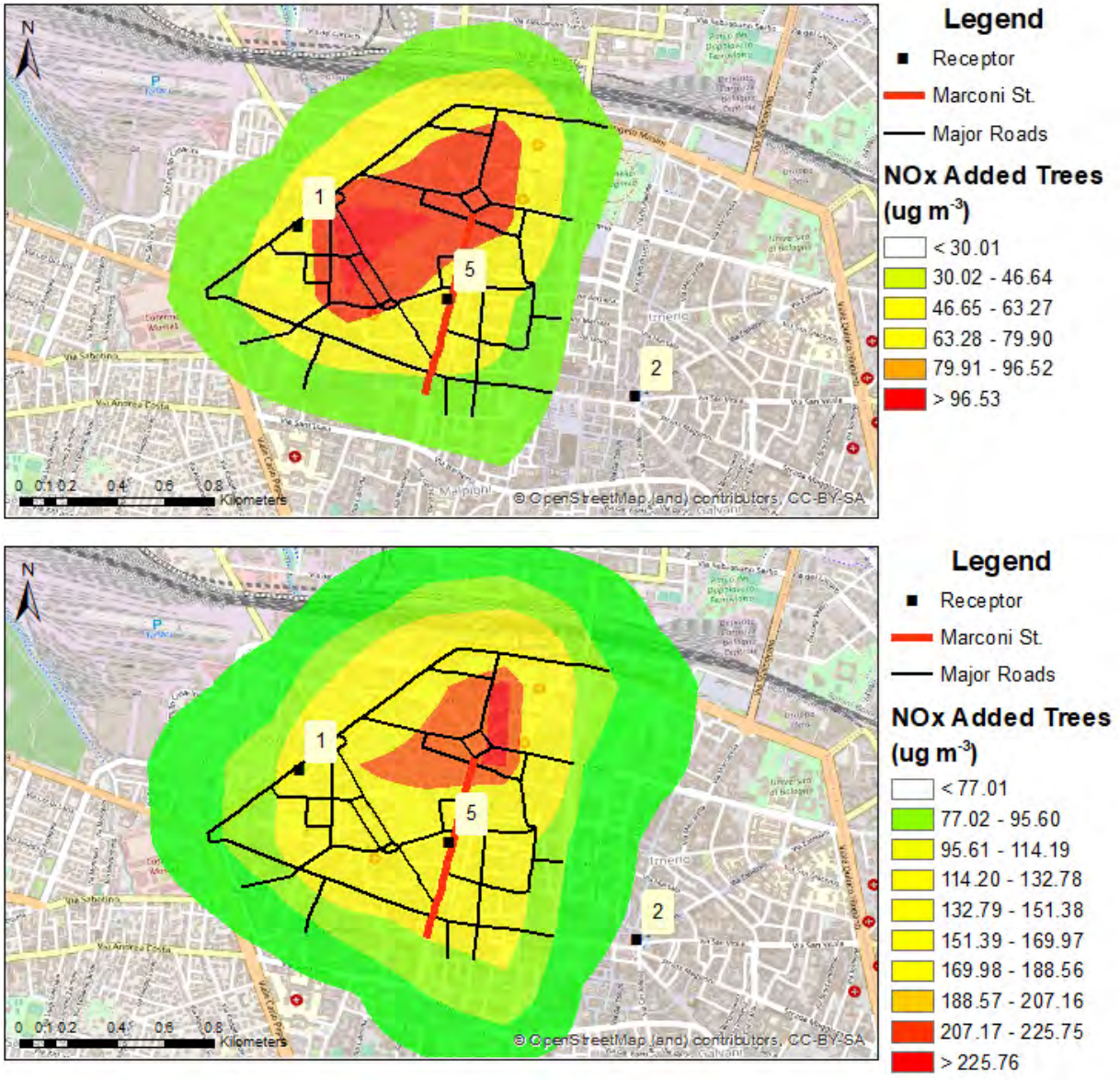

Figure 21. Concentration maps for NO_x (top: summer 2050, bottom: winter 2050) under the impact of future climate but planting trees in Marconi St. (Future Case - Added trees scenario) for a neighborhood of Marconi St. in Bologna. The maps represent concentration values averaged over the period considered. The location of the receptor sites is indicated with a number: 1) Porta S. Felice Receptor; 5) ARPAE van receptor; 2) Asinelli Receptor.

As previously done in the present climate conditions, the comparison between the two scenarios is carried out in terms of maps of concentration differences, which highlight more clearly the presence of areas of reduced or increased concentrations. Below the maps of NO_x concentrations are presented for both summer and winter period.

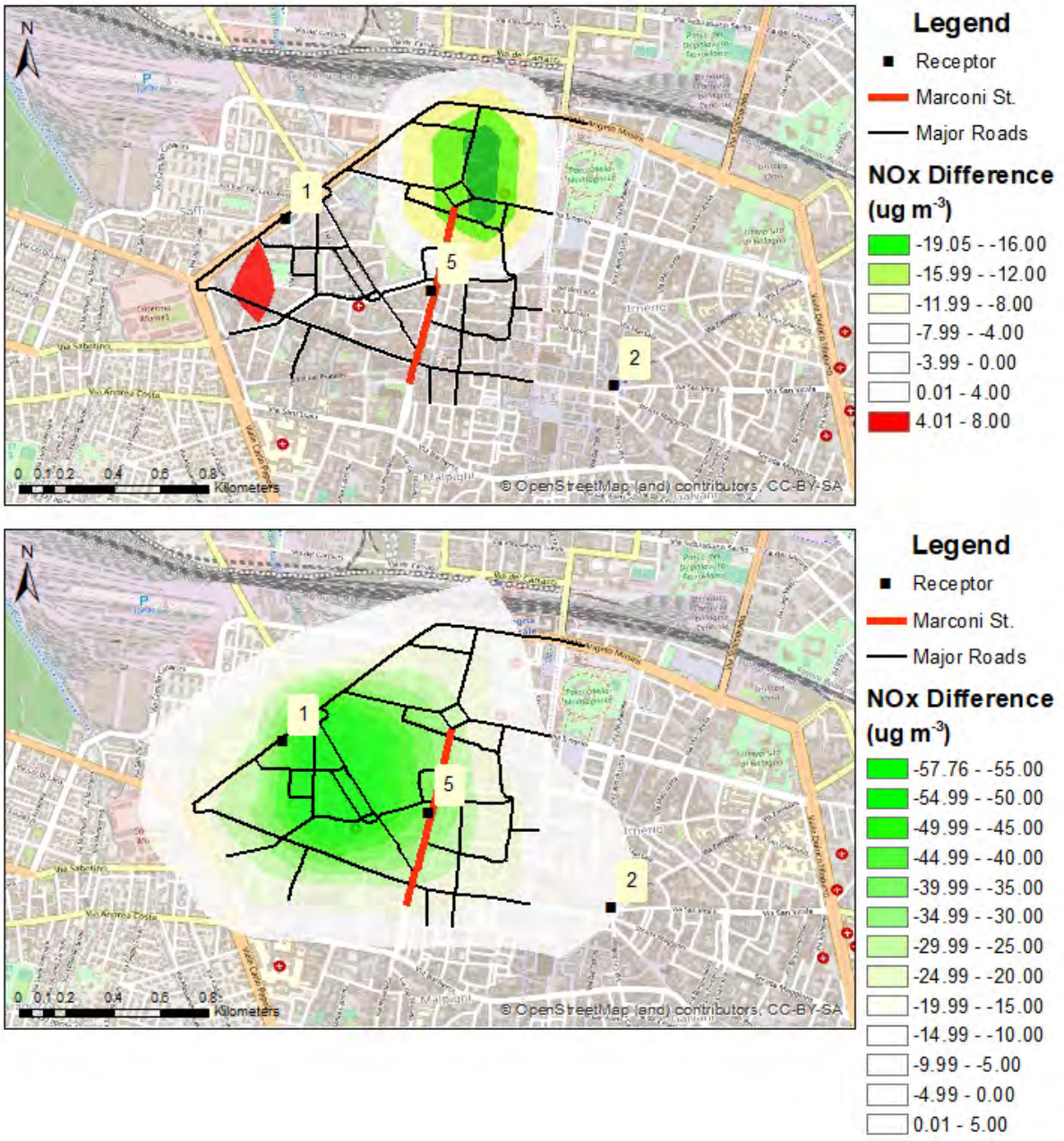

Figure 22. Maps of concentration differences for NO_x (top: summer 2050, bottom: winter 2050). The differences are calculated between the two future scenarios with and without trees (Future Case - Added Trees scenario and Future Case - Actual Trees scenario). The location of the receptor sites is indicated with a number: 1) Porta S. Felice Receptor; 5) ARPAE van receptor; 2) Asinelli Receptor.

Maps of concentration differences show how the planting of trees along Marconi St. affects the dispersion of pollutants and therefore pollutant concentrations in the neighborhood of Marconi St. In both summer and winter period, areas of concentration decreases are highlighted. In the summer period, two distinct areas are highlighted: one where the concentration increases and one where the

concentration decreases. It is in interesting to note the change in the spatial area affected by concentration decreases in the two periods, likely due to the different wind rose and dominating wind directions, SW-W in the summer and NW in the winter period (Figure 23).

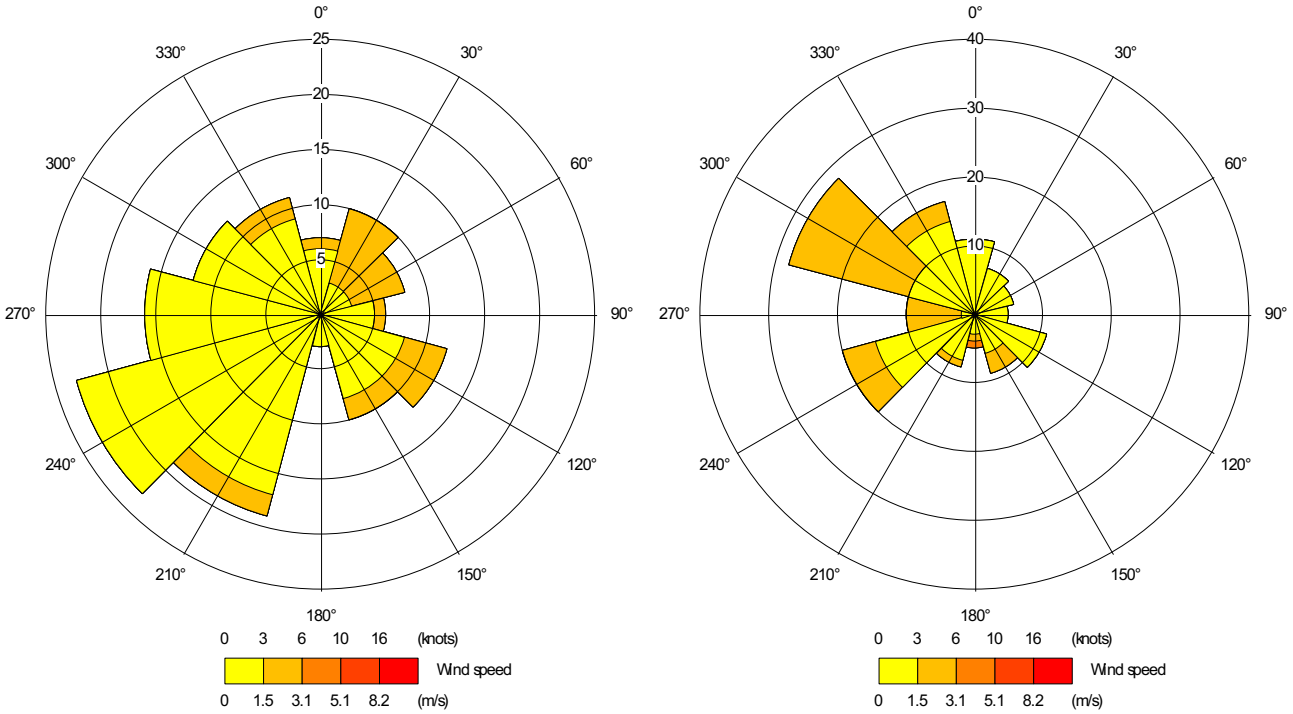

Figure 23. Wind rose for base reference case in Bologna, summer 2050 (left) and winter 2050 (right).

Receptor name	Season	NO_x
ARPAE van	Summer	32%
ARPAE van	Winter	-23%
Porta S. Felice	Summer	3%
Porta S. Felice	Winter	-25%

Table 12. Percentages of reduction/increase in concentration in the scenario of tree planting in future climate conditions compared to that without trees (Future Case - Actual Trees scenario) (calculated for ARPAE van and Porta S. Felice receptors).

Table 12 shows the variation in NO_x concentration (reduction/increase) calculated for ARPAE van and Porta S. Felice receptors, compared to the Base Case - Actual Trees. The decrease reaches a maximum of -25% in winter (Porta S. Felice receptor), while in summer the positive effect of the trees is not so evident. However, considering the entire simulation domain in Figure 24, it is possible to recognize a decrease in concentration up to a maximum of -17% even in the summer period. Therefore, the effect of the tree planting might be considered as effective in mitigating air pollution in Bologna.

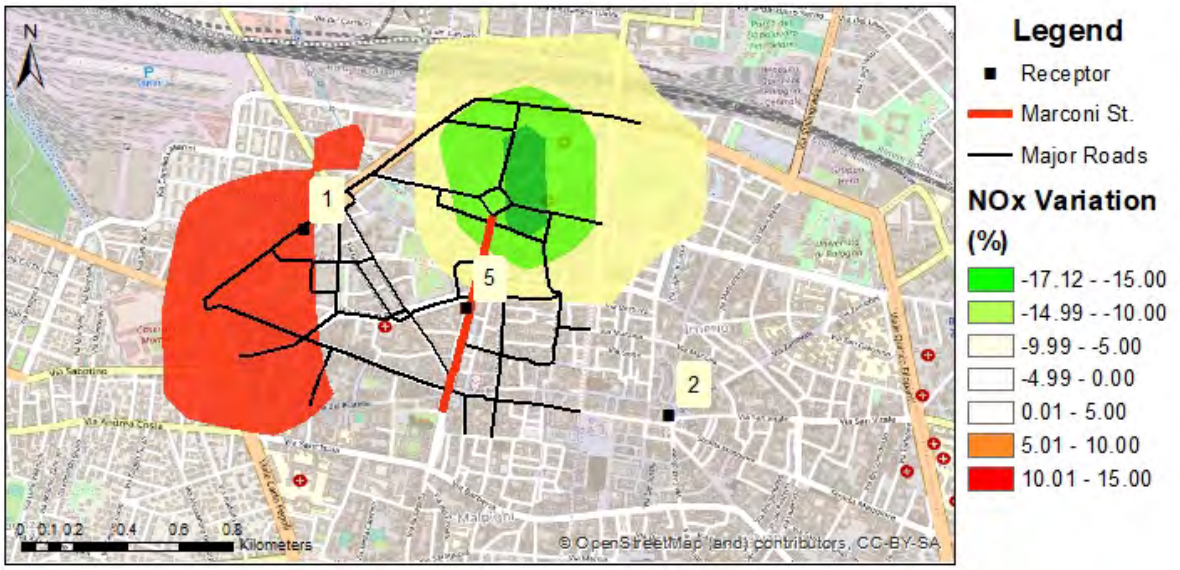

Figure 24. Maps of concentration variation for NO_x (summer 2050). The differences are calculated between the two scenarios with and without trees under future climate conditions (Future Case - Added Trees scenario and Future Case - Actual Trees scenario). The numbers indicate the position of the receptor sites: 1) Porta S. Felice Receptor; 5) ARPAE van receptor; 2) Asinelli Receptor

4.1.2 UHI simulations

As described in the methodology section, in the following we will present the evaluation of the performance in predicting the air temperature field in Bologna, followed by the results of the ADMS-TH model conducted in the current and future scenarios. Results are presented in the form of temperature maps obtained as output of long-term simulations of the ADMS-TH model.

4.1.2.1 Validation

Model performance was evaluated by comparing hourly temperature modelled values with measured ones. This comparison was carried out for three specific sites corresponding to the reference measurement stations of Bologna Urbana (BU), Asinelli (As) and Mezzolara (Mz). In Table 13 the statistical parameters for all reference stations are presented.

Station	Type	OBS mean + SD	MOD mean + SD	MB	NMSE	R	R^2	FA2	Fb
BU	Urban	27.4 ± 3.0	29.5 ± 3.2	2.11	0.01	0.99	0.77	1.00	0.07
AS	Urban	27.3 ± 3.1	28.8 ± 3.1	1.56	0.00	0.97	0.70	1.00	0.06
Mz	Rural	25.7 ± 2.6	27.9 ± 3.1	2.18	0.01	0.99	0.84	1.00	0.08

Table 13. Statistical analyses. Reference station: Bologna Urbana (BU), Asinelli (As), Mezzolara (Mz). Observed data (Obs), modelled data (Mod) (source: Original UNIBO elaboration for simulated values, Dext3r website for observations).

Overall, temperature values are well predicted (for more details see D.6.3 section 2.1.2.5) with FA2 results close to 1 showing good agreement between observed and modelled temperature values. The values of the fractional bias are very low (0.07 in BU station and in the range of 0.06 to 0.08), where the low positive values indicate the tendency of the simulations to a slight overestimation of temperature values. Also, R values close to 1, and R^2 values higher than 0.7 and even larger at Bologna Urbana and Mezzolara shows the good performance of the model simulations.

4.1.1.1 4.1.2.2 Base Case

The simulations of the ADMS-TH model in the current scenario, i.e. considering the actual land use and the hourly meteorological variables recorded by ARPAE stations during the summer 2017, have produced the following results in terms of temperature at 3m height level averaged over all meteorological conditions (Figure 25, base case – Actual Trees).

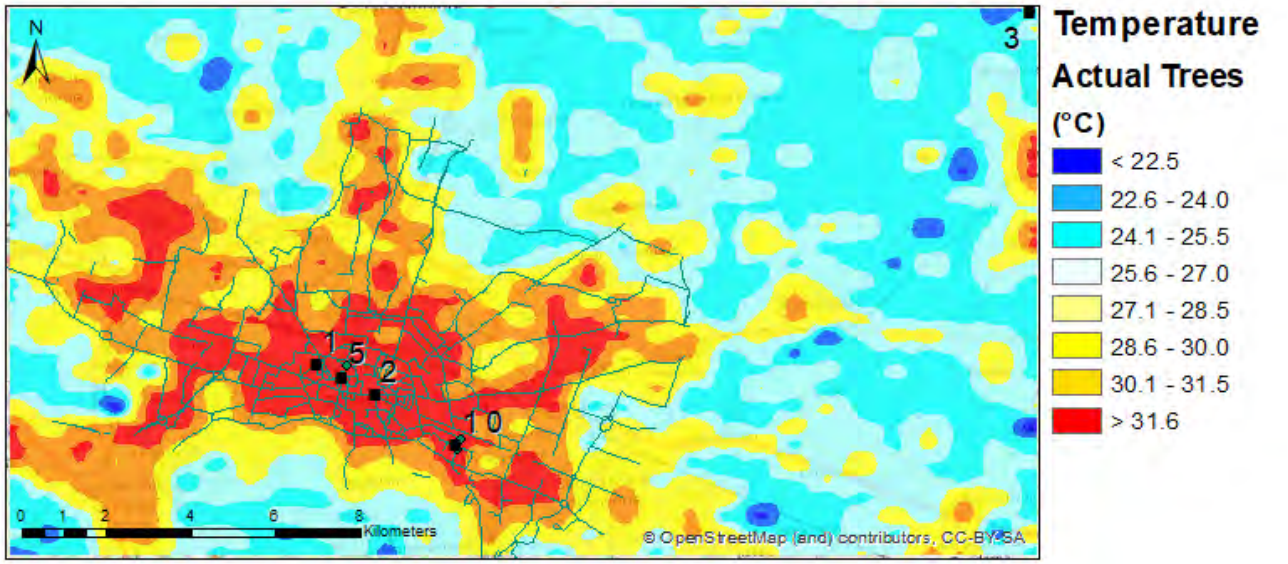

Figure 25. Maps of the temperature at a height of three meters, for Base Case –Actual Trees scenario. The location of the receptor sites is indicated with a number: 1) Bologna Urbana Receptor; 5) Marconi ARPAE van receptor; 2) Asinelli Receptor; 3) Mezzolara receptor; 10) Laura Bassi ARPAE van receptor.

The map clearly shows the urban heat island of Bologna, with higher temperatures in the city center compared with the surrounding rural areas. Following we present the temperature map obtained for the Base Case considering the GI intervention (Figure 26).

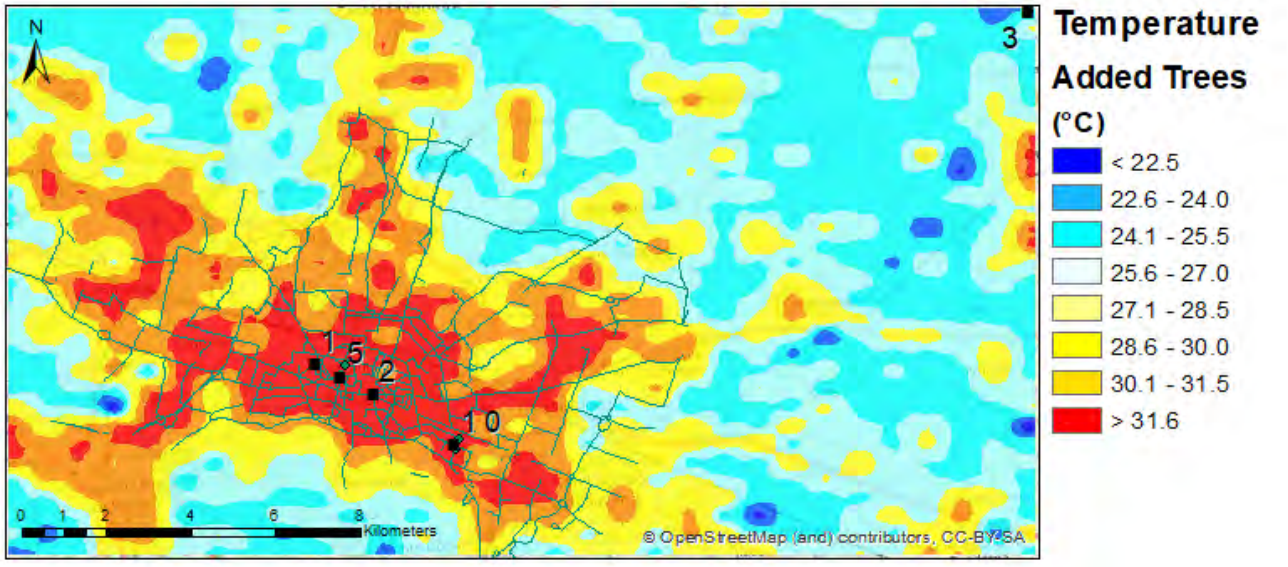

Figure 26. Maps of the temperature at a height of three meters, for Base Case –Added Trees scenario. The location of the receptor sites is indicated with a number: 1) Bologna Urbana Receptor; 5) Marconi ARPAE van receptor; 2) Asinelli Receptor; 3) Mezzolara receptor; 10) Laura Bassi ARPAE van receptor.

The spatial pattern of temperature distribution is substantially the same, but receptor values indicate a variation in the difference between urban and rural temperature.

In order to appreciate the differences between the two scenarios, the map of temperature differences is shown (Figure 27). The map shows how the introduction of trees over a small area can produce effects on the temperature observed even in the surrounding areas.

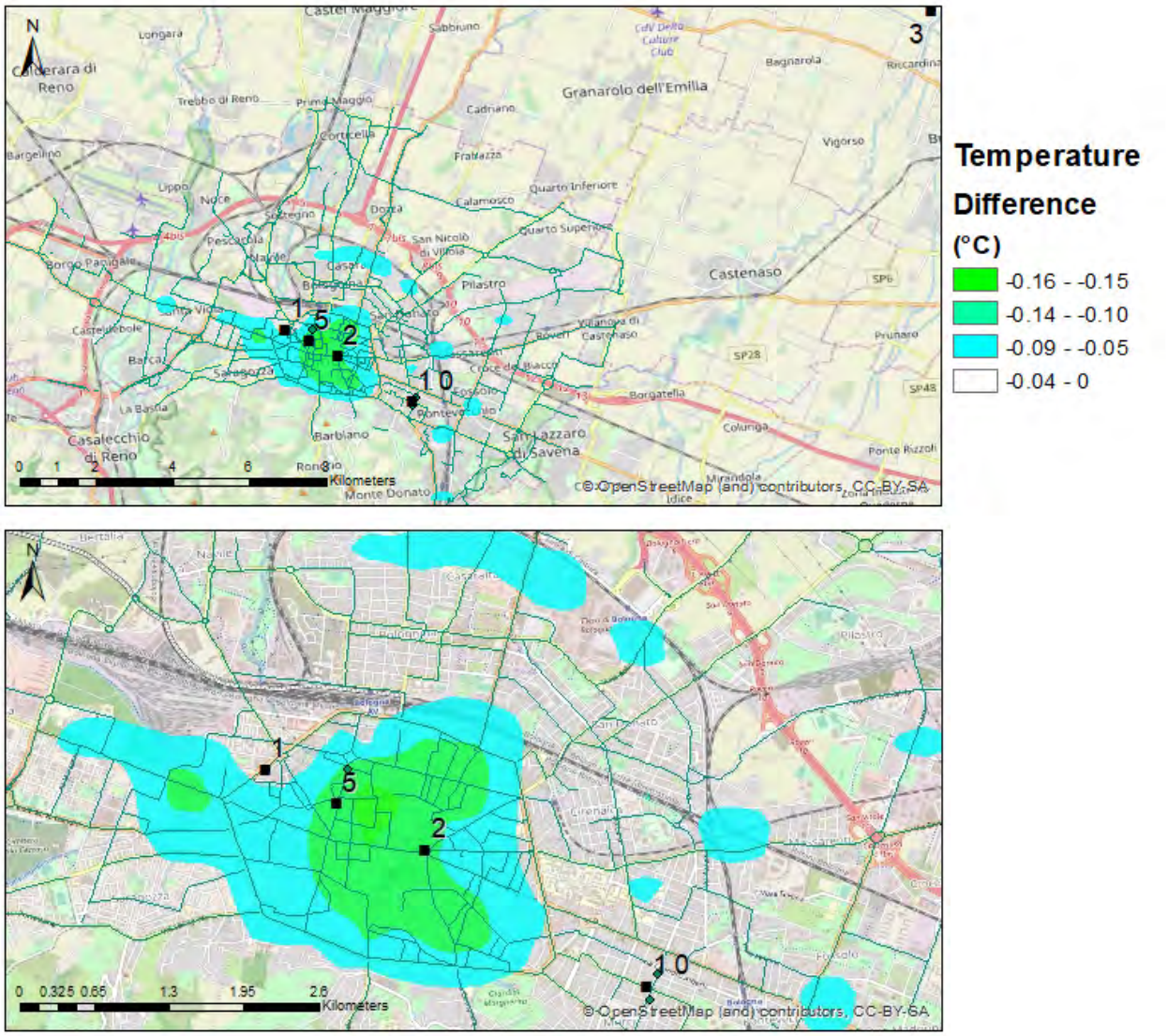

Figure 27. Difference of temperature between the Base Case - Actual Trees scenario and Base Case - Added Trees scenario (adding trees in the street canyon). Top: view of the entire domain, below: zoom on Marconi St., street canyon affected by GI intervention.

4.1.2.1 Future Case

This section shows the results of the simulations conducted in Bologna in the future climate conditions under the RCP8.5 emission scenario, the month of August 2050 was considered. As in the base case,

the results of the effect due to the presence (added trees) and the absence of trees (actual trees) are reported. The results are presented as temperature maps at 3m height level, averaged over all meteorological conditions, and temperature difference maps (added trees scenario map - actual trees scenario map).

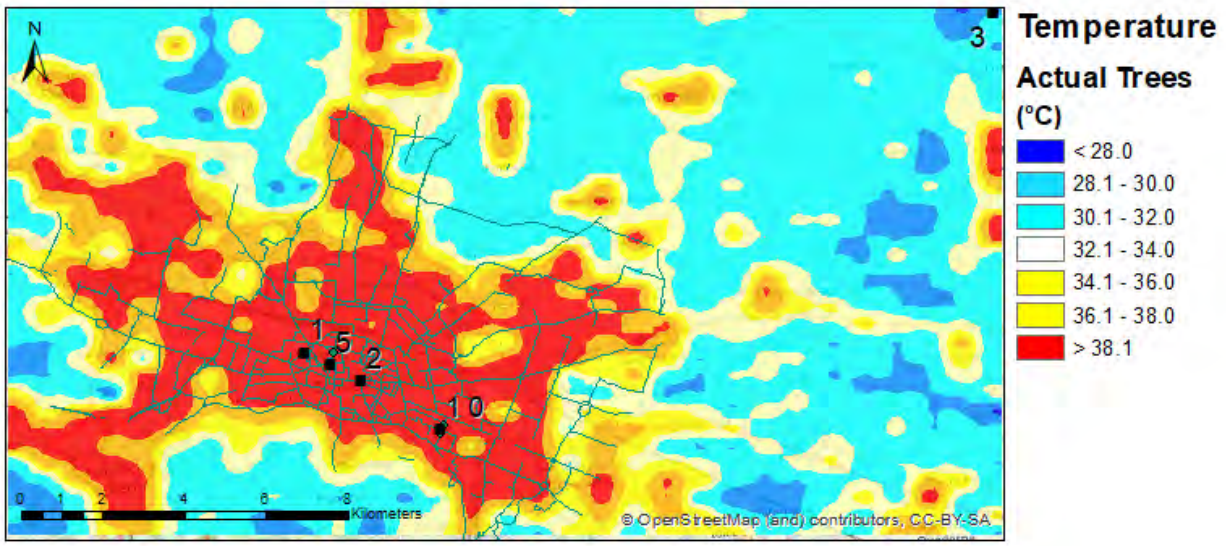

Figure 28. Maps of the temperature at a height of three meters, for Future Case –Actual Trees scenario. The location of the receptor sites is indicated with a number: 1) Bologna Urbana Receptor; 5) Marconi ARPAE van receptor; 2) Asinelli Receptor; 3) Mezzolara receptor; 10) Laura Bassi ARPAE van receptor.

The map shows, as in the base case, the urban heat island of Bologna, which tends to increase in the future as a result of climate change (22.5 - 31.6 °C for the Base Case and 28.0 - 38.1 °C for the Future Case respectively). The same spatial pattern is highlighted in the temperature map in the scenario considering the implementation the intervention planting deciduous trees in Marconi St. (Figure 29).

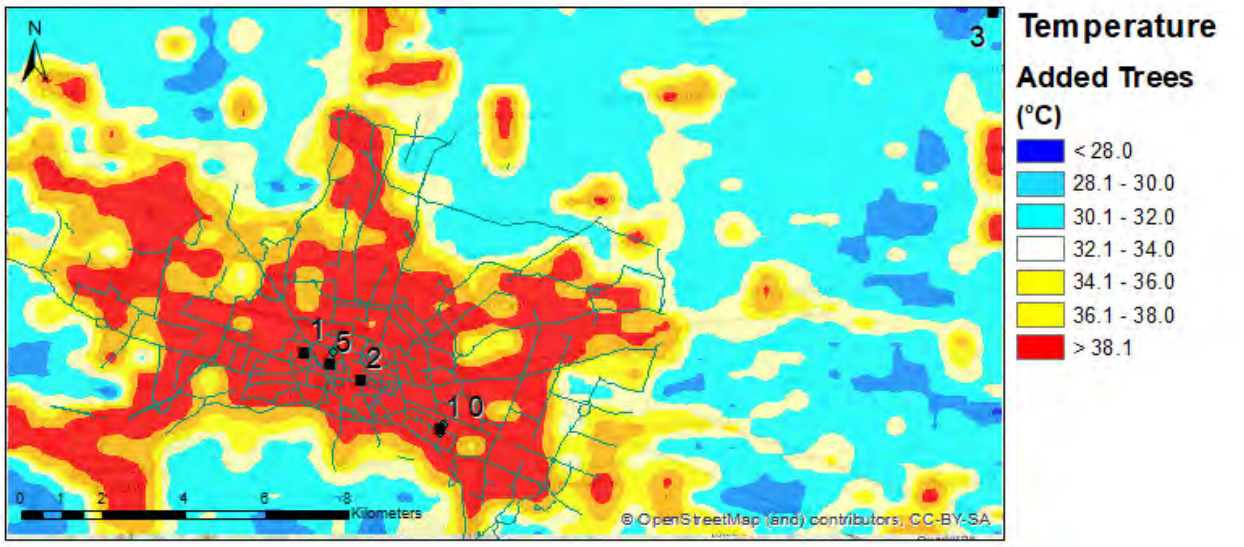

Figure 29. Maps of the temperature at a height of three meters, for Future Case – Added Trees scenario. The location of the receptor sites is indicated with a number: 1) Bologna Urbana Receptor; 5) Marconi ARPAE van receptor; 2) Asinelli Receptor; 3) Mezzolara receptor; 10) Laura Bassi ARPAE van receptor.

In order to appreciate the differences between the two scenarios, like in the base case, the map of temperature differences is shown. The map shows the same reduction values, with a slightly different pattern than in the Base Case; however also in this case we can observe how the introduction of trees over a small area potentially affects the temperature observed even in the surrounding areas.

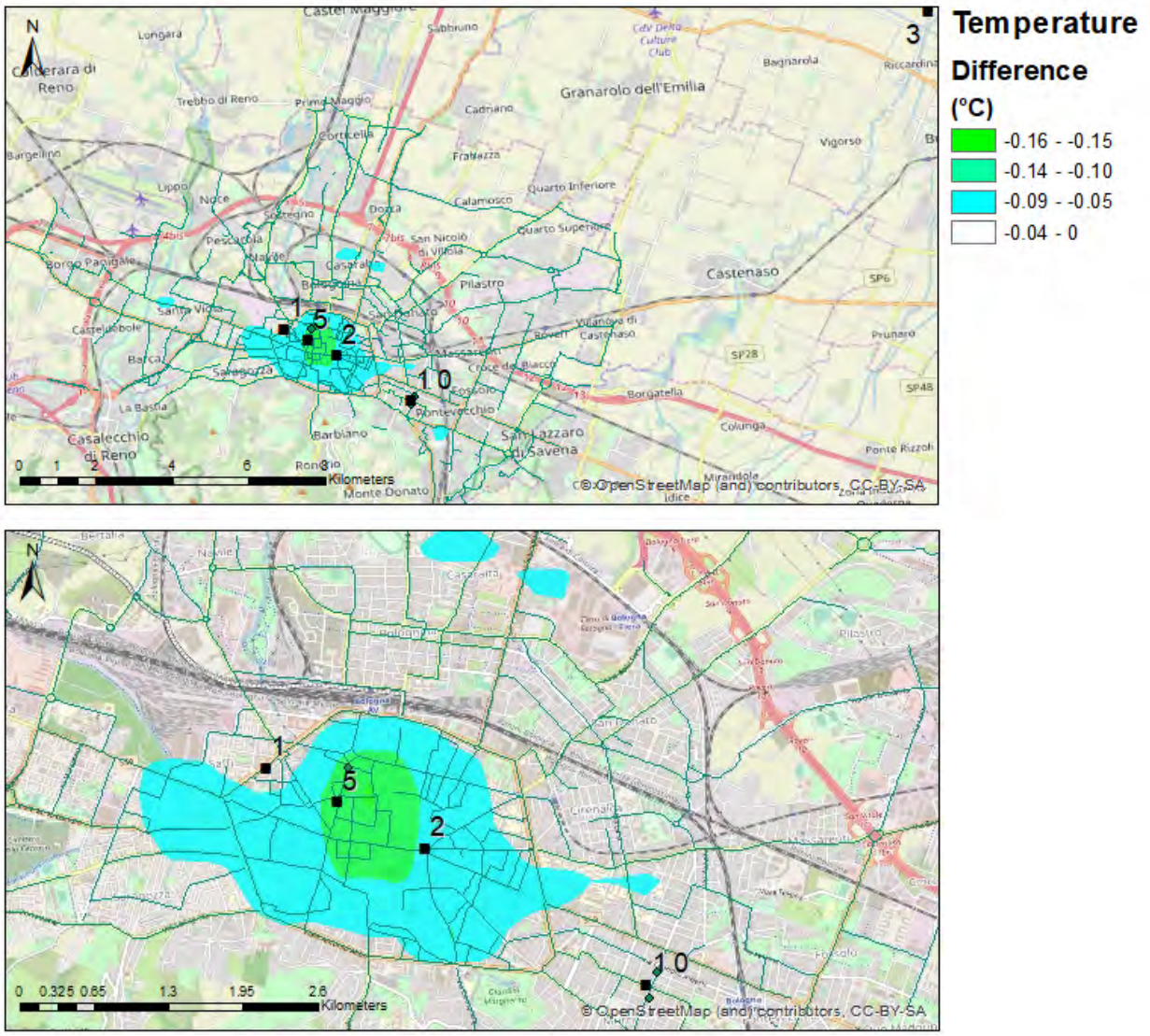

Figure 30. Difference of temperature between the Future Case - Actual Trees scenario and Future Case - Added Trees scenario (adding trees in the street canyon). Top: view of the entire domain, below: zoom on Marconi St., street canyon affected by GI intervention.

4.1.3 CFD simulations

As reported in the Methodology section, CFD simulations, whose setup was verified in D6.2 against the observations gathered within the two experimental campaigns in Bologna, were utilized to evaluate the impact of trees on ventilation in street canyons in D5.3. Here, we used the same setup using future meteorological conditions resulting from WRF high resolution numerical simulations.

The day cycles obtained from climatic projection in the future are shown in Table 14 for summer and in Table 15 for winter.

UTC – Local time	Wind direction (°) / Wind velocity (m s^{-1})	T air (°C)	T west (°C)	T east (°C)	T street (°C)
10-12	174°/0.95	31.6	55.1	48.4	46.9
12-14	122°/1.84	34.1	49.8	48.9	62.1
14-16	184°/1.47	34.2	48.4	58.4	51.6
16-18	220°/2.70	32.3	43.1	49.8	44. 6
18-20	221°/2.49	29.6	34.2	37.4	36.2
20-22	218°/2.09	27.92	29.2	30.6	30.4
22-00	221°/1.68	26.99	51.8	52.6	52.6
00-02	228°/1.20	26.32	47.9	48.8	48.6
02-04	223°/1.34	25.74	44.4	44.9	44.8
04-06	220°/0.98	25.17	40.9	41.3	41.4
06-08	317°/0.17	24.36	39.8	39.9	39.9
08-10	319°/0.35	26.93	47.0	44.4	47.3
10-12	182°/0.99	29.86	55.3	48.1	57.1

Table 14. Future summer day cycle as simulated by WRF high-resolution numerical simulations for Bologna.

UTC – Local time	Wind direction and velocity (m s^{-1})	T air (°C)	T west (°C)	T east (°C)	T street (°C)
11-12	299°-1.97	12.5	17.4	14.2	14.2
13-14	298°-1.64	13.6	15.8	16.2	14.3
15-16	324°-1.13	13.5	14.6	14.9	11.4
17-18	53°-0.95	11.9	12.5	12.3	9.5
19-20	123°-1.02	10.2	10.3	9.6	5.9
21-22	185°-0.45	10.0	10.7	9.9	6.6
23-00	206°-0.77	9.7	10.2	9.4	5.1
01-02	127°-0.70	9.6	10.2	9.4	6.9
03-04	120°-1.01	7.8	8.3	7.7	5.5
05-06	121°-1.13	7.0	8.0	7.3	5.0
07-08	190°-0.29	7.0	7.8	6.8	3. 7
09-10	306°-0.97	7.7	8.2	7.6	4.2
11-12	320°-0.96	10.6	15.6	10.9	6.2

Table 15. Future winter day cycle as simulated by WRF high-resolution numerical simulations for Bologna.

The wind direction and velocity and the air temperature have been extracted by WRF simulations, while the temperature on west and east sides of the buildings as well as the temperature on the street have been obtained by modelling the solar radiation heat transfer on the surfaces. CFD simulations were ran using the boundary conditions presented in Table 14 and Table 15, in order to evaluate the outputs considering two representative cases in summer and winter and compare them with what obtained under the present climate in the following section.

4.1.3.1 Future without trees

In this section, the pollution concentration and temperature distributions are obtained under the hypothesis that the geometry of buildings in Marconi street, a real urban street canyon in the middle of the city of Bologna will not be modified until 2050. As reported in D6.2, Marconi street is a four lanes limited traffic car zone, characterized by a considerable transit of buses (almost all bus lanes pass from this street). It is characterized by the presence of portici (arcades), which are not modelled in these simulations, and therefore also by high pedestrian traffic. Marconi street is almost completely free from trees, apart from the first part of the street. The street orientation compared to North-South direction is 20°. Riva di Reno street, in East-West direction in Figure 31, is a two lanes road characterized by intense cars and buses traffic.

Figure 31. Overview of Marconi street and surrounding area (left) and Marconi street canyon view (right).

As previously mentioned, the CFD simulations utilized here for a neighbourhood of the city of Bologna have been validated by comparing hourly values as obtained from the numerical simulations with the measurements performed during the two experimental campaigns described in D5.2 and D6.2. Pollutant emissions for the future climate scenario were kept the same as in the baseline simulations, for consistency with the RCP8.5 s("business-as-usual") cenario.

Figure 32 and Figure 33 show the comparison between the simulations and the experimental measurements for Marconi street during the summer campaign. Figure 32 shows the temperature and Figure 33 the CO concentration. As described in D6.2, instrumentation for measuring CO concentrations was located on the top of an ARPAE van located at ground level, while temperature, velocity and TKE were measured over a balcony 8 m high and 1 m distant from the building wall.

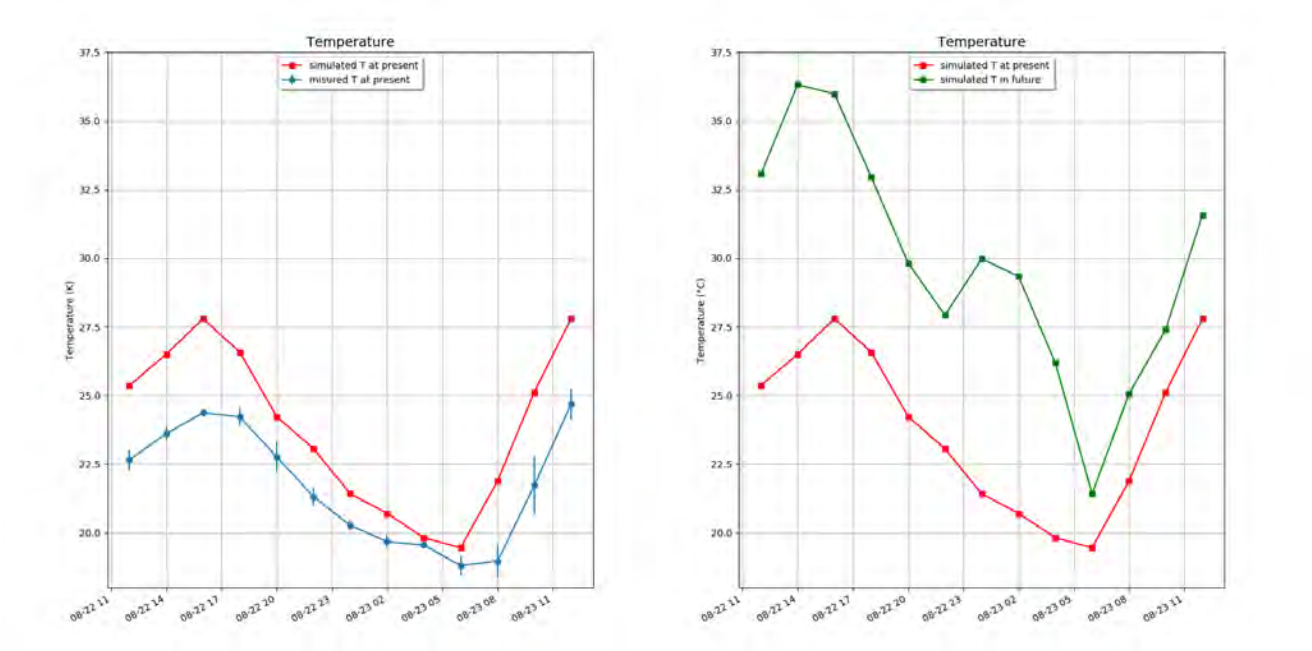

Figure 32. Marconi street, summer. Temperature obtained in the position where the ARPAE station was located. Left: comparison between numerical results (red) and experimental results (blue) under present meteorological conditions. Right: comparison between numerical results obtained under present (red) and under future climate conditions (green).

Figure 32 shows the comparison between the temperature obtained from CFD simulations and the measured temperature in the present (left); the Figure also shows the comparison between the outputs of the CFD simulations under future conditions with those obtained for the present.

The temperature increase obtained under future climate conditions ranges from 2 to 10°C, with a maximum during the afternoon and night hours. Table 14 shows that, during the future day cycle, the wind direction falls predominantly within the range 180°-220°, i.e. from South-South-West, while in the present the wind direction varies from 90° and 180°, i.e. mostly from East-South-East. Figure 32 also shows that local temperature within the canyon can be increased up to 10°C locally under future climate in summer.

The comparison between the CO concentrations obtained from CFD simulations and those measured in the present is shown in Figure 33 (left). The Figure also shows the comparison between CFD simulation obtained for the future conditions on those obtained for the present

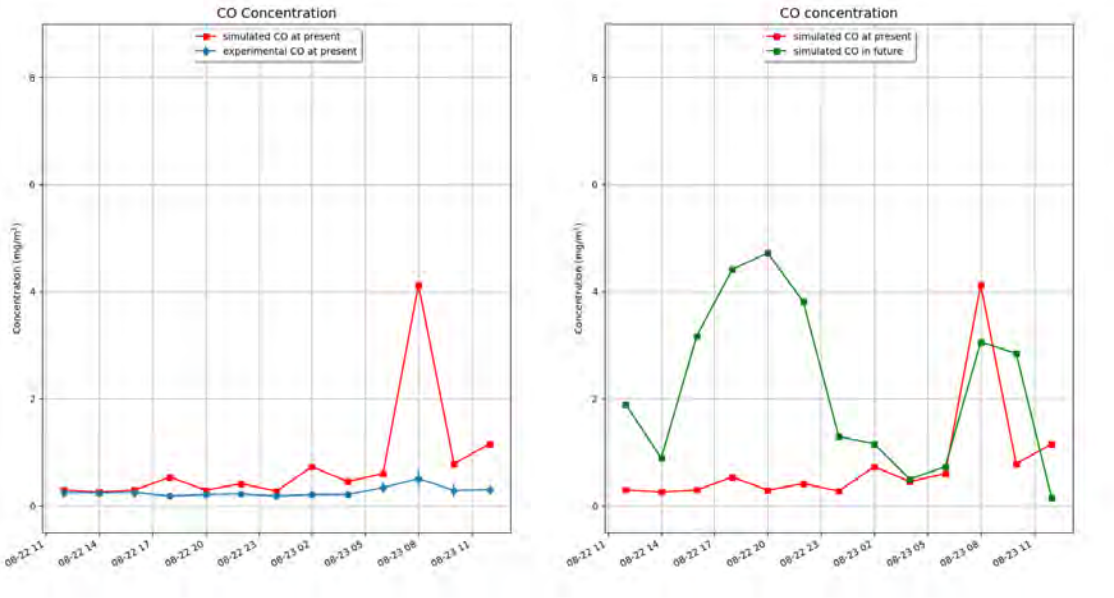

Figure 33. Marconi street, summer. CO concentration obtained in the position where the ARPAE station was located. Left: comparison between the numerical results (red) and experimental results (blue) under present meteorological conditions. Right: comparison between numerical results obtained under present (red) and under future climate conditions (green).

Figure 33 shows that a strong increase in the CO concentrations is obtained under future conditions during the afternoon and evening hours, i.e. when the wind direction is from South to South-West.

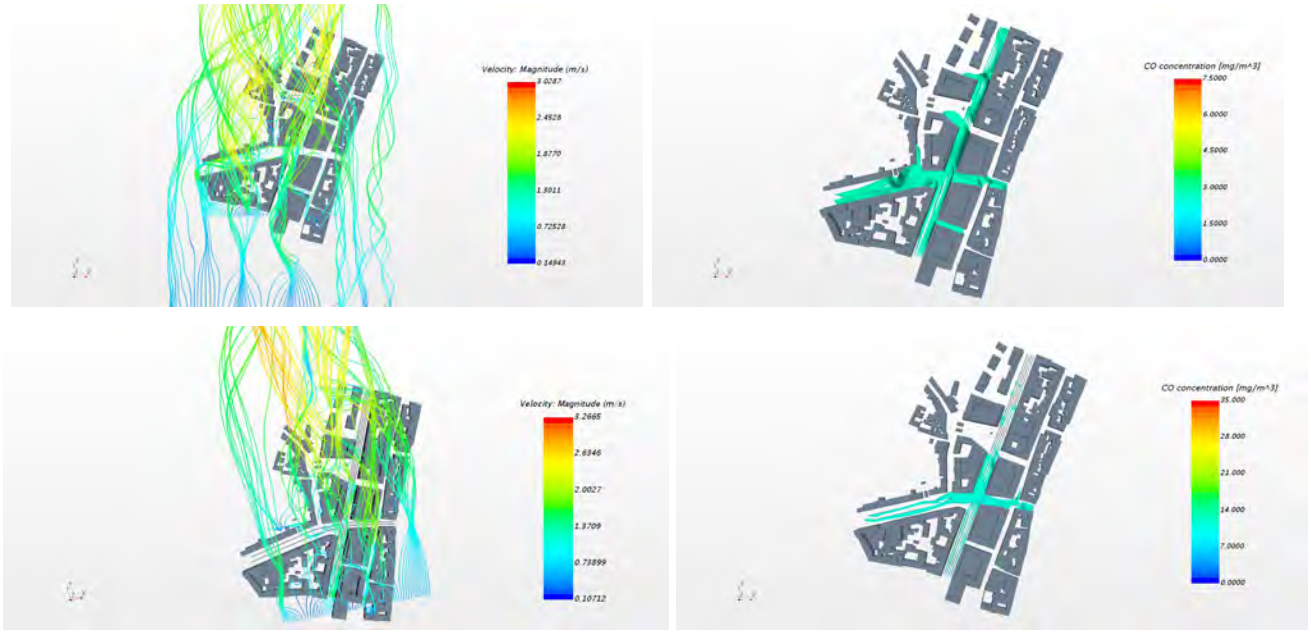

Figure 34: Future summer cases at UTC 10 (top) and UTC 14 (bottom) for Bologna, Marconi St. Streamlines (left) and CO concentration (right).

Figure 34 shows the streamlines and the CO concentrations obtained for the afternoon hours, for UTC 10 and UTC 14. In particular, the wind direction in the two cases is similar, as shown in Table 14 (174° and 184° respectively), but the wind velocity is higher in the second case. This difference in wind intensity results in similar streamlines in the northern part of Marconi street but different streamlines in the street perpendicular to the flow (Riva Reno street). In the first case (UTC 10), vortices are visible at the sides of the intersection, with different shapes with respect to the second case (UTC 14). As shown in Figure 35, this results in a different CO distribution on Riva Reno street, but a similar one on Marconi street.

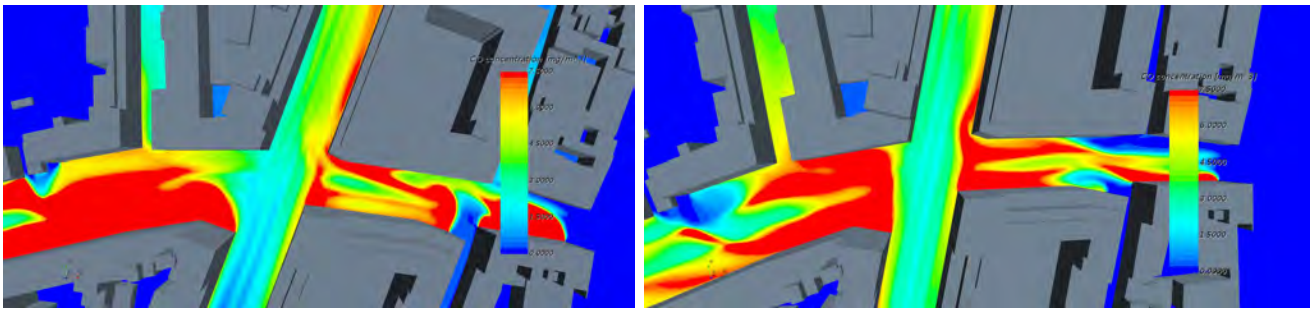

Figure 35: Future summer cases at UTC 10 (left) and at UTC 14 (right) for Bologna, Marconi St. CO concentration at 1.5 m height.

The results obtained in the time interval from UTC 16 to UTC 4 are quite similar, as the wind direction ranges from 218 º to 228 º, i.e. it is from South-West. For this reason, only the results obtained for UTC 16 is provided as representative of both cases.

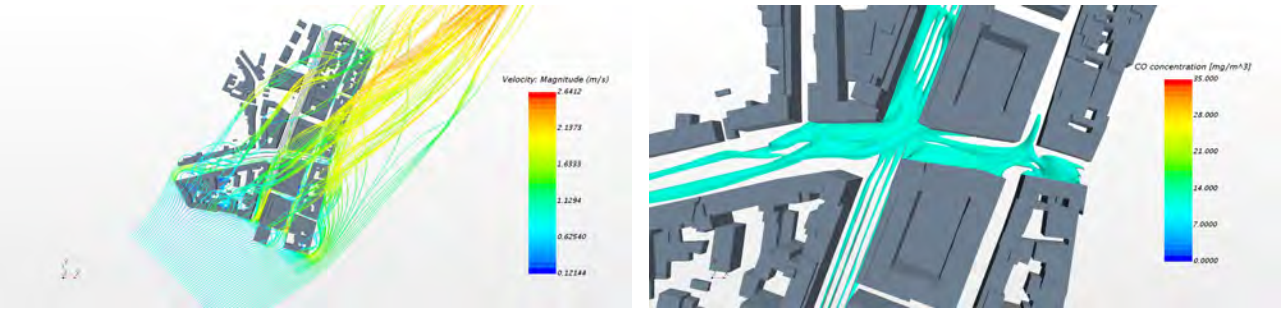

Figure 36: Future summer case, UTC 16, for Bologna, Marconi St. Streamlines (left) and CO concentration (right).

Figure 36 shows the streamlines and CO concentrations obtained for UTC 16. As reported in Table 14, the wind direction for this case is 220º. The streamlines show channelling flows both in Marconi street and in Riva Reno street, with some vortices in Riva Reno street with different shapes. As shown in Figure 37, CO concentration peaks on Riva Reno street can be observed in correspondence of the vortices.

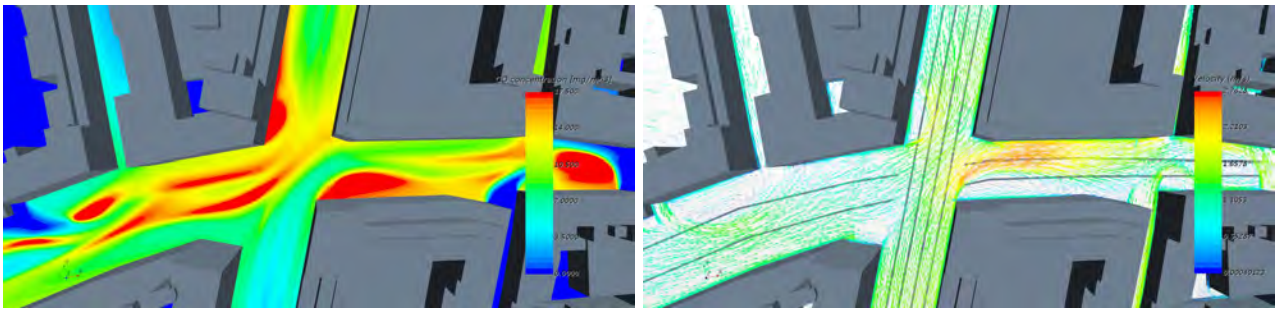

Figure 37: Future summer case, UTC 16, for Marconi St. in Bologna. CO concentration (left) and air velocity vectors (right).

A second CO concentration peak can be observed in Figure 32 at UTC 6 and UTC 8. Figure 38 shows the streamlines and CO concentrations obtained for the case of UTC 6 in future summer. As reported in Table 14, the wind direction for this case is 317º. The streamlines show vortices both in Riva Reno street and in Marconi street, as the wind direction is from North-west, i.e. it forms a 45º angle with both streets.

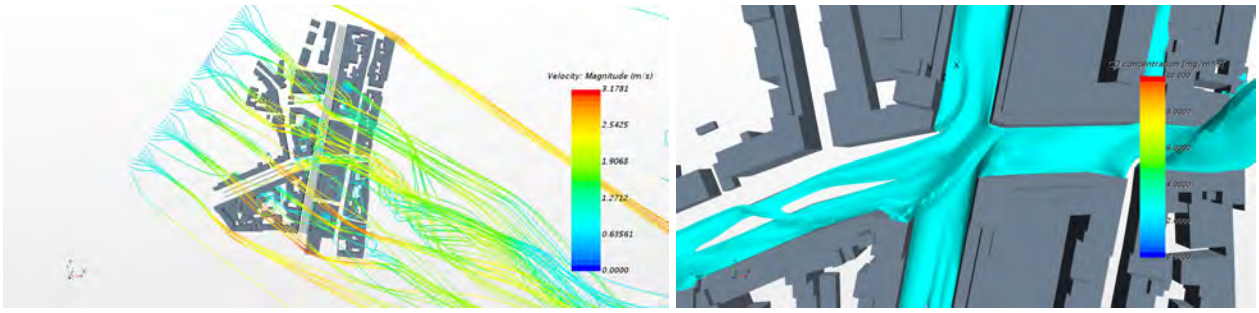

Figure 38: Future summer case, UTC 6, for Bologna, Marconi St. Streamlines (left) and CO concentration (right).

Most of the vortices are formed downstream the intersection, with different shapes. This results in some CO peaks on Marconi street near the intersection, as shown in Figure 39.

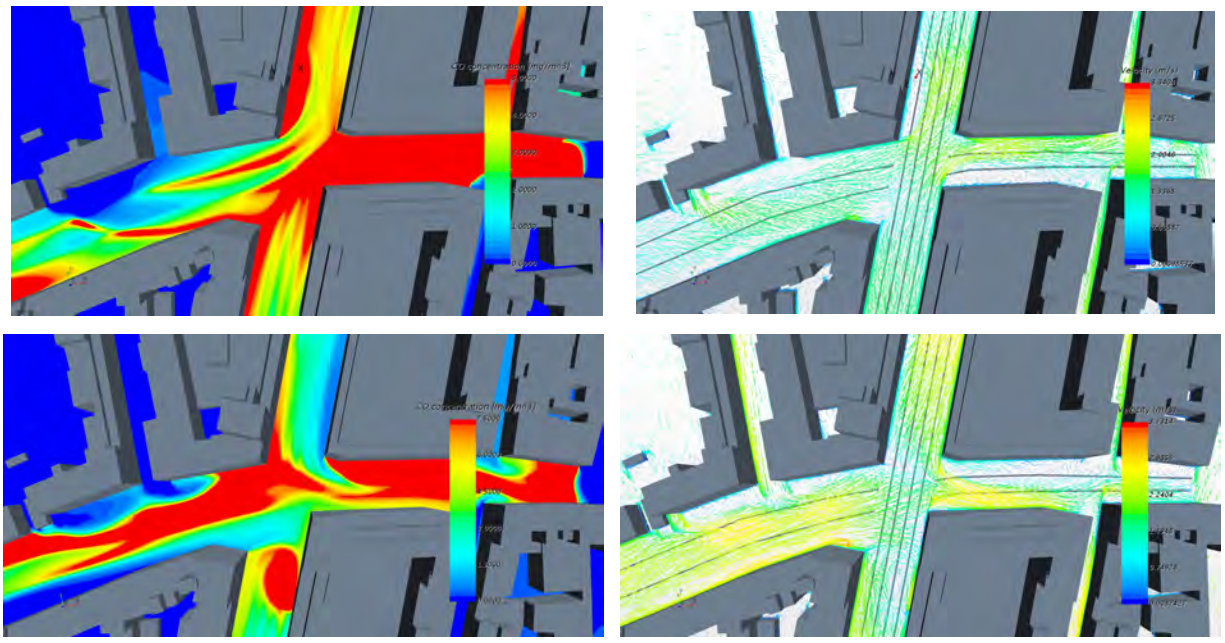

Figure 39: Future summer case for Marconi St., Bologna, UTC 6 (top) and UTC 8 (bottom). CO concentration (left) and air velocity vectors (right).

During winter, the wind configuration that characterises the two future summer cases UTC 6 and UTC 8 is verified twice, once in afternoon and once in the morning. Figure 40 shows the streamlines and CO concentrations obtained for the future winter case at UTC 13. As shown in Table 15, the wind direction for this case is 298º. The streamlines show channelling flows both in Marconi street and in Riva Reno street, with flow separation generated near the buildings' edges. As shown in Figure 41, high CO concentration gradients can be observed near the flow separation. This result is very different from that obtained under present winter conditions in winter, characterized by a wind direction in the range 75 º - 104 º.

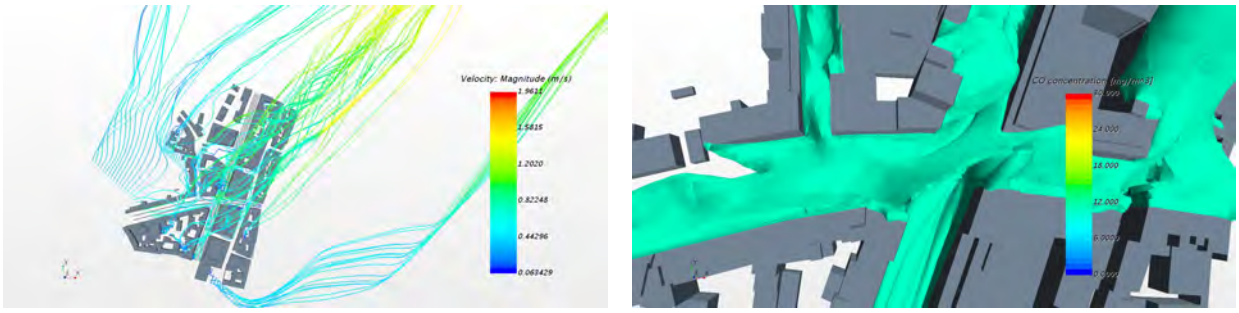

Figure 40: Future winter case, for Marconi St., Bologna, UTC 13. Streamlines (left) and CO concentration (right).

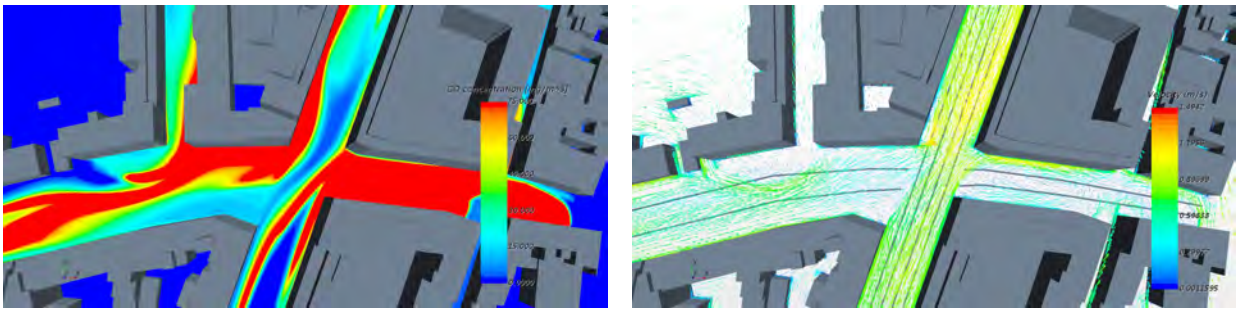

Figure 41: Future winter case for Marconi St., Bologna, UTC 13. CO concentration (left) and air velocity vectors (right).

To conclude this section, we extrapolate the pollutant distribution near a real traffic intersection (TI) in Bologna resulting under future climate. In particular, Table 16 shows the quantification of the increase of pollutant concentration at the sides of the TI.

Wind direction	Traffic	Recirculation vortices	Vortex width V_w/W	Vortex length V_l/W	Vortex height V_h/W	CO_{TI}/CO_p
Parallel	Peak	Both sides	1	>5	2.5	3.5
	Off-peak	Both sides	0.7	0.7	1.5	2.1
45º	Peak	Both sides	1	>5	2.7	3.8
	Off-peak	Both sides	0.7	0.7	1.7	2.5
Perpendicular	Peak	Both sides	1	>5	2.7	3.6
	Off-peak	Both sides	0.7	0.7	1.8	2.4

Table 16. Quantification of the increase in pollutant concentration at the side of the traffic intersection between Marconi and Riva di Reno St., considering different wind configurations.

The table displays the results for the area of influence of the TI in terms of the presence and dimensions of the recirculation vortices at the sides of the TI and the percentage difference in pollutant concentrations between TI and pathways along Marconi street (CO_{TI}/CO_p). The wind direction refers to

Marconi street, so that parallel means that the wind direction is parallel to Marconi street axis, 45º means that the angle between Marconi street and wind direction is 45º and perpendicular means that the wind direction is perpendicular to Marconi street axis. By comparing Table 16 with Table 20 in report D6.2, we can conclude that the presence of recirculation vortices at both sides of the TI for all the wind directions during peak traffic conditions will not change in the future. The pollutant concentrations on the TI sides are always higher than those corresponding to the pathways. The dimensions of the recirculation zones in the future are higher than those obtained for the present and with higher percentage differences in pollutant concentrations between TI peaks and pathways. On the basis of these observations, we can conclude that in the future the effects of pollution hotspots will be stronger near the intersections.

4.1.3.2 Future with trees

In this section, we analyse the results obtained under the future summer case at UTC 12, considering the insertion of "Populus tremula" tree in the middle of Marconi street canyon at a regular distance of 3.5 m. In this case the wind direction is 122° and the wind velocity is 1.84 m s^{-1}. The shape of the trees and Leaf Area Density (LAD) are shown in Table 17.

Populus tremula

Average height	Crown width	LAD
10.5 m	3.5 m	2.03 m^2 m^{-3}

Table 17: Characteristics of the Populus tremula tree species chosen for the planting tree scenario in Marconi street.

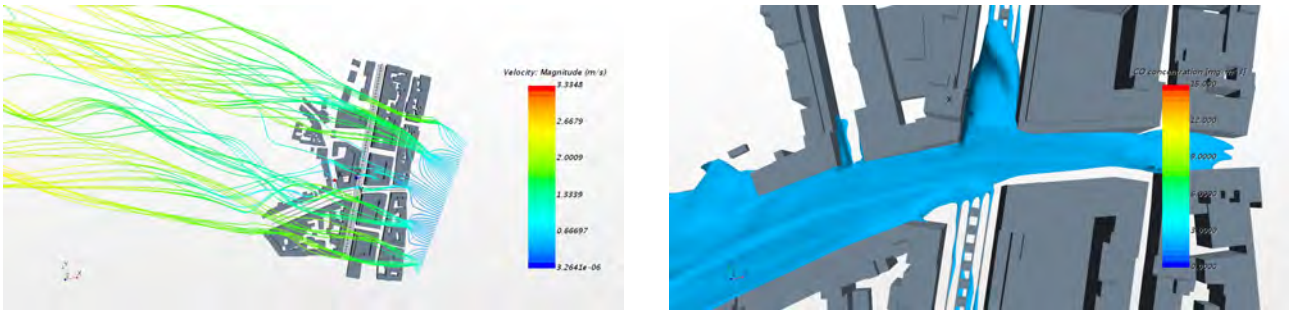

Figure 42: Future summer case for Marconi St., Bologna, at UTC 12, under a scenario of tree planting. Streamlines (top, left); CO concentration (top, right and bottom).

Figure 42 shows that the presence of trees inhibits the formation of recirculation vortices at the street intersection between Marconi and Riva Reno streets. Therefore, the CO concentration peaks are not

visible on the lateral sides of the intersection. Figure 43 presents the CO concentration and air velocity vectors obtained at 1.5 m height.

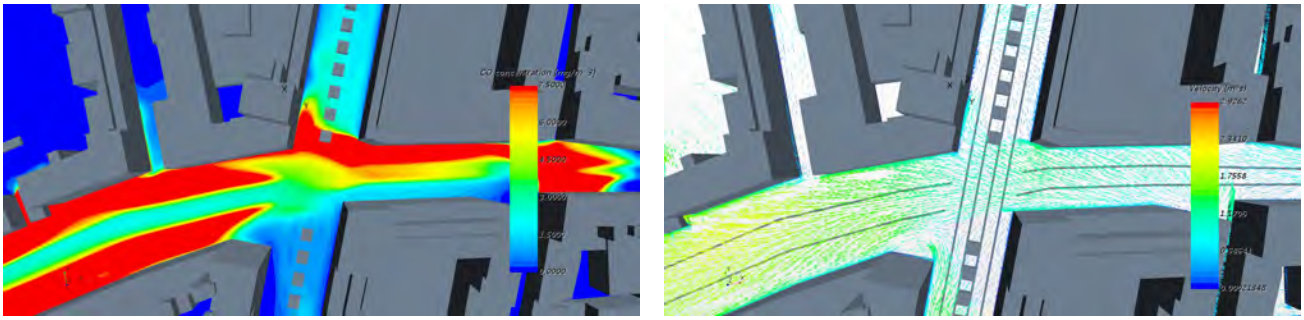

Figure 43: Future summer case for Marconi St., Bologna, UTC 12 ***with trees****. Velocity vectors (left); CO concentration (left).*

The vector map obtained for this scenario shows a main flow on Riva Reno street with secondary flows from the two sides of Marconi street, dragged by the main flow without the creation of vortices. The crowns positioned at the center of Marconi street inhibit the recirculation of air along Marconi street, while, as shown in Figure 44, in the absence of trees two CO concentration peaks are observed at both sides of the intersection.

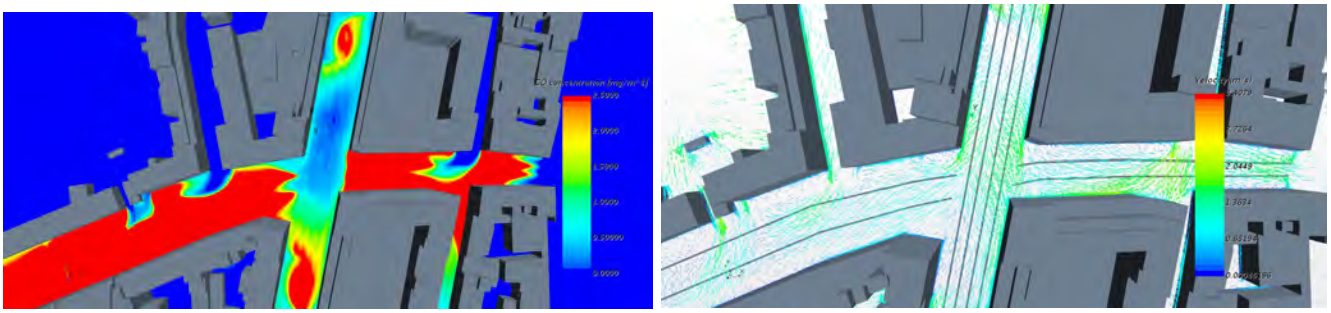

Figure 44: Future summer case for Marconi St., Bologna, UTC 12 ***without trees****. Velocity vectors (left); CO concentration (left).*

As done in D6.2 presenting the results of CFD simulations obtained under present meteorological conditions, Figure 45 reports the CO concentration obtained on a vertical plane section where the measurement station was located. The right side of Figure 45 shows the temperature distribution obtained on the same plane. CO is concentrated on the bottom-right part of the canyon, and in proximity of the higher CO concentrations, also higher temperatures are observed (bottom, left).

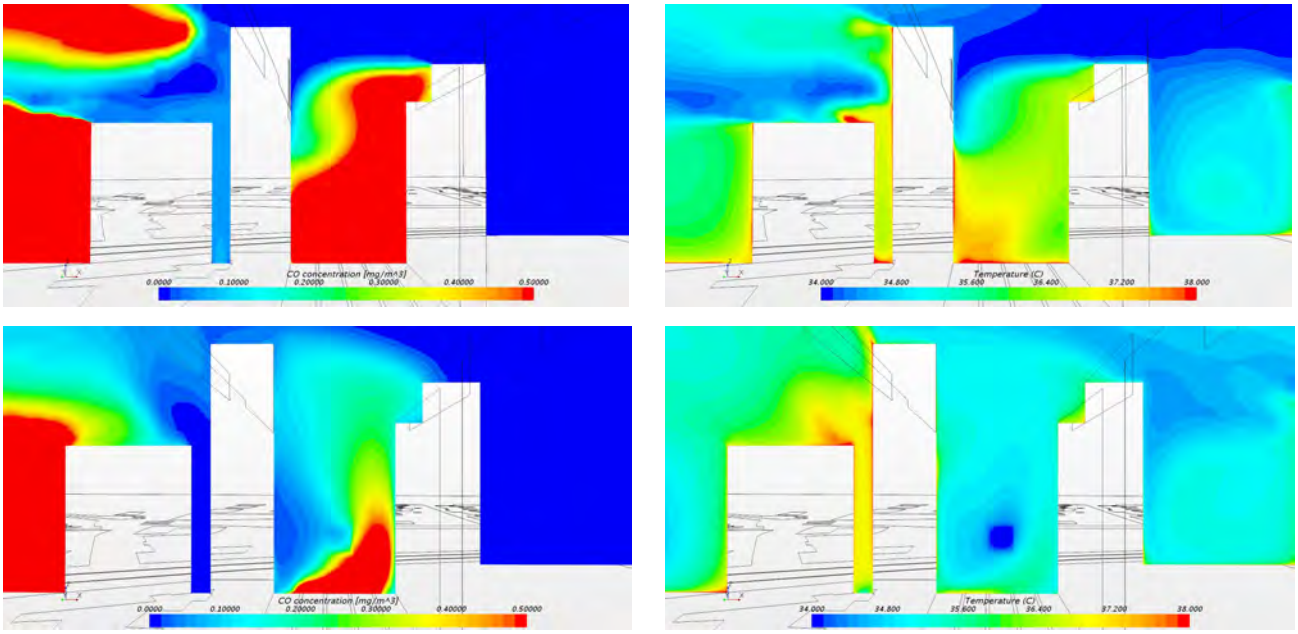

Figure 45: Comparison of CO concentration (left) and temperature (bottom) obtained for the future summer case in Marconi St., Bologna, at UTC 14, without (top) and with trees (bottom).

The Figure shows that in the scenario with trees both CO concentration and temperature are lower than those obtained for the case without trees.

We can conclude that the right choice of trees might be a win-win approach for contrasting climate change, with lower temperatures and lower pollutant concentrations within urban street canyons such as Marconi St. in Bologna.

4.2 Vantaa

In this section, we describe the results obtained with the methodology previously outlined for Vantaa, starting with the verification of the model setup and followed by the evaluation of the impact of the intervention on air quality and air temperature in the present and future climate conditions.

4.2.1 Present scenario

As previously described, dispersion model simulations for the present scenario in Vantaa were conducted using hourly meteorological observations gathered at the Vantaa airport in 2017, for a winter (January 2017) and for a summer month (July 2017) as input meteorological data to the dispersion model simulations. Those observations were complemented with an additional parameter, the surface roughness at the dispersion and meteorological sites, obtained as an output from the SURFEX high resolution simulations conducted by FMI. The use of real meteorological observations gathered at the

airport in a real year, enabled to verify the performance of the model setup in correctly predicting air pollutant concentrations in the base reference case in Tikkurila, while adding the surface roughness terms we were able to represent changes in the urban layout when considering the intervention scenarios.

Conversely, the analysis of the impact of urban layout on air temperature was analysed considering the output of the SURFEX model considering changes when altering the urban layout but forced with and the same atmospheric forcing generated as an artificial test year representing the past recent climate.

4.2.1.1 Validation

As reported in Section 3, the statistical evaluation of the performance of the ADMS-Urban model was carried out comparing graphically simulated pollutant concentrations with measured values in the Tikkurila air quality station (managed by HSY Helsinki Region Environmental Services Authority) and calculating some statistical parameters previously presented, considering one winter and one summer month (January and July 2017).

Figure 46 and Figure 47 present the comparison of hourly simulated and observed concentrations at the Vantaa Tikkurila air quality station for the two months considered. The comparison was carried out only for pollutants measured in the Tikkurila air quality station, i.e. NO_2 and $PM_{2.5}$.

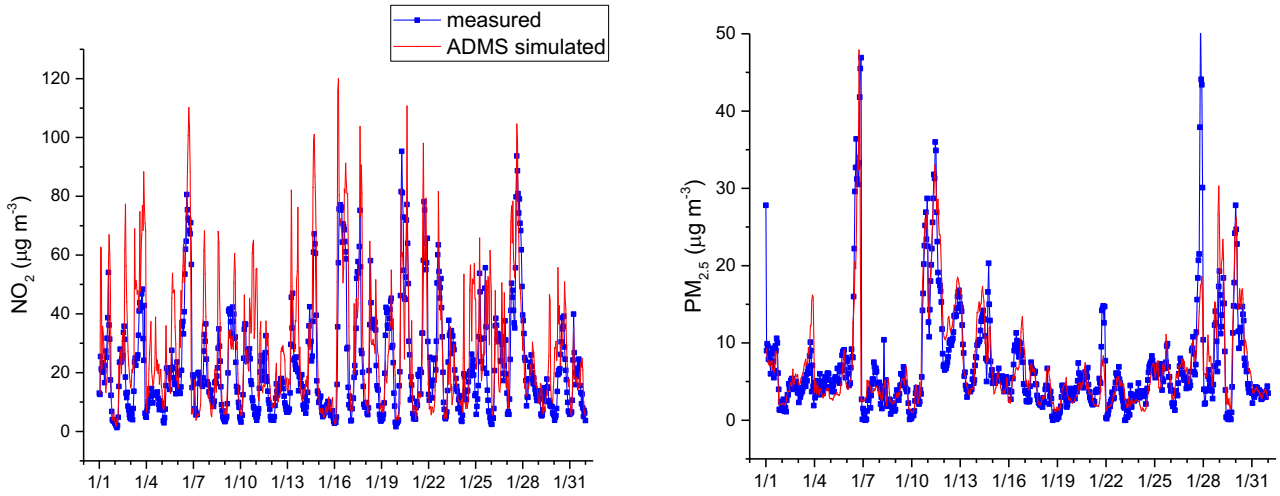

Figure 46. Comparison of hourly observed and simulated NO_2 and $PM_{2.5}$ concentrations at the Vantaa air quality station of Tikkurila in January 2017.

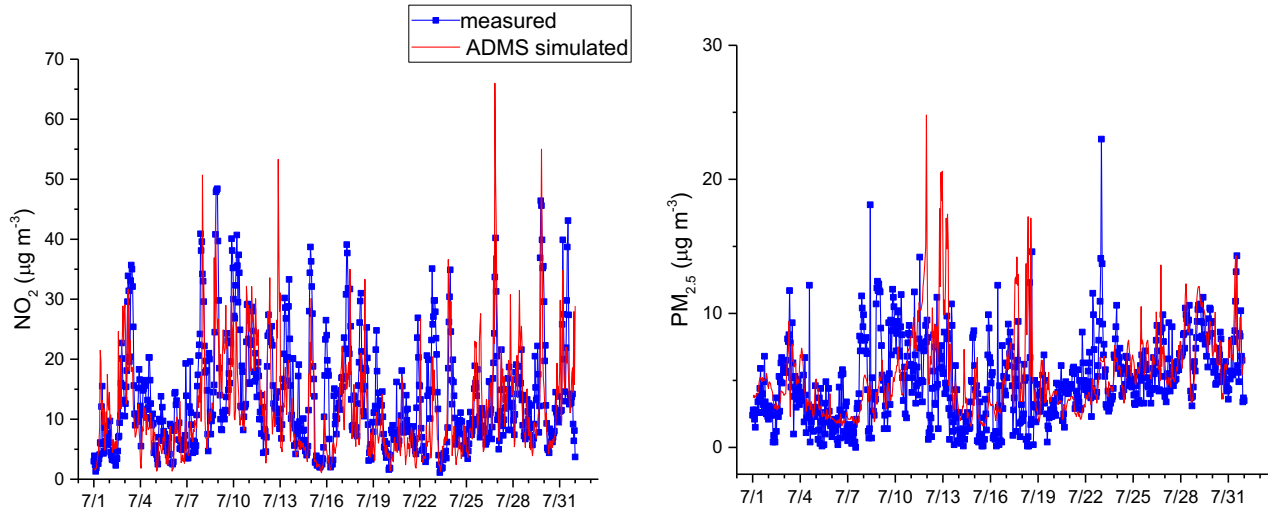

Figure 47. Comparison of hourly observed and simulated NO_2 and $PM_{2.5}$ concentrations at the Vantaa air quality station of Tikkurila in July 2017.

Figure 46 and Figure 47 show that the model represents correctly the overall pattern of $PM_{2.5}$ concentrations especially in the winter period, while the summer pattern is caught less well in the simulations. For NO_2, the reverse seems to hold, though the general simulated pattern is consistent with observations in both moths. In addition, simulated NO_2 concentrations present a general tendency to be overestimated, which may result from incorrect and too high local NO_2 emissions.

Statistical parameters for the ADMS model simulations of NO_2 and $PM_{2.5}$ concentrations are reported in Table 18 and generally indicate a good performance of the dispersion simulations for Tikkurila: FA2 results show good agreement between observed and simulated concentrations, R correlation coefficients are in the range 0.64-0.90 (respectively for $PM_{2.5}$ in summer and winter), the normalized mean square error is low for all the pollutants, while the values of the fractional bias indicate a slight overestimation of NO_2 during winter and a slight underestimation of NO_2 during summer. This difference between the summer and winter case seems to indicate, more than a problem with NO_x emissions and/or NO_x treatment in the ADMS-Urban, an issue with the NO_x chemistry module, possibly resulting from solar radiation values used as input data, which in the absence of O_3 local observations cannot be further elucidated.

Month	Pollutant	Mean ± SD		NMSE	R	R^2	FA2	Fb
		Modelled	Observed					
Jan-17	NO_2	29.1 ± 12.3	22.6 ± 10.2	0.13	0.84	0.70	0.97	0.25
Jan-17	$PM_{2.5}$	7.1 ± 4.6	6.9 ± 4.5	0.08	0.90	0.82	1.00	0.03
Jul-17	NO_2	11.9 ± 4.9	13.5 ± 4.6	0.09	0.73	0.50	0.97	-0.13
Jul-17	$PM_{2.5}$	5.5 ± 2.3	5.0 ± 1.7	0.13	0.64	0.40	0.97	0.09

Table 18. Statistics of daily observed and modelled NO_2 and $PM_{2.5}$ concentrations ($\mu g/m^3$) in Vantaa Tikkurila air quality station in the months of January and July 2017.

Figure 48 and Figure 49 represent the comparison of the weekly and diurnal pattern of observed and simulated NO_2 and $PM_{2.5}$ concentrations in Tikkurila air quality station. The Figures clearly indicate that the model represents correctly diurnal patterns of observed concentrations, particularly so in winter whereas the summer weekly pattern present some biases though on average is also in agreement with the observations. In most cases and in both months the simulated NO_2 and $PM_{2.5}$ patterns fall in the 95% confidence intervals around the mean, suggesting that the biases of simulated values are within the standard deviations of observed values. As such, the comparison between simulated and measured concentrations suggests the reasonableness of time-varying emission factors utilized in the dispersion simulations.

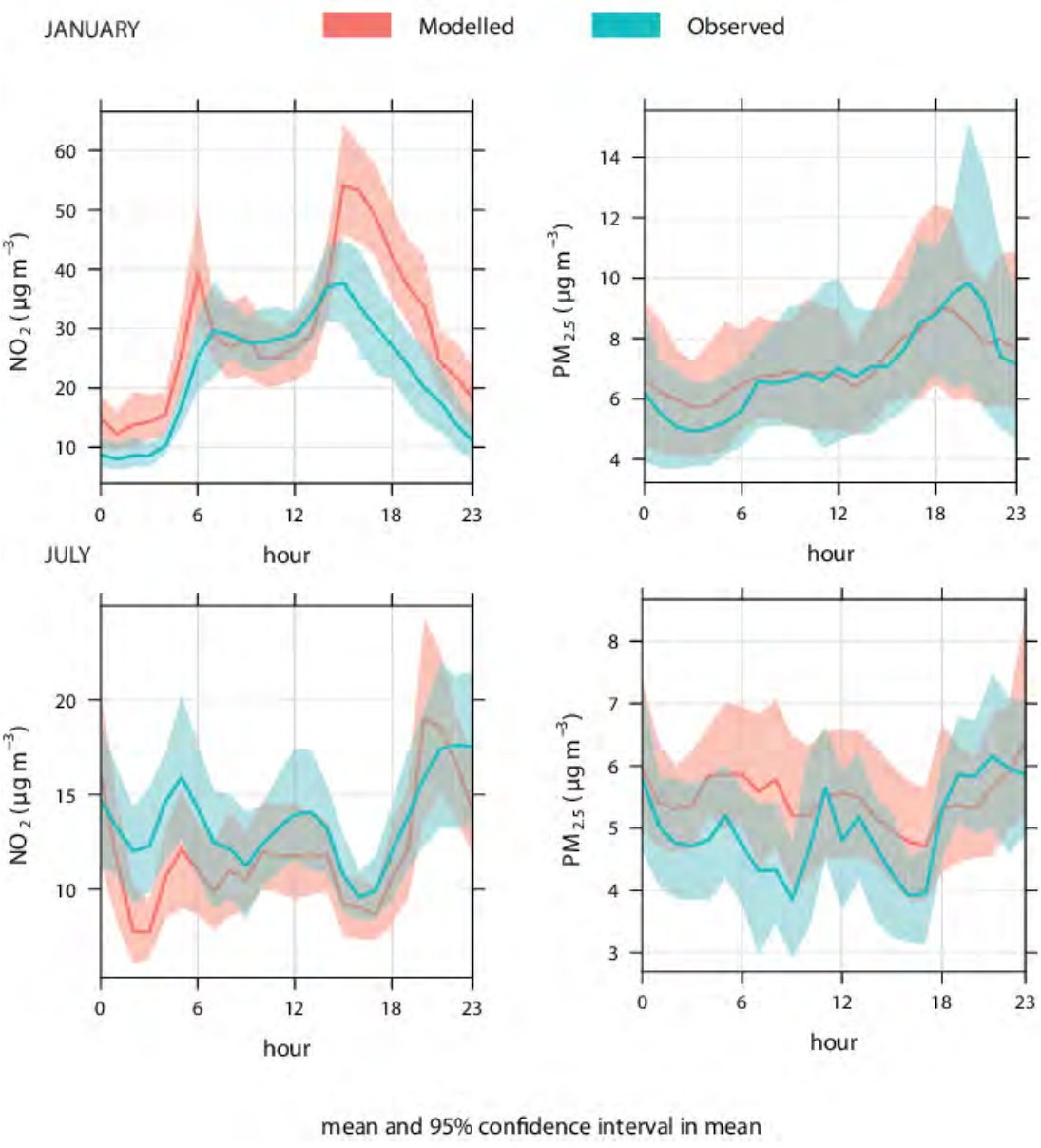

Figure 48. Mean measured and simulated diurnal patterns for NO_2 and $PM_{2.5}$ concentrations in the months of January and July 2017 in Vantaa Tikkurila air quality station.

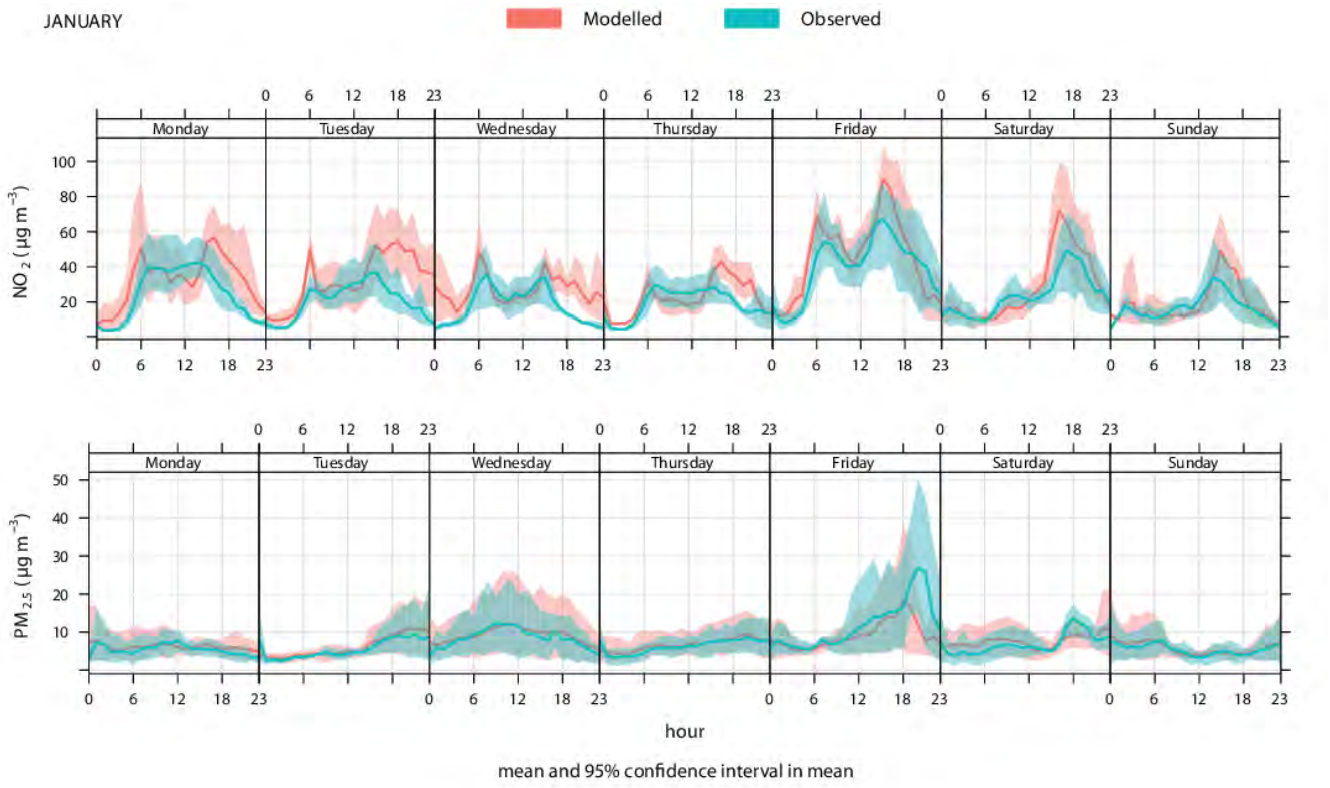

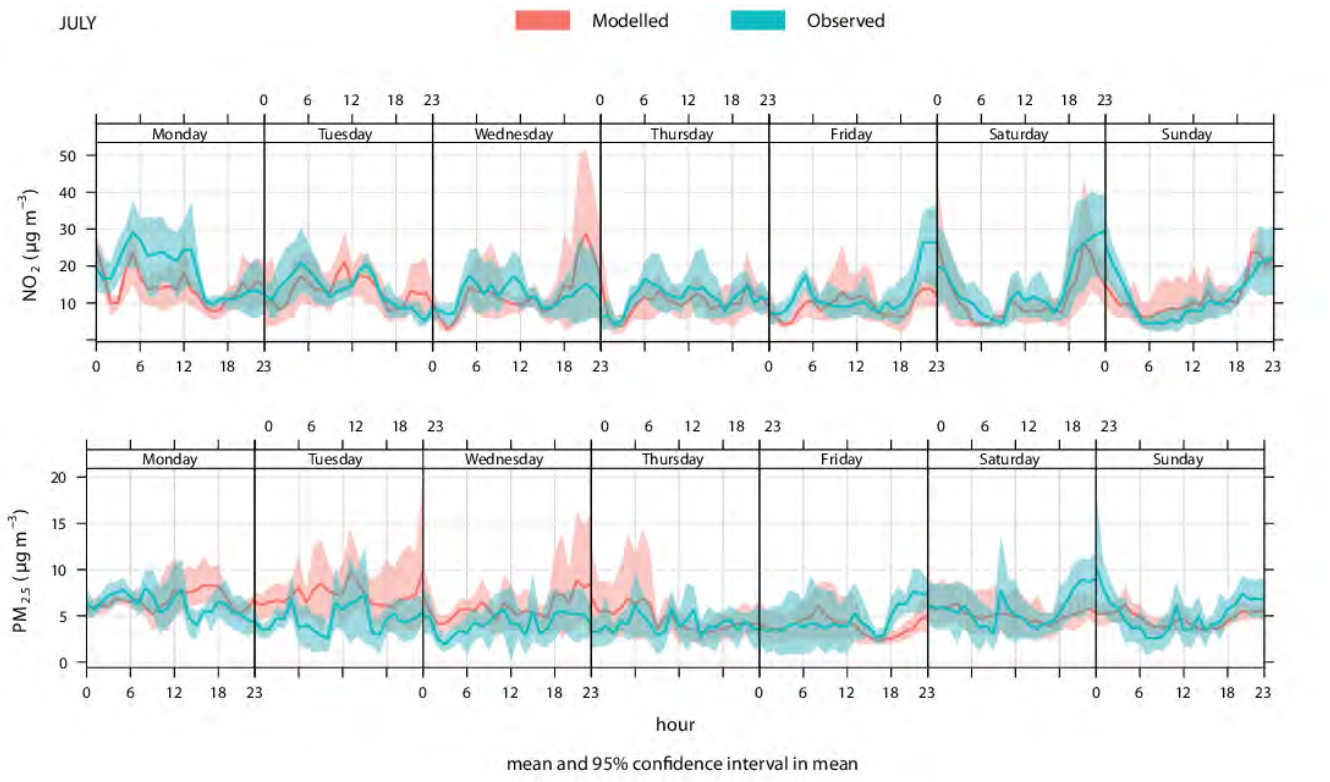

Figure 49. Mean measured and simulated weekly diurnal patterns for NO_2 and $PM_{2.5}$ concentrations in the months of January and July 2017 in Vantaa Tikkurila air quality station.

4.2.1.2 Effects of vegetation on air quality

In the following, we present first of all the results of long-term simulations conducted for the baseline reference case in the present climate conditions (January and July 2017), previously verified against observed pollutant concentrations at the Tikkurila air quality station.

As reported in D4.5, in Vantaa both NO_2 (Figure 50) and $PM_{2.5}$ (Figure 51) show reduced concentrations in January. Areas of local enhanced pollutant concentrations are situated in proximity of major roads, even though concentrations are comparatively low with respect to other European cities like Bologna previously presented. Concentrations tend to reduce towards the outer region of the simulation domain, and in case of $PM_{2.5}$ the external western border seems to be characterized by lower concentrations than the eastern one. This result might depend on the wind rose of the period, dominated by W and SW winds (Figure 52). The wind rose of the period indeed causes the appearance of a plume of NO_2 and $PM_{2.5}$ extending to the NE of the simulation domain.

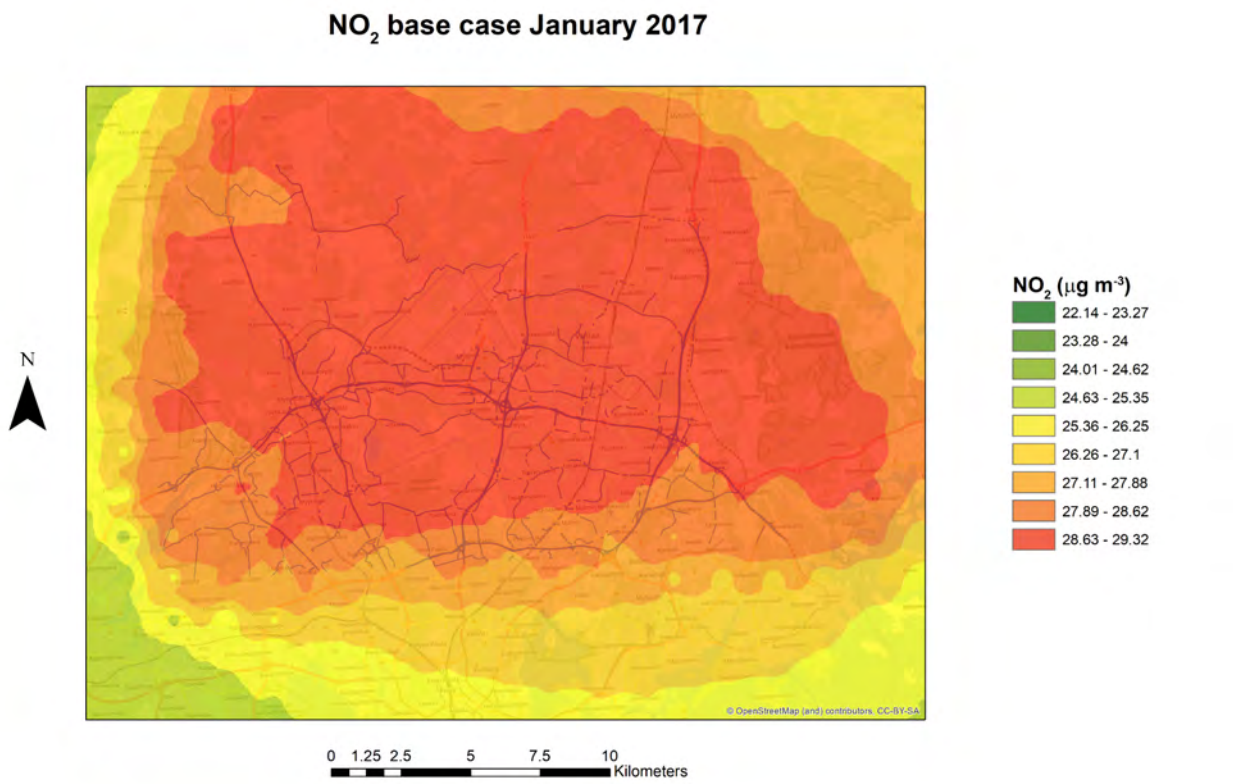

Figure 50. NO_2 concentration map for the Vantaa present reference scenario (January 2017 mean). Also shown are the major roads considered in the simulations.

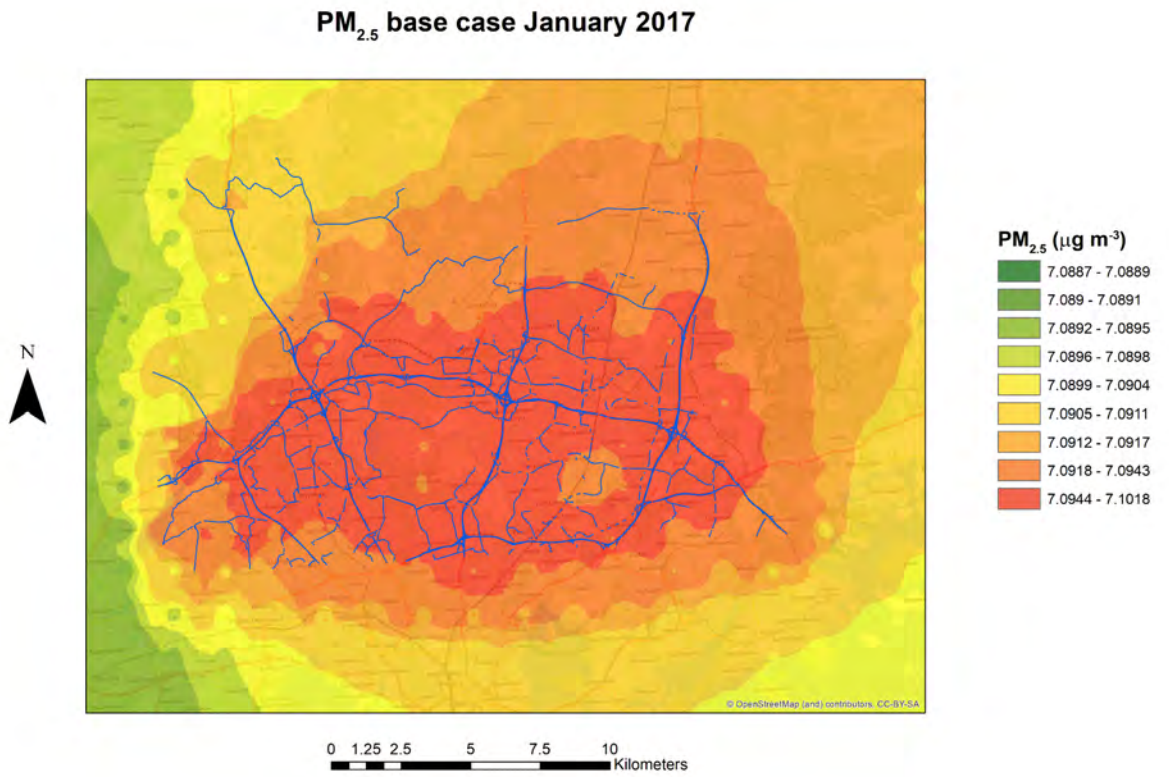

Figure 51. $PM_{2.5}$ concentration map for the Vantaa present reference scenario (January 2017 mean). Also shown are the major roads considered in the simulations.

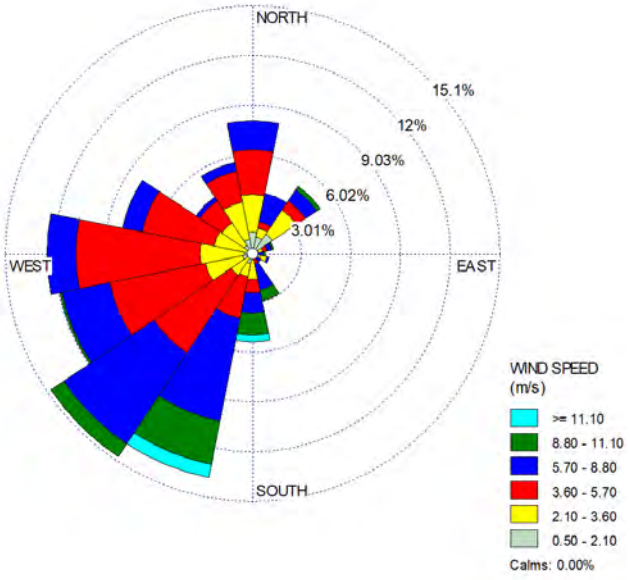

Figure 52. Wind rose for January 2017 in Vantaa.

Figure 53, Figure 54 and Figure 55 present the outputs of long-term simulations for NO_2, $PM_{2.5}$ and O_3 concentrations. Even though O_3 concentrations were not validated against observations, the dispersion pattern of this secondary pollutant was analysed in particular to compare its concentrations in the base case to that of the intervention scenario. NO_2 and $PM_{2.5}$ concentrations are even lower than those simulated in the winter case, as due to the contribution to photochemical reactions leading to formation of O3 during summer under the influence of solar radiation in the case of NO_2, and to enhanced nucleation in cold winter conditions for $PM_{2.5}$ (Pakkanen et al., 2006). In the summer case, while NO_2 present comparatively reduced concentrations in the south-western part of the simulation domain, PM2.5 presents localized lower concentrations even in the southeastern border and a local hotspot towards the northern part; this pattern, besides emissions, is likely caused by the wind rose of July 2017 (Figure 56), characterized by winds with similar intensities to the winter month, but from NW and SW quadrants, while N and S were less frequently observed during the simulation period.

O_3 shows, as expected, a complementary dispersion map to NO_2, with minima in the city centre where ozone quickly reacts with NO in the vicinity of NO_x emissions and higher levels in the simulation borders far away from NO_x traffic sources where NO levels are low and O_3 locally produced or therein transported is not removed efficiently (e.g., Hagenbjörk et al., 2017).

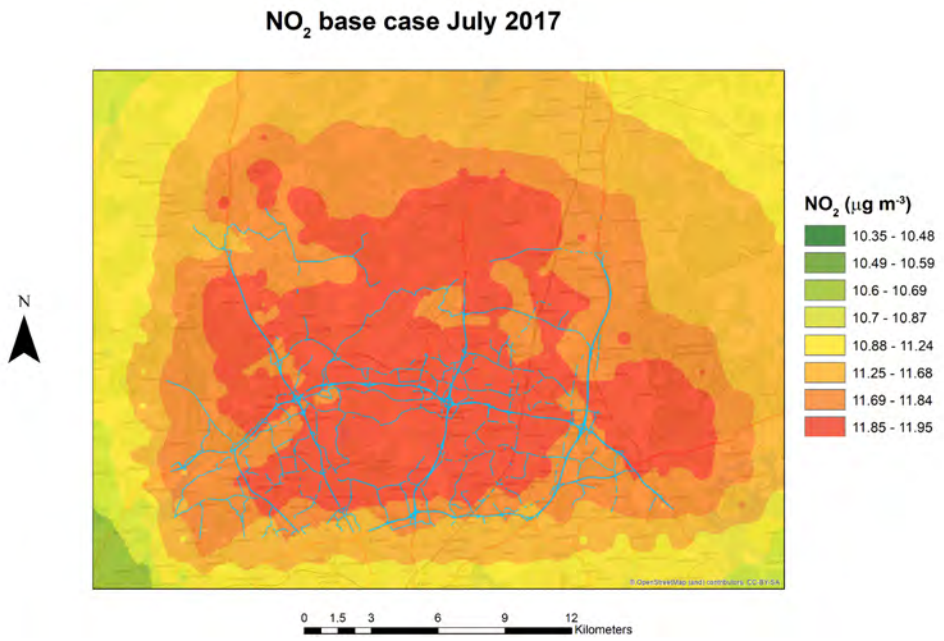

Figure 53. NO_2 concentration map for the Vantaa present reference scenario (July 2017 mean). Also shown are the major roads considered in the simulations.

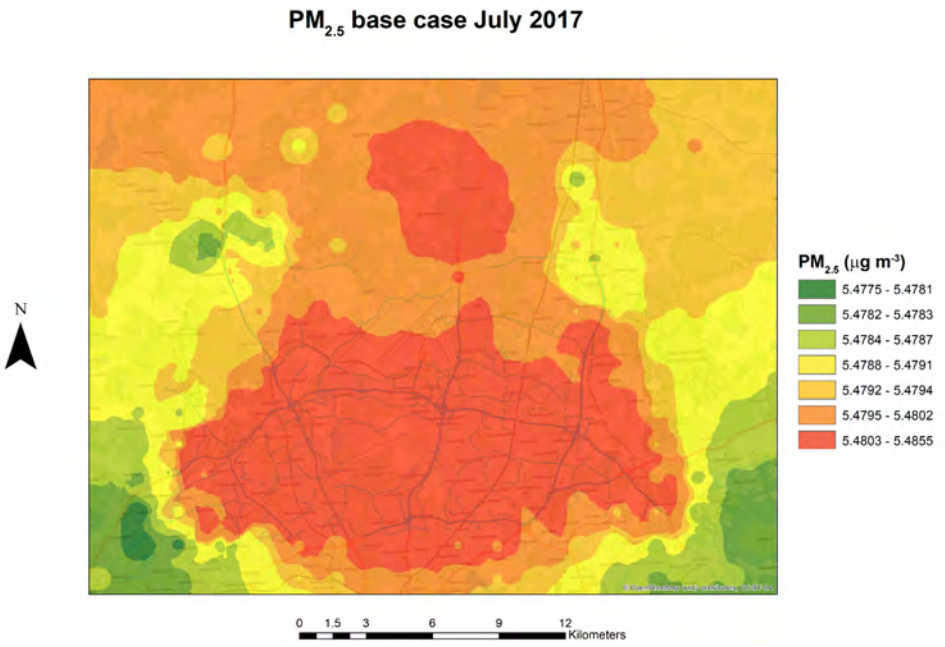

Figure 54. $PM_{2.5}$ concentration map for the Vantaa present reference scenario (July 2017 mean). Also shown are the major roads considered in the simulations.

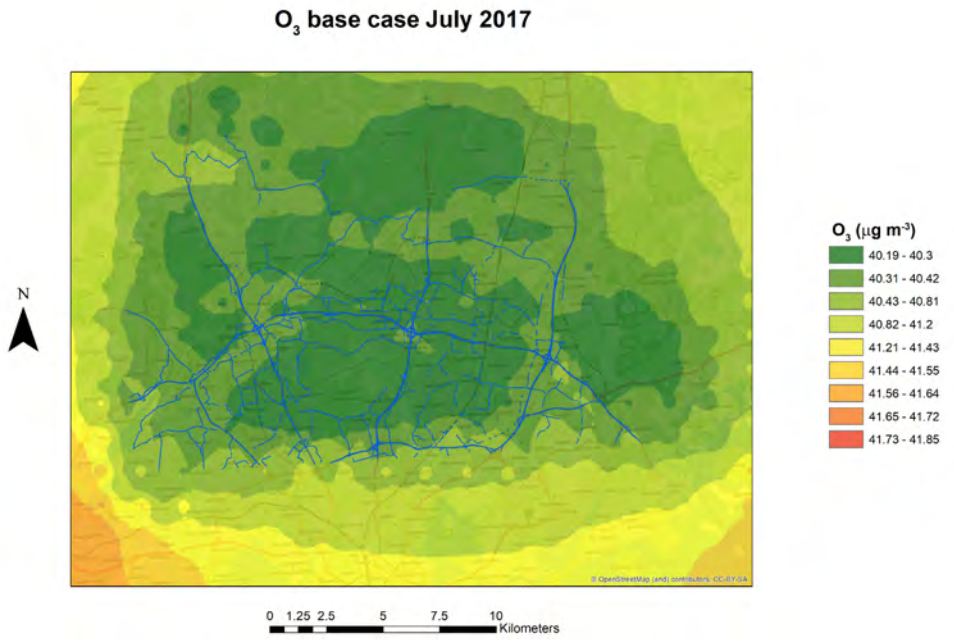

Figure 55. O_3 concentration map for the Vantaa present reference scenario (July 2017 mean). Also shown are the major roads considered in the simulations.

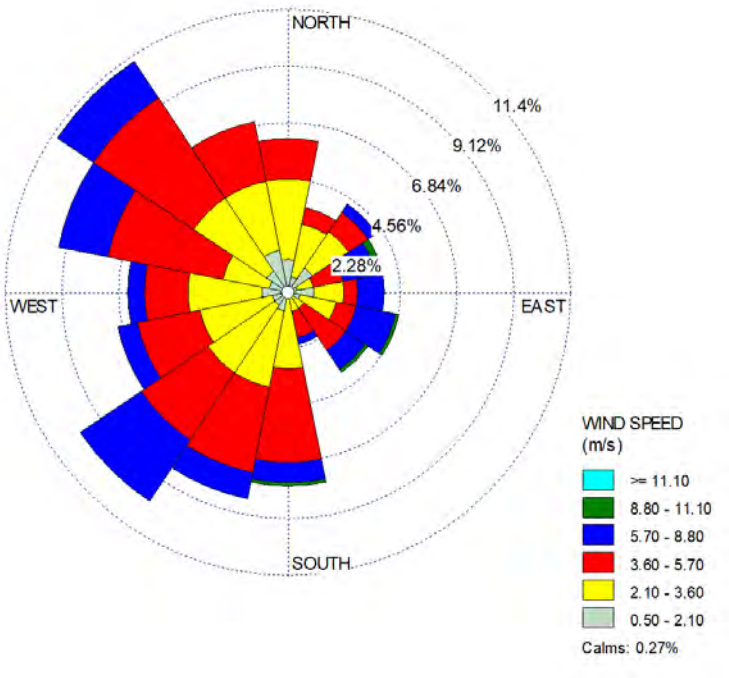

Figure 56. Wind rose for July 2017 in Vantaa.

As previously detailed, the effects of vegetation on air quality when altering the urban layout and substituting urban dense areas with lower and less dense buildings and a larger fraction of vegetated spaces were simulated through modifications of the surface roughness at the dispersion site, while maintaining the same atmospheric forcing and the same roughness length at the meteorological site. Specifically, the atmospheric forcing consisted in hourly observations of meteorological parameters (air temperature, air relative humidity, solar radiation, wind intensity and wind direction) at Vantaa airport in January and July 2017. Surface roughness at the dispersion and meteorological sites were obtained from the outputs of the SURFEX model, which observed a halving of the roughness length when substituting dense built areas with more vegetated areas ("intervention" scenario).

Figure 57 and Figure 58 show NO_2 and $PM_{2.5}$ concentration maps for a scenario considering the implementation of the intervention consisting in a change of the urban layout in the present climate conditions during a winter period. The pollutant spatial distribution does not present major changes, and local areas of maximum concentrations remain localized in proximity of major roads. Pollutant concentrations present also only minor changes with respect to the base reference case previously examined.

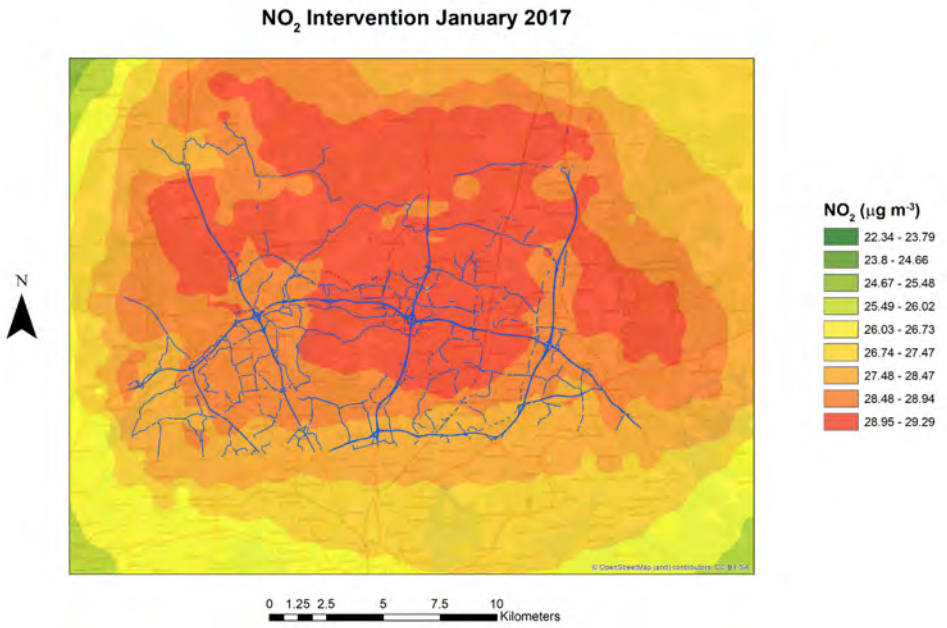

Figure 57. NO_2 concentration map for the Vantaa intervention scenario in the present climate conditions (January 2017 mean). Also shown are the major roads considered in the simulations.

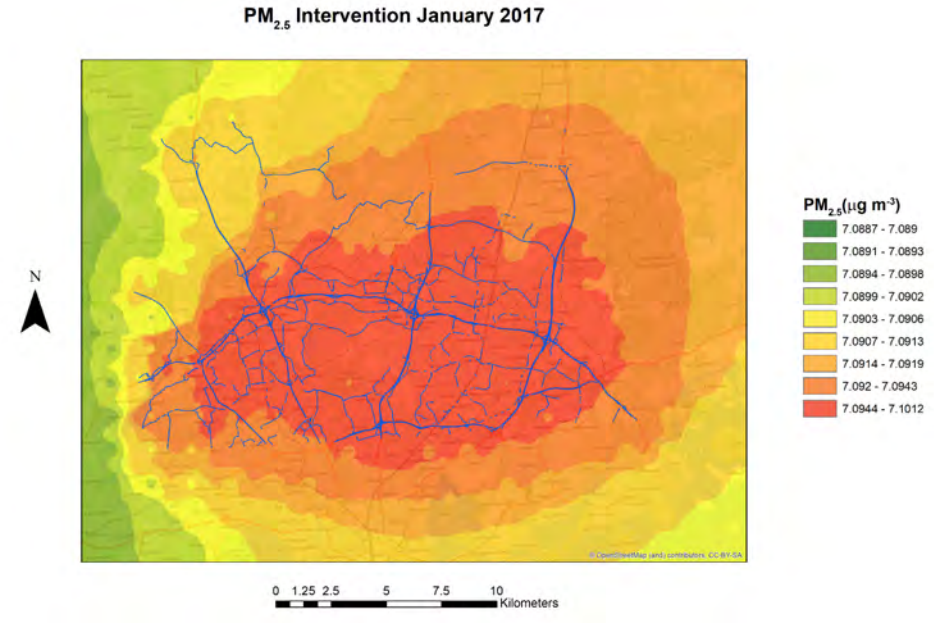

Figure 58. $PM_{2.5}$ concentration map for the Vantaa intervention scenario in the present climate conditions (January 2017 mean). Also shown are the major roads considered in the simulations.

A closer look at the effect of the intervention is gained examining the concentration differences maps between the intervention scenario and the base reference case, for NO_2 and $PM_{2.5}$ concentration case during January 2017 (Figure 59 and Figure 60). For NO_2, Figure 59 indicates that the intervention does not alter much the pollutant concentrations, presenting a widespread minor reduction over the city centre, and slight enhancements far away from the city center. $PM_{2.5}$ (Figure 60) presents practically no variations with respect to the base case reference scenario. The minor impact of the intervention on pollutant concentrations is in agreement with the very modest effect shown by the intervention on meteorological parameters observed in D6.4.

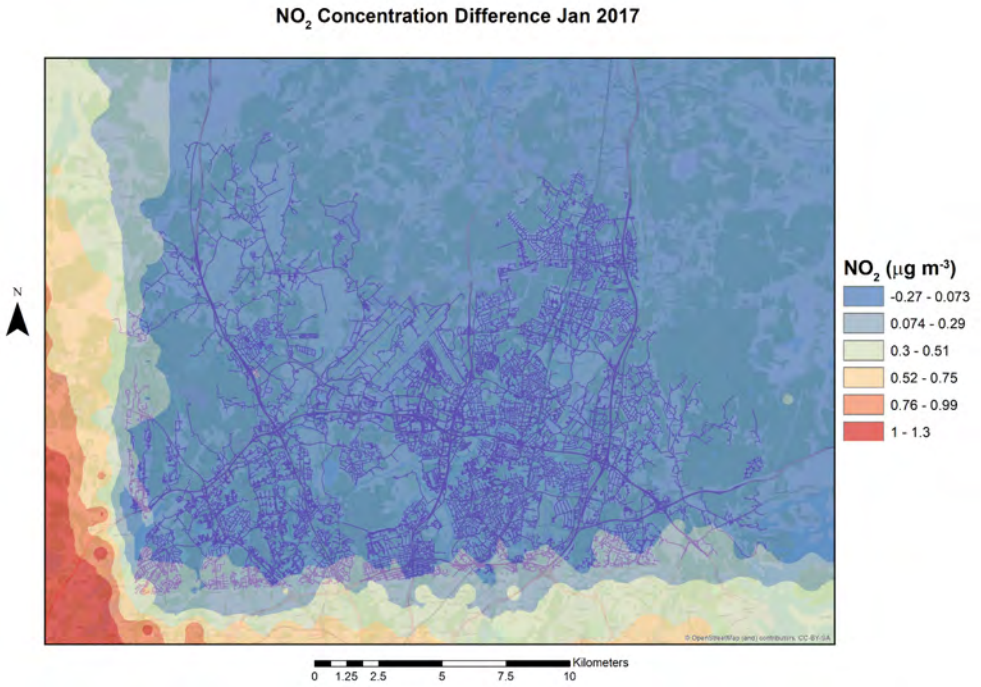

Figure 59. NO_2 concentration difference map between the Vantaa intervention scenario and the base reference case in the present climate conditions (January 2017 mean).

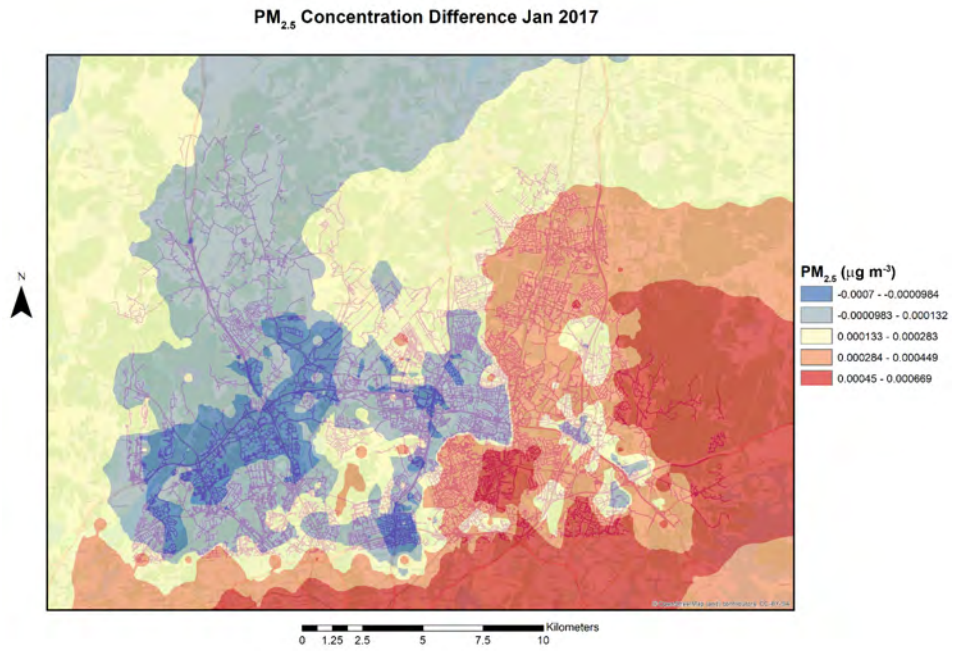

Figure 60. $PM_{2.5}$ concentration difference map between the Vantaa intervention scenario and the base reference case in the present climate conditions (January 2017 mean). Also shown are the major roads considered in the simulations.

Figure 61, Figure 62 and Figure 63 present NO_2, $PM_{2.5}$ and O_3 concentration maps for the scenario of application of the intervention in a summer month with the present climate conditions. Similar to the winter case, the pollutant spatial distribution presents similar patterns with the base reference case. Likewise, minimum and maximum pollutant concentrations show minor changes, with minor reductions in concentration local maxima for $PM_{2.5}$ and O_3.

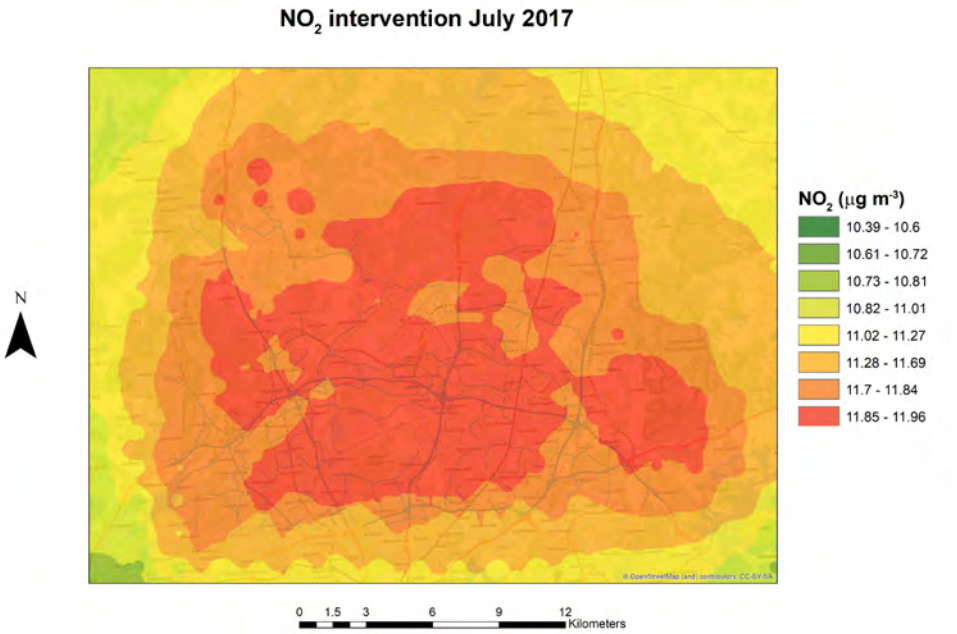

Figure 61. NO_2 concentration map for the Vantaa intervention scenario in the present climate conditions (July 2017 mean). Also shown are the major roads considered in the simulations.

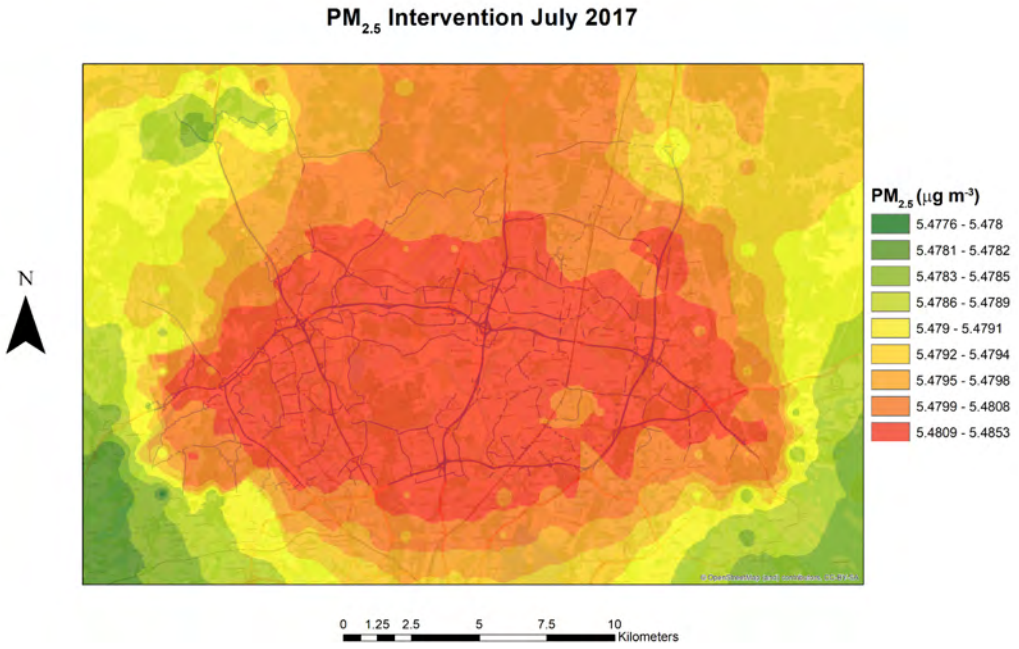

Figure 62. $PM_{2.5}$ concentration map for the Vantaa intervention scenario in the present climate conditions (July 2017 mean). Also shown are the major roads considered in the simulations.

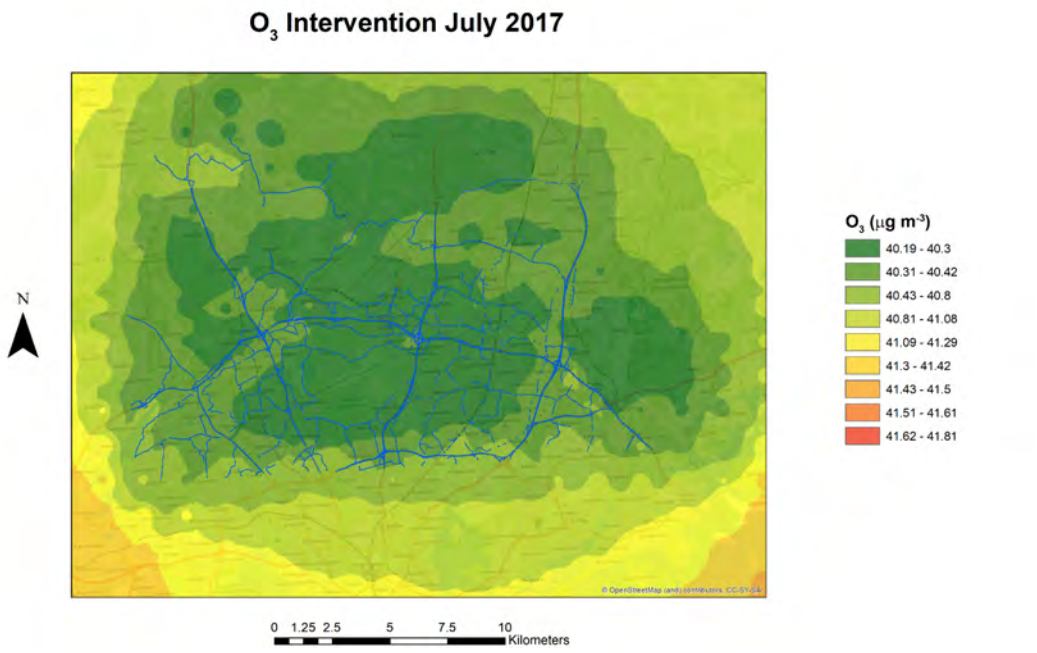

Figure 63. O_3 concentration map for the Vantaa intervention scenario in the present climate conditions (July 2017 mean). Also shown are the major roads considered in the simulations.

Again, a detailed analysis of impacts of the intervention in terms of air pollution is carried out examining concentration difference maps for the three pollutants between the intervention scenario and the base reference case in July 2017. Concentration difference maps (Figure 64, Figure 65 and Figure 66) show that the impact of the intervention is very limited, both in terms of reduction and enhancements in pollutant concentrations, even in July. In particular, NO_2 presents again a widespread minor reduction in the city centre, accompanied by a slight enhancement far from the trafficked roads, whereas $PM_{2.5}$ presents practically no changes with respect to the base case. The clearer, but still not very high, reductions in O_3, which is the only pollutant showing no region of enhancement, is likely caused by the increased albedo adopted in the intervention scenario.

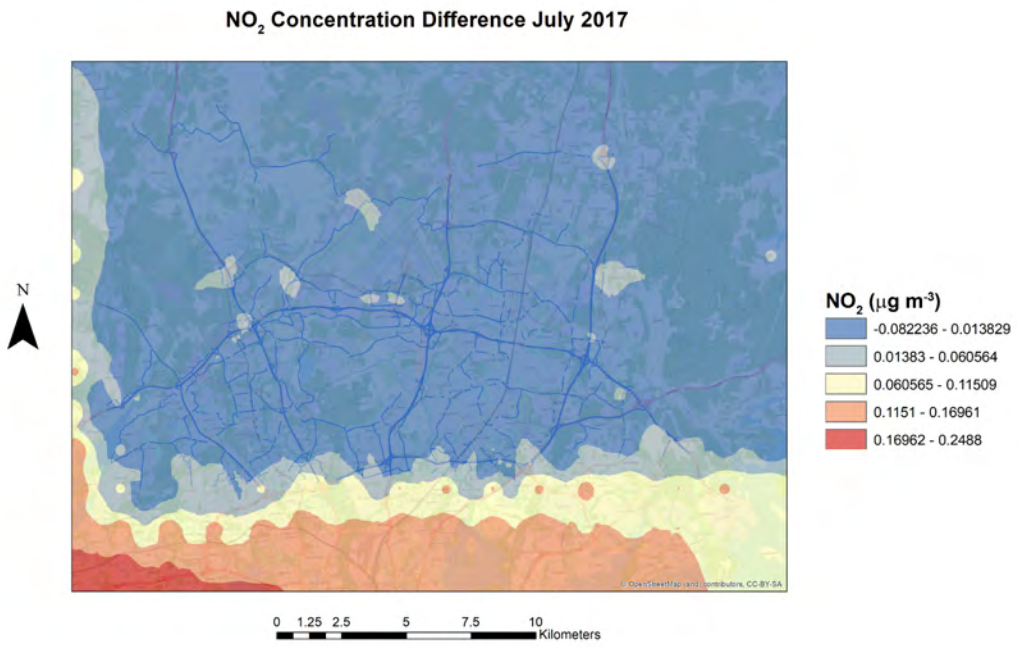

Figure 64. NO_2 concentration difference map between the Vantaa intervention scenario and the base reference case in the present climate conditions (July 2017 mean).

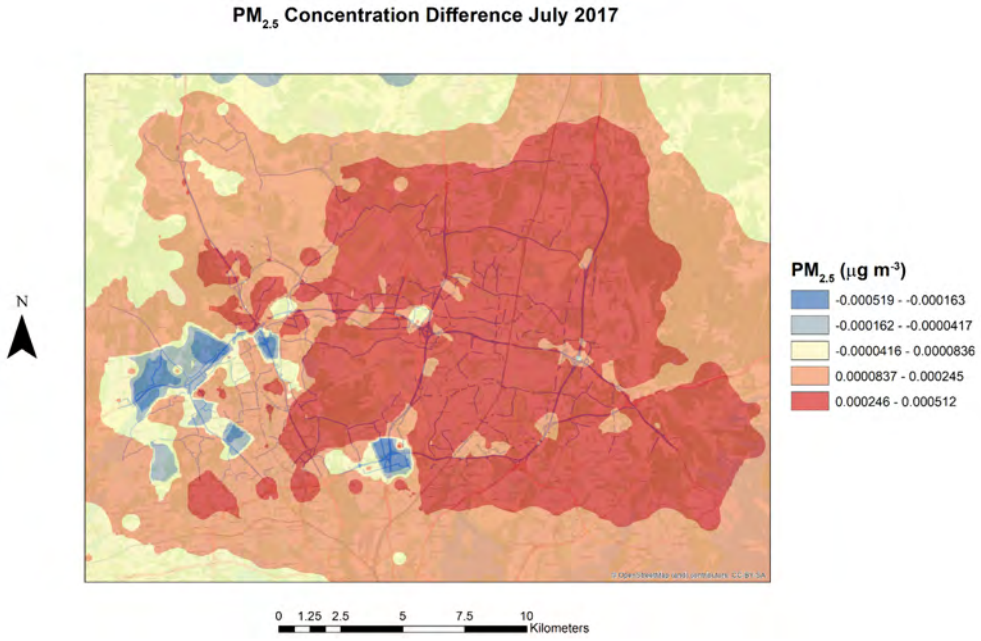

Figure 65. $PM_{2.5}$ concentration difference map between the Vantaa intervention scenario and the base reference case in the present climate conditions (July 2017 mean).

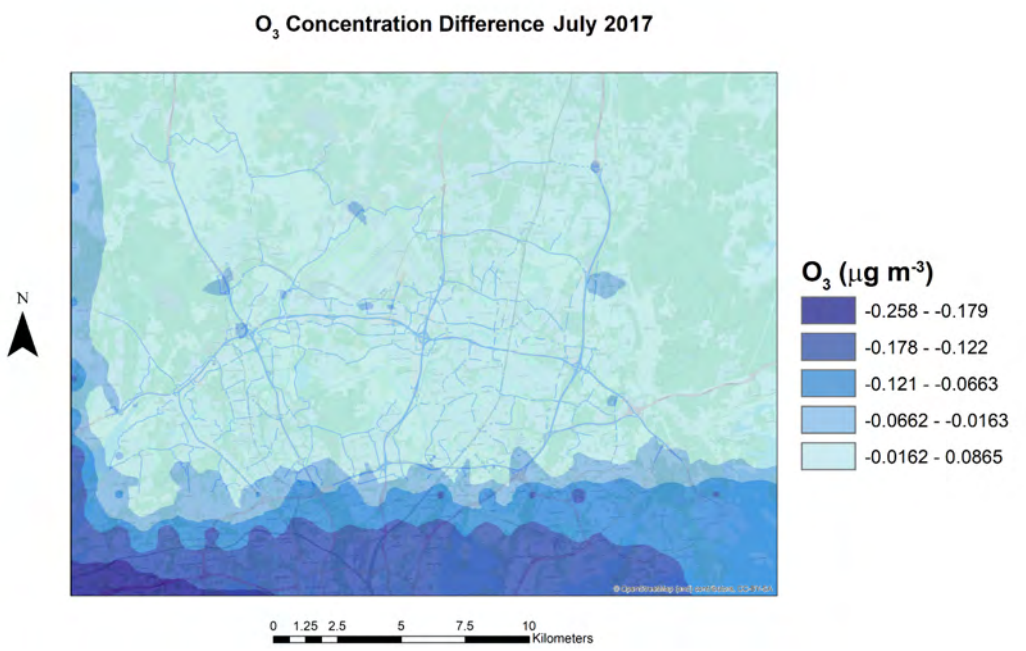

Figure 66. O_3 concentration difference map between the Vantaa intervention scenario and the base reference case in the present climate conditions (July 2017 mean).

To conclude with, we indicate the percentage differences in pollutant concentrations between the intervention scenario and the base case in the two months, calculated at the Tikkurila air quality station as difference between long term mean obtained in the intervention scenario and in the base case, normalized over the base case (Table 19). The Table confirms the limited impact of the intervention, as results from the limited differences presented by all the pollutants in both months.

% Difference	NO_x	NO_2	O_3	PM_{10}	$PM_{2.5}$
Jan-17	-2.25E-03	2.48E-02	-1.66E-02	2.72E-03	2.82E-03
Jul-17	3.41E-02	5.46E-02	-1.24E-02	6.98E-03	8.57E-03

Table 19. Percentage differences for pollutant concentrations at the Tikkurila air quality station between the intervention scenario and the base reference case in the two analyzed months (January and July 2017).

4.2.1.3 Effects of vegetation on air temperature

As reported in D6.4, the presence of built-up areas in the Helsinki-Vantaa region has a pronounced impact on local microclimate simulated by the SURFEX model, in particular with higher air temperatures both in winter and in summer (Figure 67 and Figure 68).

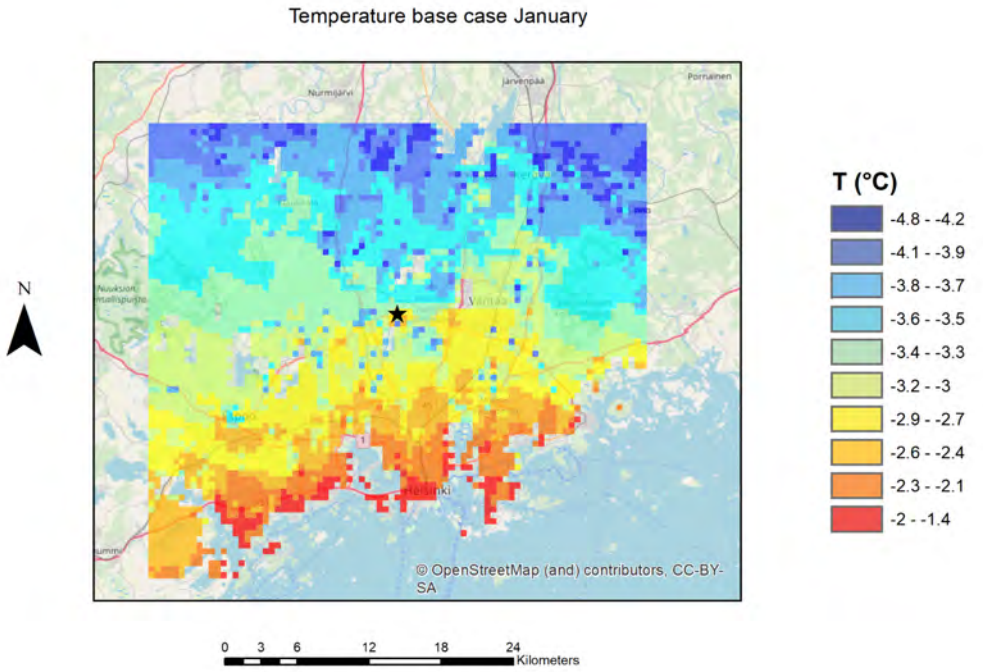

Figure 67. Monthly mean air temperature as simulated by SURFEX in January, in the test reference year for the present climate conditions. The commercial area of Tikkurila is indicated with the black star.

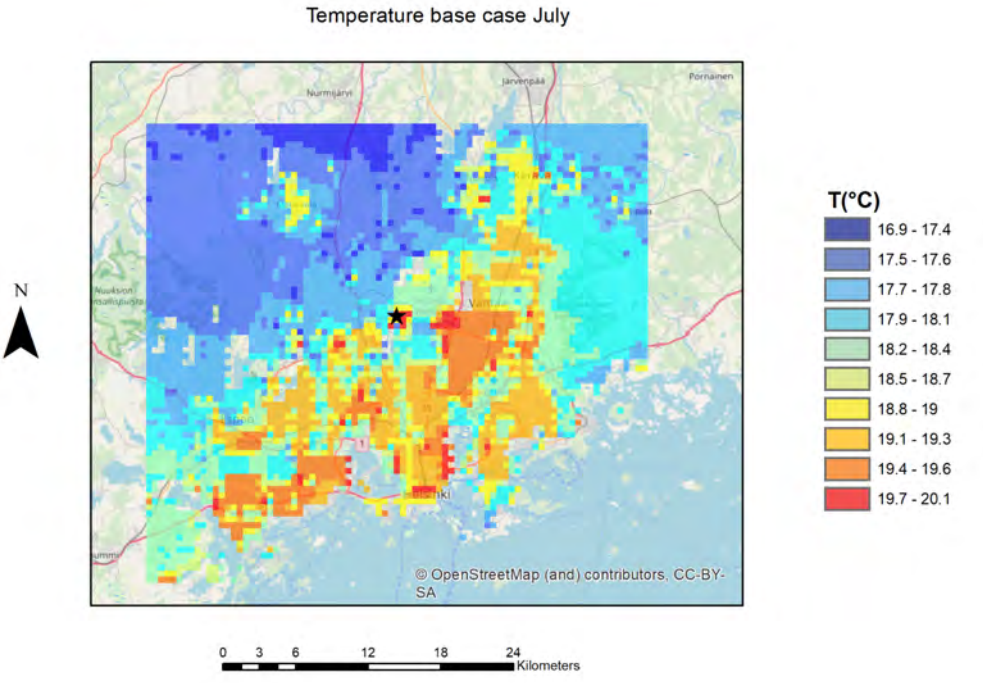

Figure 68. Monthly mean air temperature as simulated by SURFEX in July, in the test reference year for the present climate conditions. The commercial area of Tikkurila is indicated with the black star.

When replacing the dense urban layout with a suburban type structure the spatial pattern of air temperature shows no major changes (Figure 69 and Figure 70), with practically no variations in the minimum and maximum temperatures (only January maximum temperature is slightly reduced in the intervention scenario).

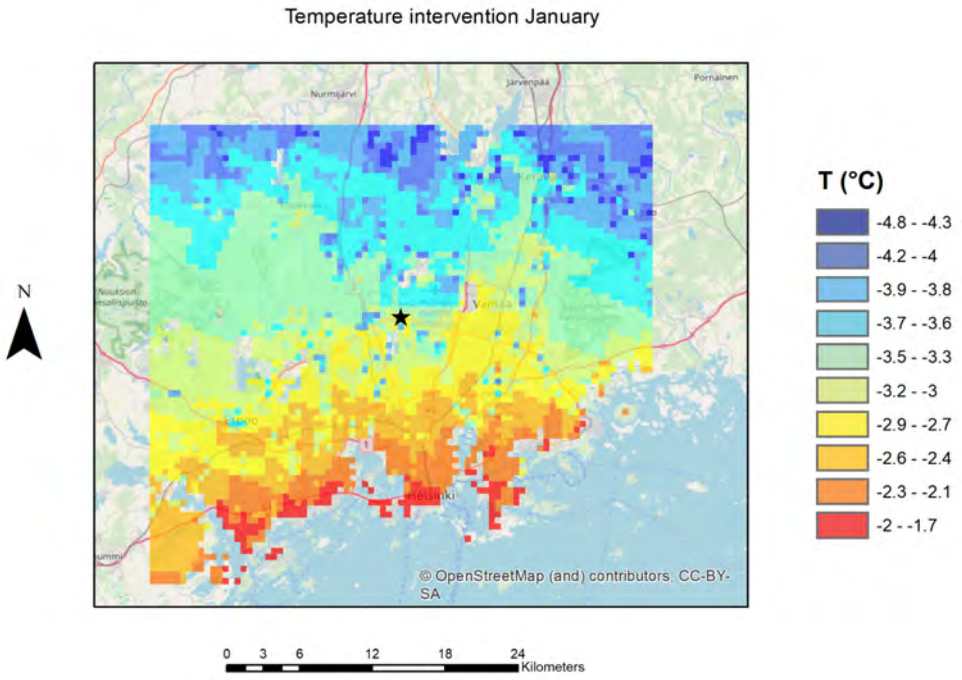

Figure 69. Monthly mean air temperature as simulated by SURFEX in January, in the intervention scenario for the present climate conditions. The commercial area of Tikkurila is indicated with the black star.

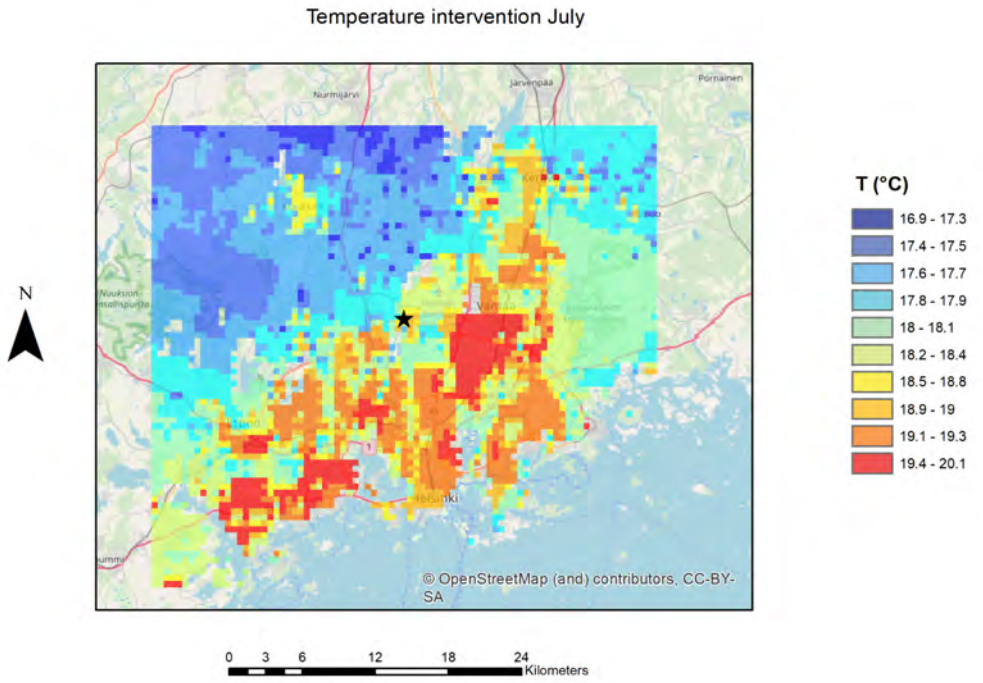

Figure 70. Monthly mean air temperature as simulated by SURFEX in January, in the intervention scenario for the present climate conditions. The commercial area of Tikkurila is indicated with the black star.

However, the analysis of temperature difference maps (Figure 71 and Figure 72) show the presence of areas with reductions as high as 0.4°C in January and 0.8 in July; therefore, even though reductions are spatially very localized, the intervention may lead to improvements in thermal comfort in some neighborhoods of the city center.

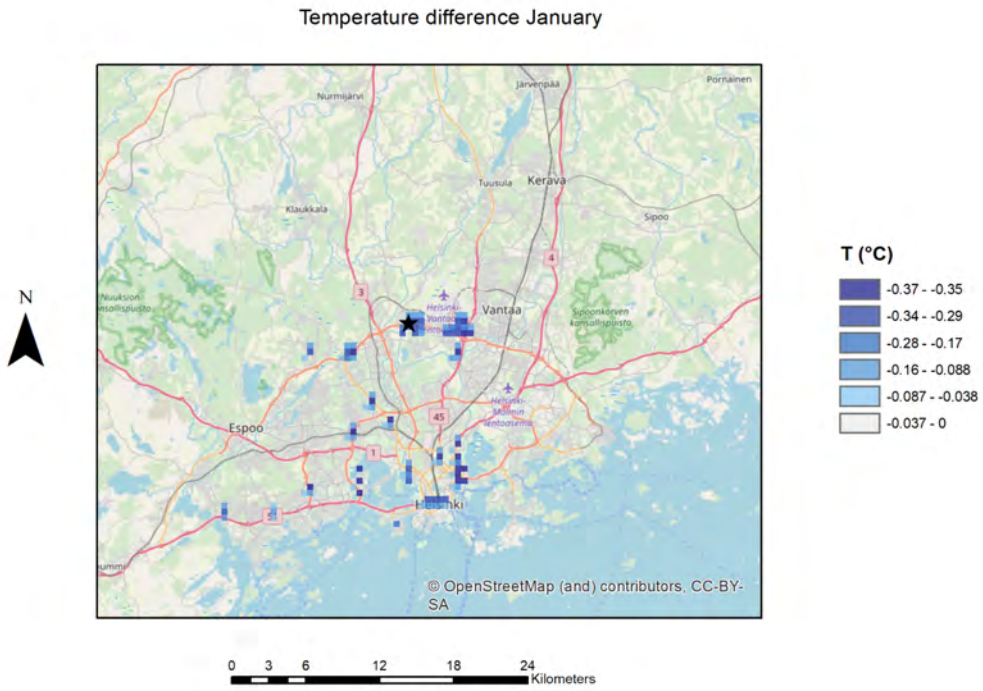

Figure 71. Temperature difference map between the intervention scenario and the base case in January in the present climate conditions. The commercial area of Tikkurila is indicated with the black star.

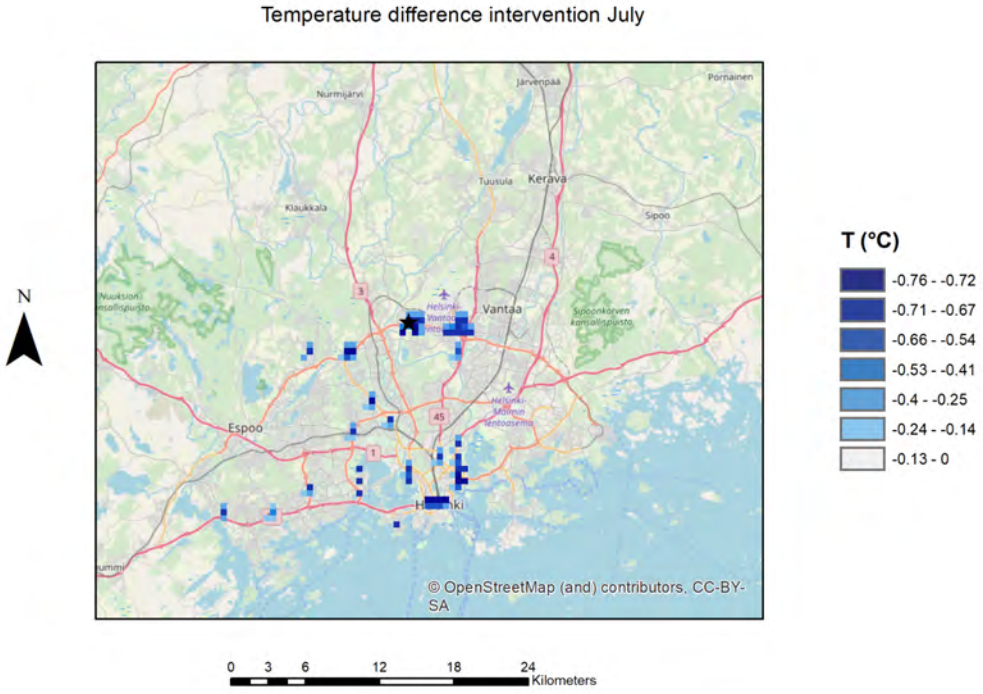

Figure 72. Temperature difference map between the intervention scenario and the base case in July in the present climate conditions. The commercial area of Tikkurila is indicated with the black star.

4.2.2 Future scenario

As previously detailed, the future scenario was constructed by applying morphing adjustment to the baseline test-year forcing for the Vantaa airport. This forcing was used as input data to dispersion model simulations to derive information on the impact of climate change on air pollution in Vantaa. Further, the same forcing was also used as input to the SURFEX model to simulate the effects of the altered urban layout on air temperature. Again, simulations were conducted for one winter and one summer month (January and July, respectively), to compare better with the results obtained for the present climate conditions.

4.2.2.1 Effects of vegetation on air quality

As previously done in the present scenario, before presenting the effects of the intervention on air pollution, we show the results obtained by dispersion model simulations carried out with the future meteorology representative of the mid-2050s in Vantaa under the RCP8.5 scenario. In particular, in this case, while the input meteorological data were changed with morphing adjustment of the meteorology in the synthetic reference year, emissions were left unchanged, so that variations in pollutant concentrations account only for the climatic changes.

As reported in D6.4, the most affected parameter is the temperature, as we will see in the next section. Little changes are observed instead for wind speed, while the share of westerly winds is projected to slightly increase. These minor changes in winds are not predicted to impact much on pollutant concentrations in Vantaa.

As done in the present scenario, we first present the concentration maps obtained by dispersion modeling simulations conducted in the two months, January and July 2050s, considering only the impact of climate change and without alteration of the present urban layout. Figure 73 and Figure 74 present maps of NO_2 and $PM_{2.5}$ in Vantaa in January 2050, under the effect of climate change. Comparing with the results obtained in January 2017, we can observe that changes in meteorology will affect pollutant concentrations only slightly, with a minor tendency of increasing maximum concentrations but maintaining a similar dispersion pattern.

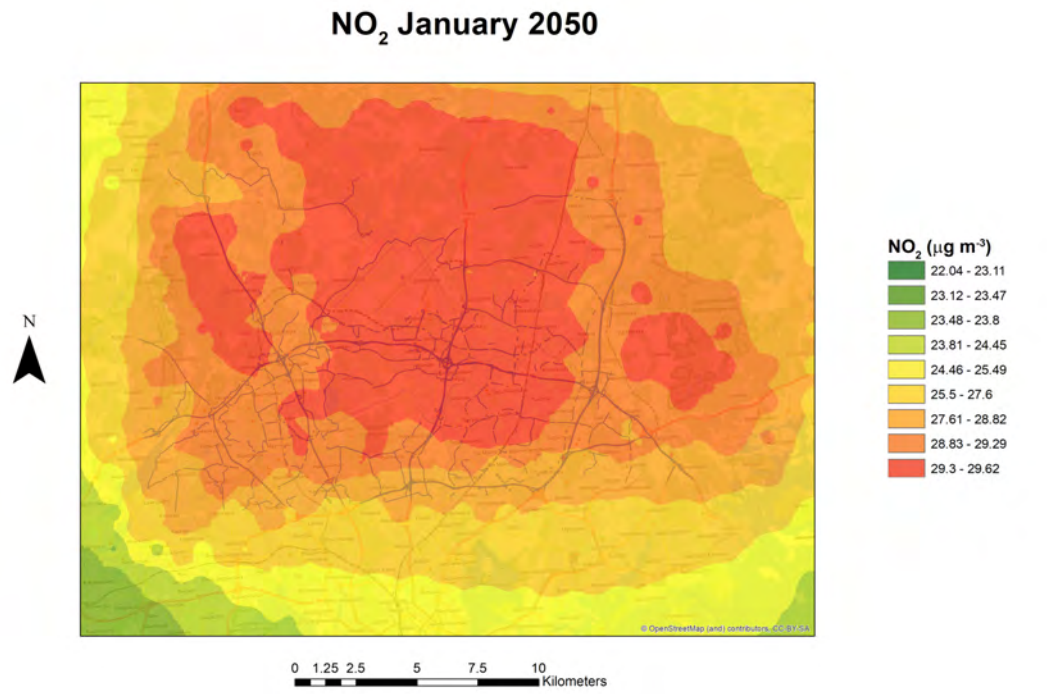

Figure 73. NO_2 concentration map for the Vantaa future scenario (January 2050 mean), considering the effect of climate change only. Also shown are the major roads considered in the simulations.

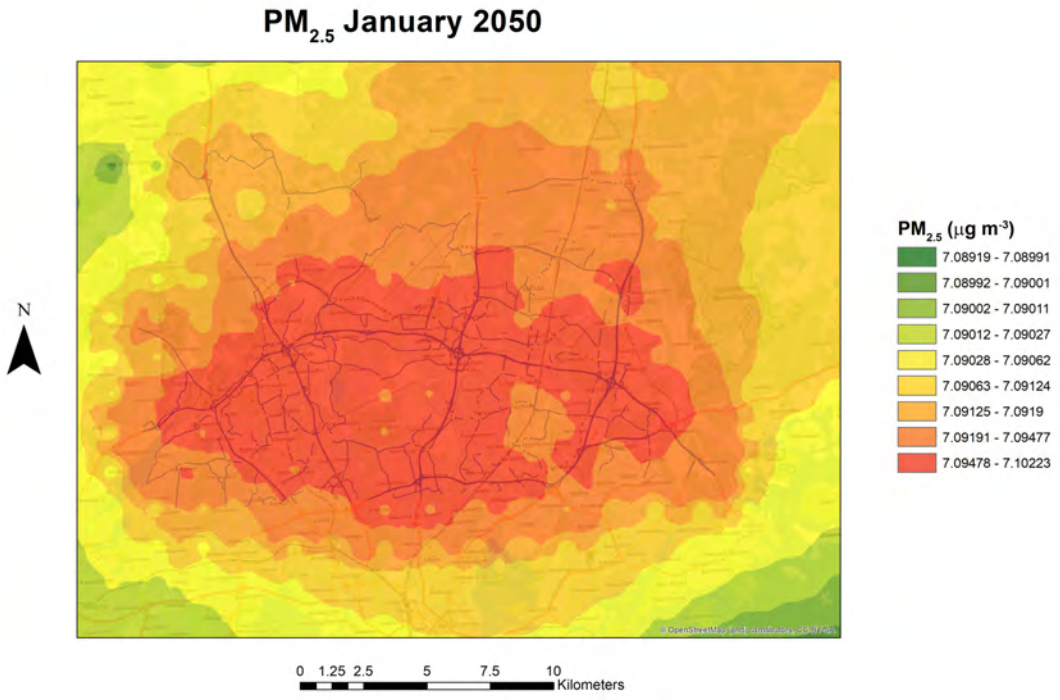

Figure 74. $PM_{2.5}$ concentration map for the Vantaa future scenario (January 2050 mean), considering the effect of climate change only. Also shown are the major roads considered in the simulations.

However, the wind rose of the period (Figure 75) presents a different pattern with respect to that of January 2017, with an increase of westerlies and a reduction of SW winds, while wind intensities do not present major changes. These slight variations in wind direction patterns are responsible of only minor changes in the position of minimum concentrations far from the city center even in the future, whereas concentration hotspots will be still located in the city center close to major traffic roads.

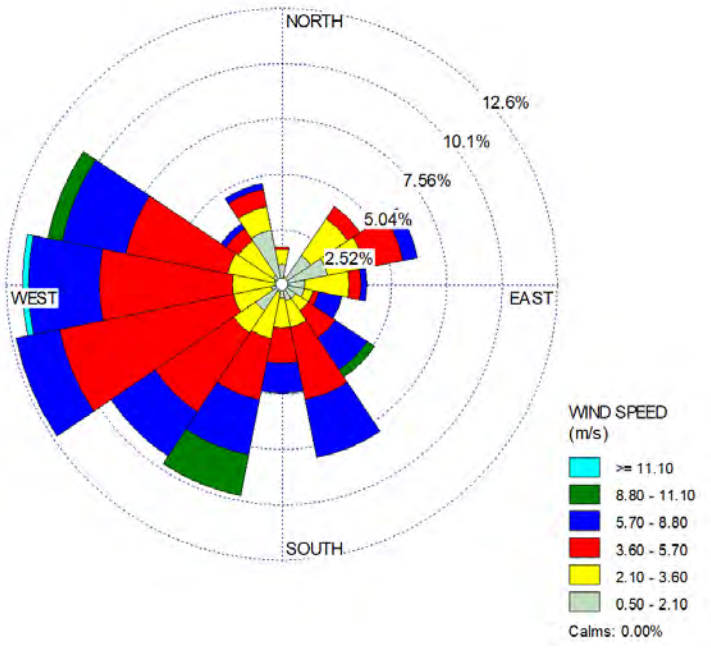

Figure 75. Wind rose of January 2050 in Vantaa.

Examining concentration maps in future July for NO_2, $PM_{2.5}$ and O_3 (Figure 76, Figure 77 and Figure 78), we may observe that the spatial pattern will be affected by more important changes in summer. In particular, while NO_2 presents minimum concentrations in the eastern border of the simulation domain, $PM_{2.5}$ is especially impacted with a movement of concentration hotspots that besides in vicinity of major trafficked roads are also located to the western border. This can be attributed to a noticeable change in wind directions impacting Vantaa, with a decrease in NW winds in favor of an increase of NE directions (Figure 79).

As in the present scenario, O_3 presents a complementary pattern to that of O_3, as due to the well-known and previously explained equilibrium which involves NO_2, NO and O_3.

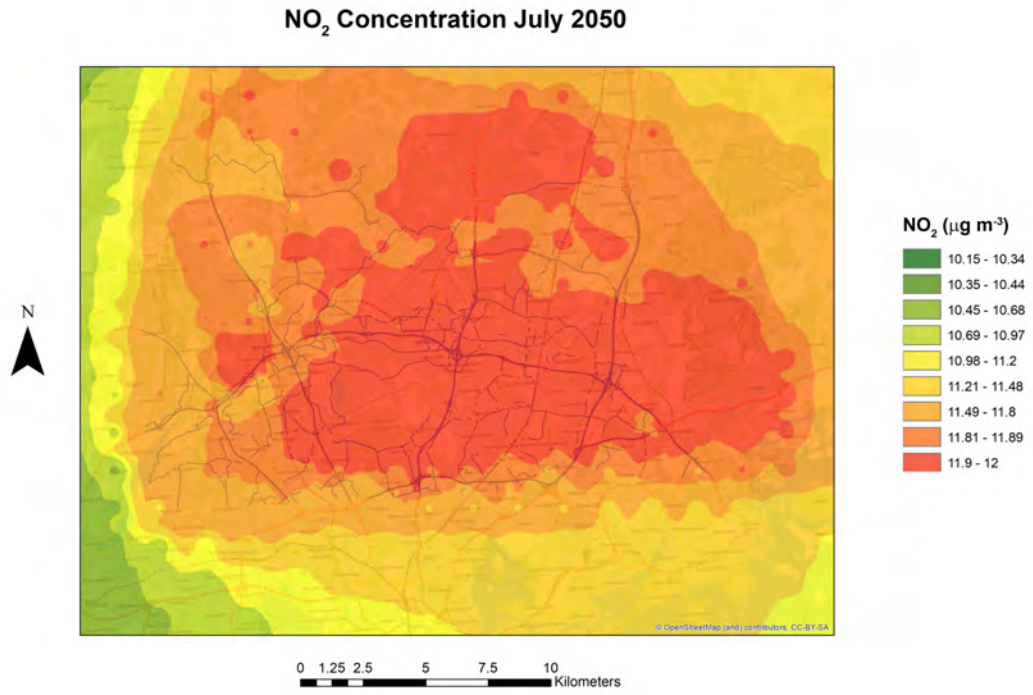

Figure 76. NO_2 concentration map for the Vantaa future scenario (July 2050 mean), considering the effect of climate change only. Also shown are the major roads considered in the simulations.

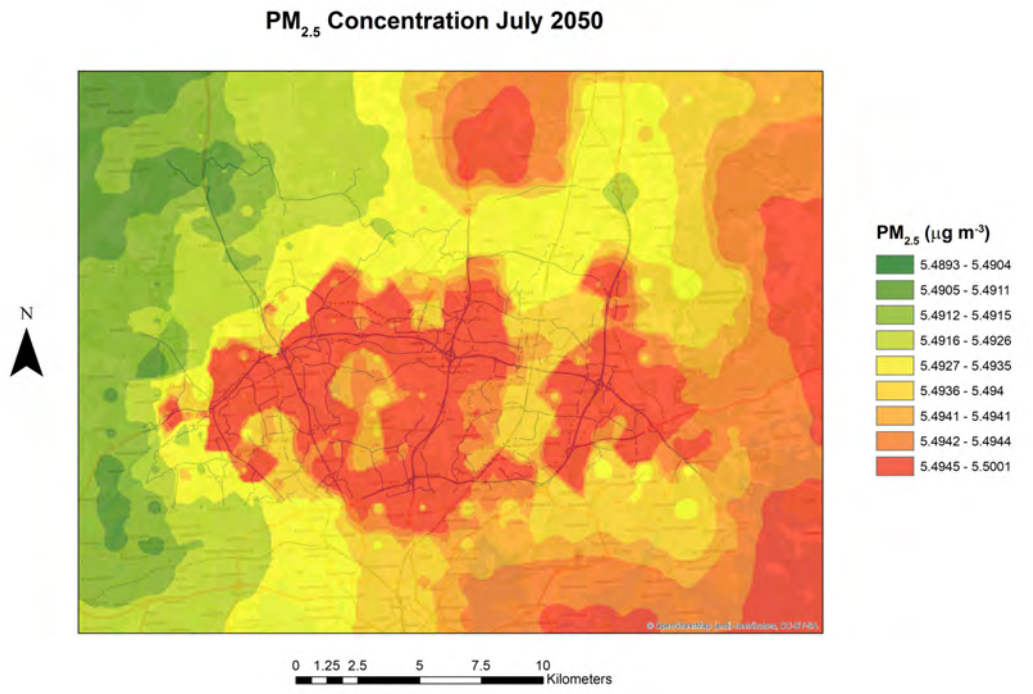

Figure 77. $PM_{2.5}$ concentration map for the Vantaa future scenario (July 2050 mean), considering the effect of climate change only. Also shown are the major roads considered in the simulations.

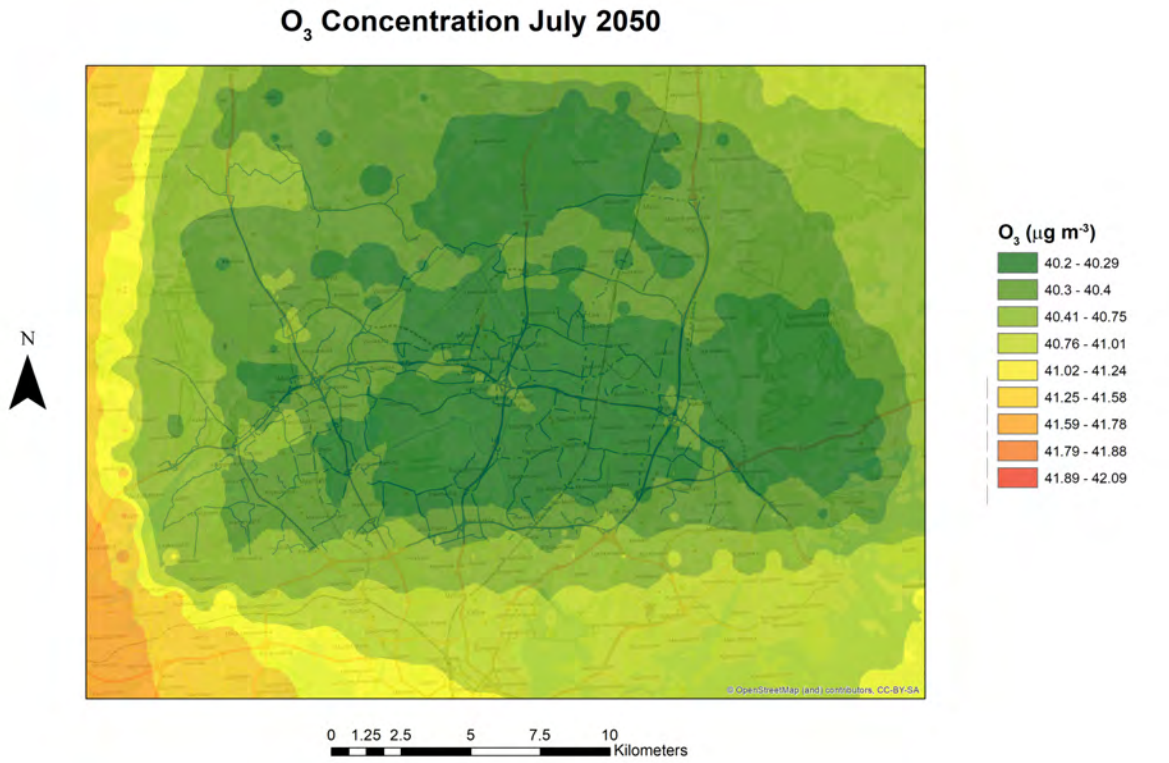

Figure 78. O_3 concentration map for the Vantaa future scenario (July 2050 mean), considering the effect of climate change only. Also shown are the major roads considered in the simulations.

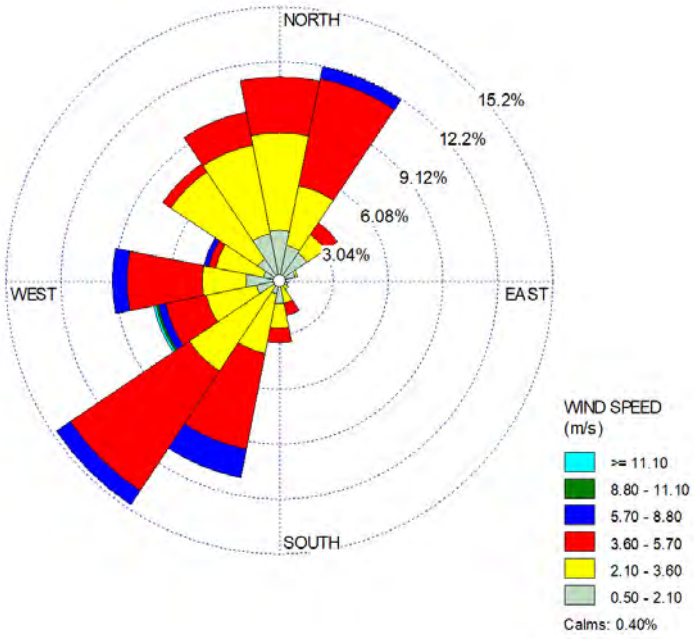

Figure 79. Wind rose of July 2050 in Vantaa.

Next, we can examine the effects of the intervention on pollutant concentrations under the future climate scenario.

Figure 80 and Figure 81 present NO_2 and $PM_{2.5}$ concentration maps in Vantaa for a scenario considering the implementation of the intervention altering the urban layout in future January. The maps show that the spatial patterns of pollutant concentrations will not be affected by the implementation of this intervention. Likewise, the position and magnitude of pollutant concentrations do not seem to present major variations, in agreement with the results obtained for the present scenario.

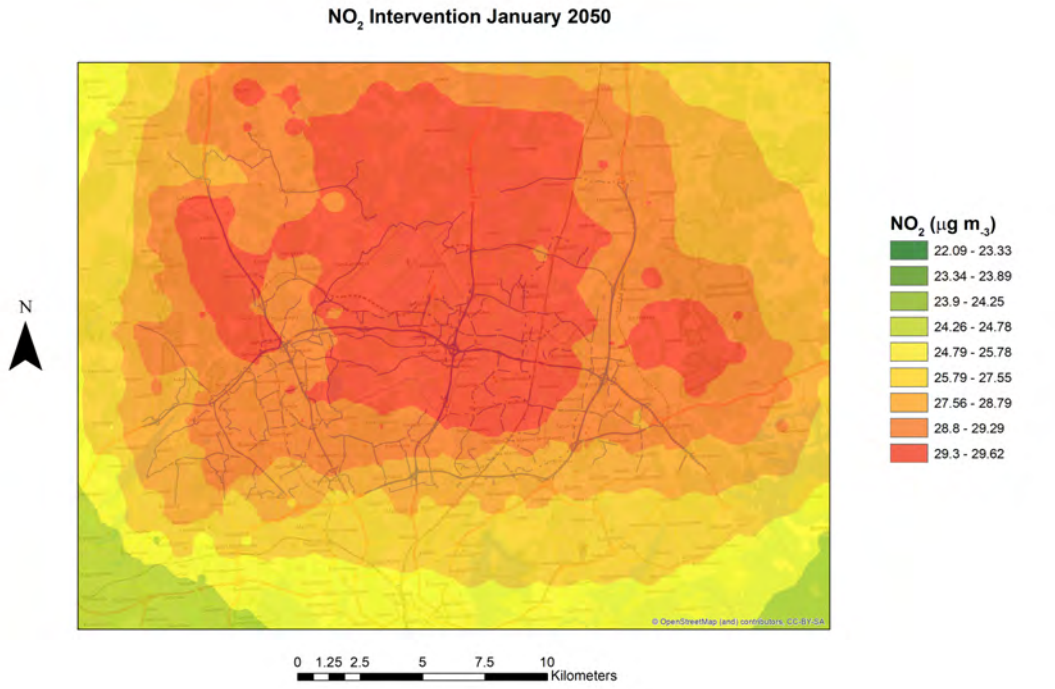

Figure 80. NO_2 concentration map for the Vantaa intervention scenario in the future climate conditions (January 2050 mean). Also shown are the major roads considered in the simulations.

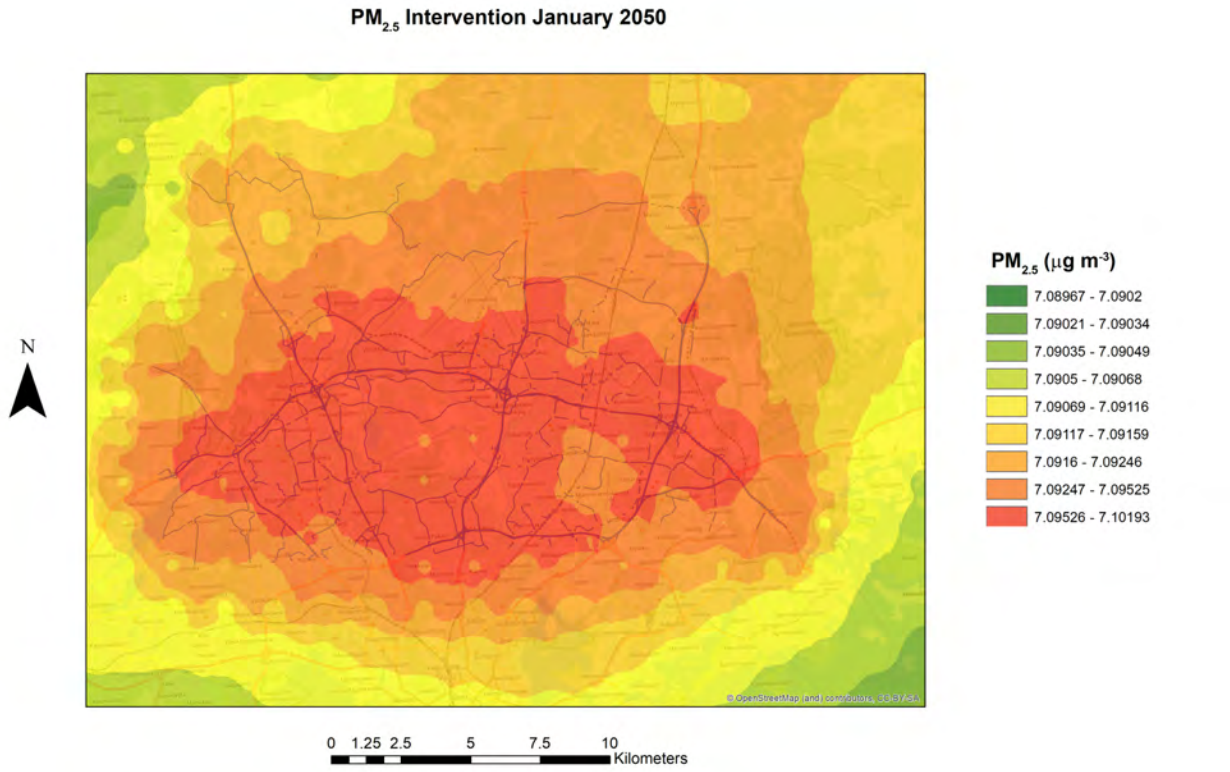

Figure 81. $PM_{2.5}$ concentration map for the Vantaa intervention scenario in the future climate conditions (January 2050 mean). Also shown are the major roads considered in the simulations.

Figure 82, Figure 83 and Figure 84 present NO_2, $PM_{2.5}$ and O_3 concentration maps for the scenario considering the implementation of the intervention altering the urban layout in the future July in Vantaa. Again, we may observe that the implementation of the intervention does not alter the pollutant concentration spatial pattern, while the magnitude of pollutant concentrations is only slightly changed with respect to the scenario when considering the effect of climatic changes only.

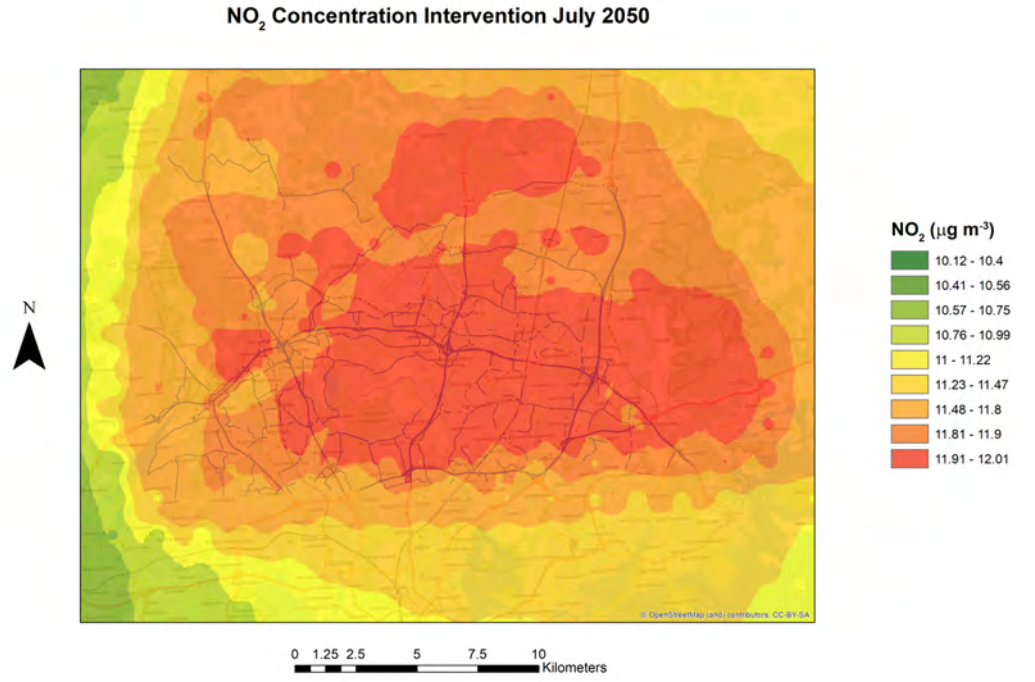

Figure 82. NO_2 concentration map for the Vantaa intervention scenario in the future climate conditions (July 2050 mean). Also shown are the major roads considered in the simulations.

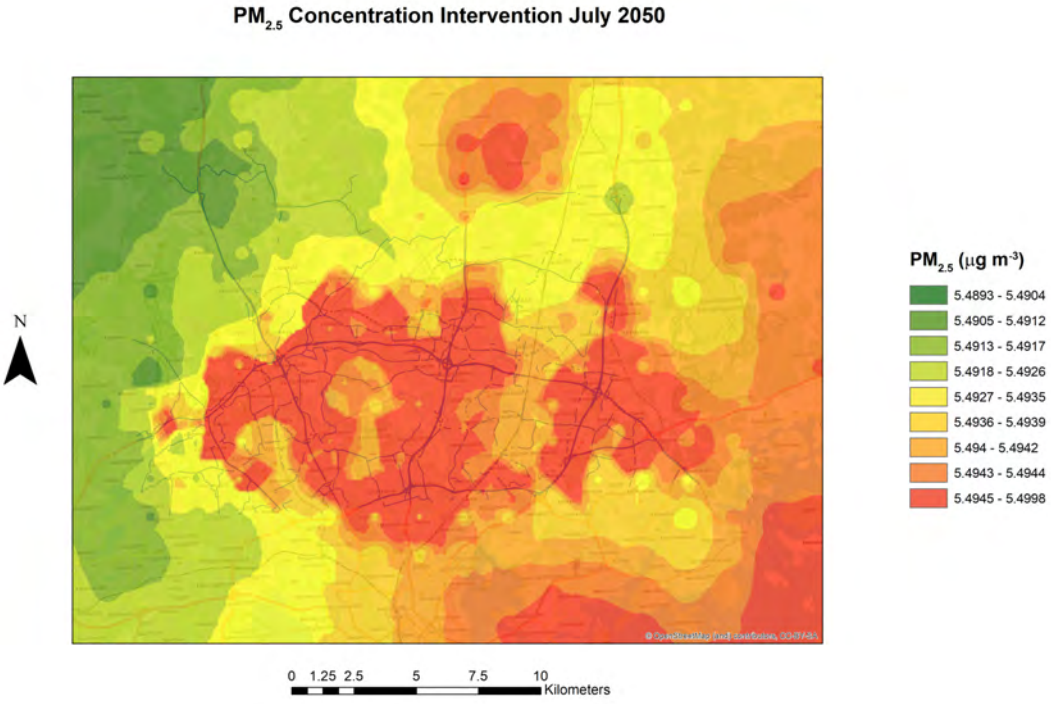

Figure 83. $PM_{2.5}$ concentration map for the Vantaa intervention scenario in the future climate conditions (July 2050 mean). Also shown are the major roads considered in the simulations.

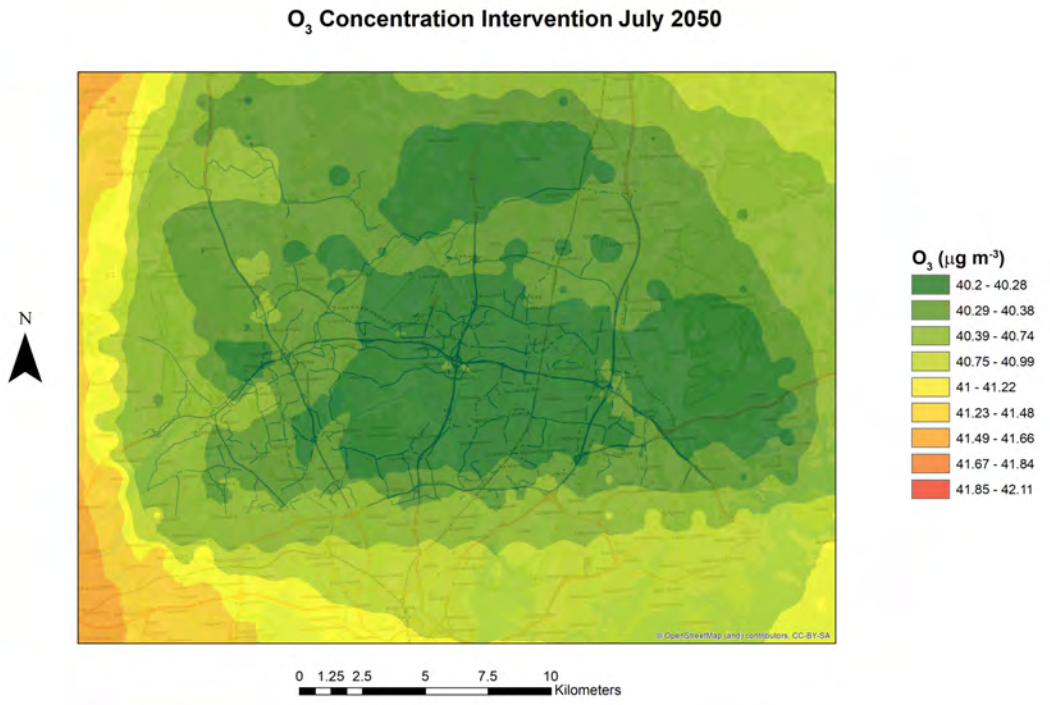

Figure 84. O_3 concentration map for the Vantaa intervention scenario in the future climate conditions (July 2050 mean). Also shown are the major roads considered in the simulations.

To conclude this analysis and to better examine the entity of the impacts of the intervention altering the urban layout in the two months, as previously done in the present scenario, we observe concentration difference maps between the two scenarios, the one with the intervention and climate changes and the one considering the effect of climatic changes only.

Figure 87, Figure 88 and Figure 89 report maps of concentration differences between the scenario of implementation of the intervention and the scenario considering the effect of climate change only in future January. As observed in the present scenario, the intervention is not very effective in producing changes in pollutant concentrations in Vantaa. NO_2 concentrations are observed to decrease slightly in the city center close to major roads and to increase slightly far away from the city center. Instead, PM2.5 concentrations are practically not affected by the intervention.

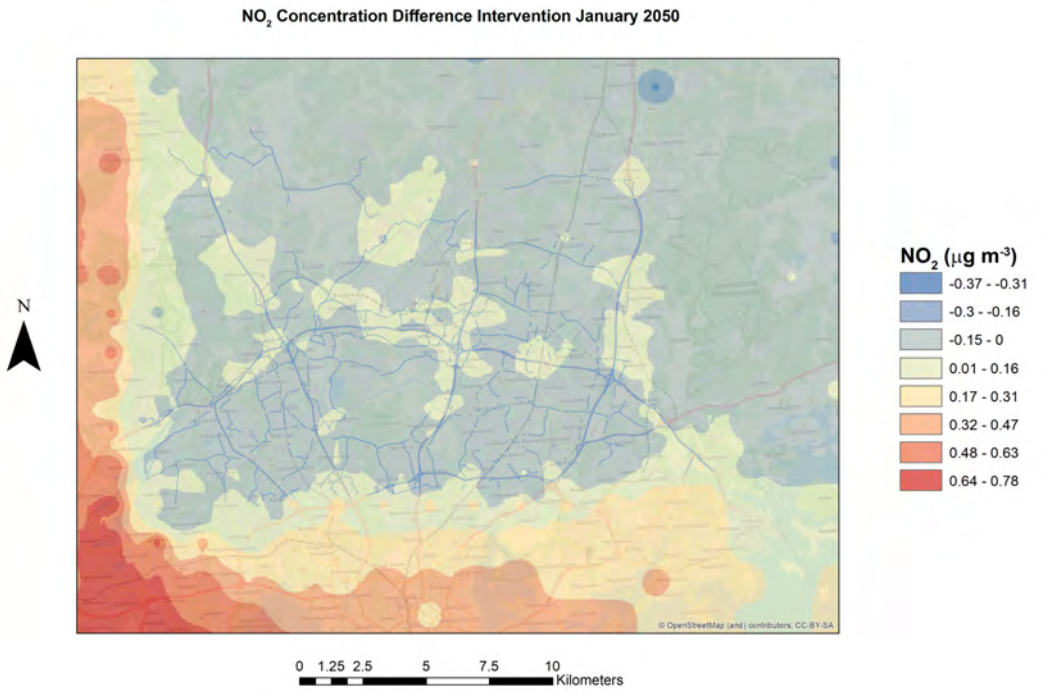

Figure 85. NO_2 concentration difference map between the Vantaa intervention scenario and the scenario considering the effects of climatic changes only (January 2050 mean).

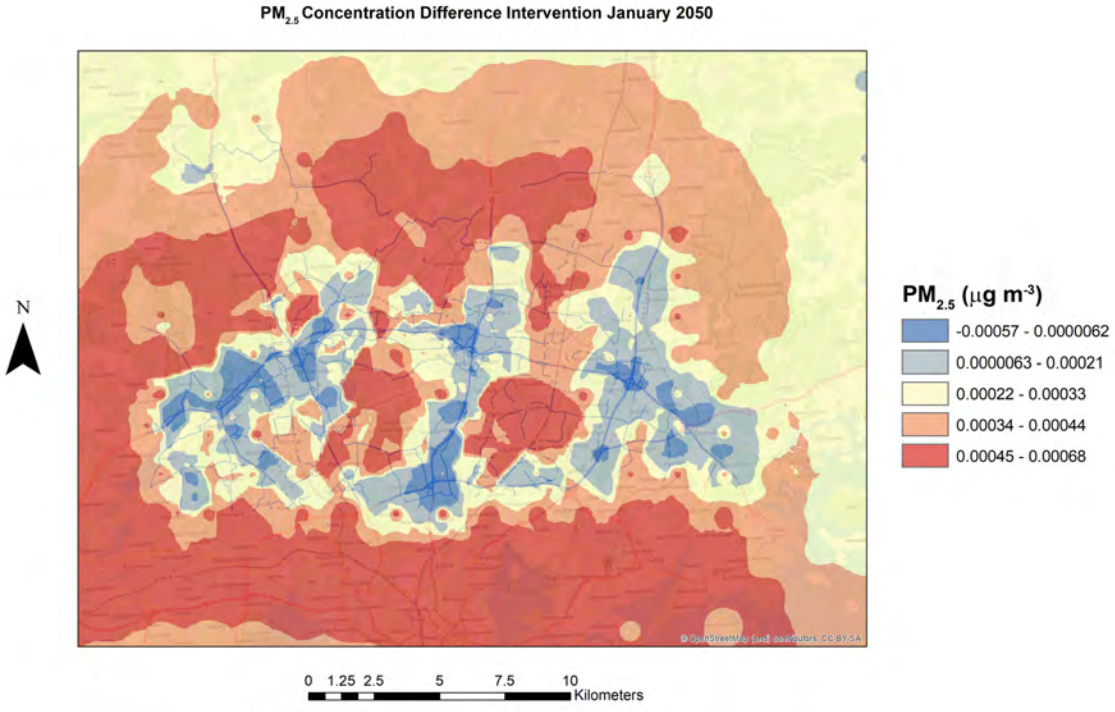

Figure 86. $PM_{2.5}$ concentration difference map between the Vantaa intervention scenario and the scenario considering the effects of climatic changes only (January 2050 mean).

Figure 87, Figure 88 and Figure 89 present concentration differences maps for the scenario considering the implementation of the intervention and the scenario impacted by climatic changes only in future July. We can observe that NO_2 and $PM_{2.5}$ present reduced variations when implementing an intervention consisting in an alteration of the urban layout. Similar to January and to the present scenario, the intervention reduces slightly NO_2 concentrations in the city center and increases concentrations to the SW of the simulation domain.

The stronger reduction observed for O_3 is likely to be caused by the change in albedo used in the intervention scenario, even though the spatial pattern of the reduction is complementary to that of NO_2, with increases in the city center and to the E of the simulation domain, and conversely the largest reductions observed to the SW, probably connected to the wind rose of the period, dominated as previously observed by winds from NW, SW and W, and with absence of winds from the E direction.

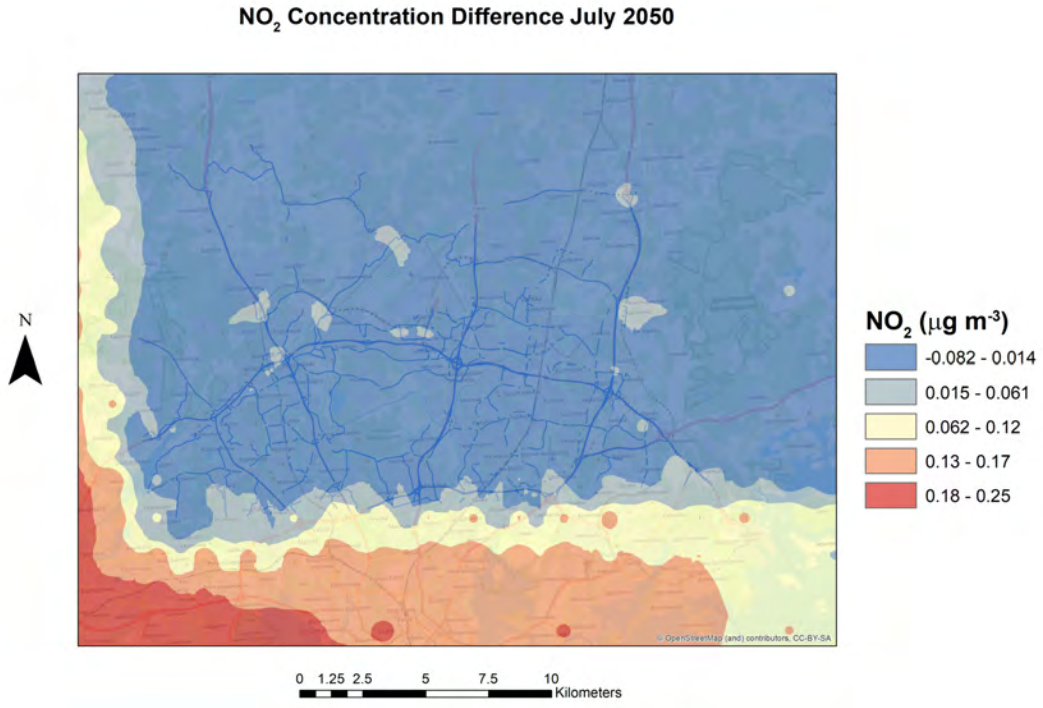

Figure 87. NO_2 concentration difference map between the Vantaa intervention scenario and the scenario considering the effects of climatic changes only (July 2050 mean).

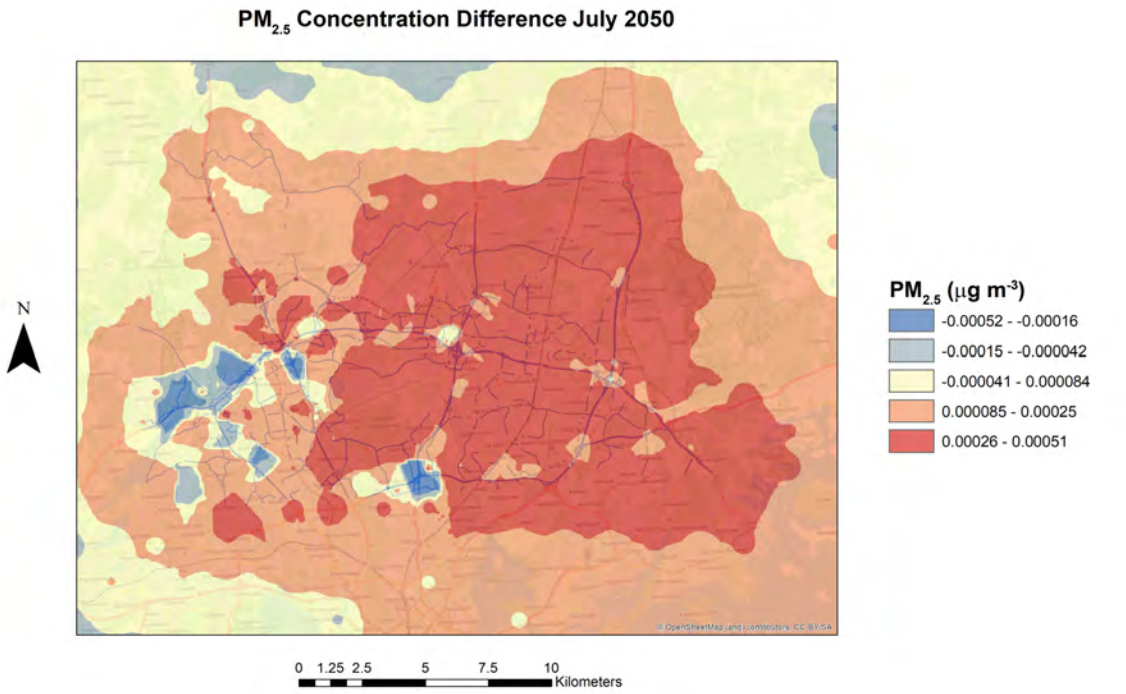

Figure 88. $PM_{2.5}$ concentration difference map between the Vantaa intervention scenario and the scenario considering the effects of climatic changes only (July 2050 mean).

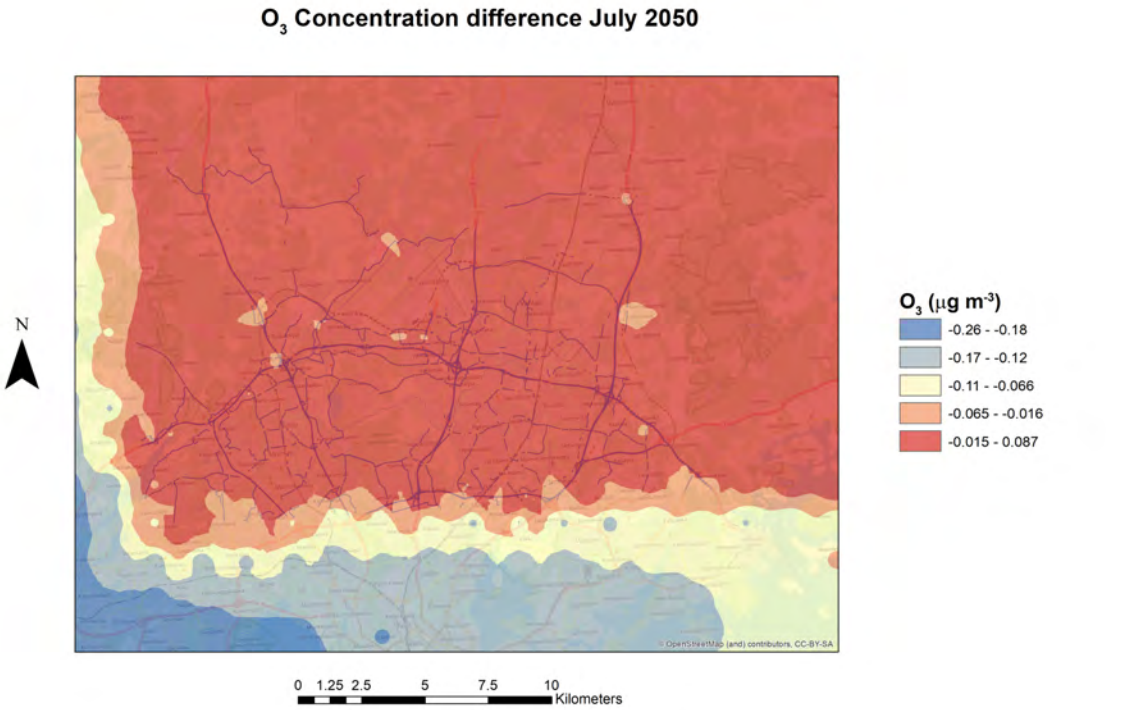

Figure 89. O_3 concentration difference map between the Vantaa intervention scenario and the scenario considering the effects of climatic changes only (July 2050 mean).

We finally conclude our analysis of the effects of the intervention on air quality in the future climate examining the differences between the two scenarios (with and without the intervention) in the two months at the Tikkurila air quality station, considering all the pollutants.

% Difference	NO_x	NO_2	O_3	PM_{10}	$PM_{2.5}$
Jan-50	1.10E-02	-2.79E-02	2.31E-02	5.44E-03	4.65E-03
Jul-50	1.62E-02	9.71E-02	-2.78E-02	2.32E-03	2.18E-03

Table 20. Percentage differences for pollutant concentrations at the Tikkurila air quality station between the intervention scenario and the scenario without intervention under the effect of future climate conditions in the two analyzed months (January and July 2050).

Table 20 confirms the limited impact of the intervention on pollutant concentrations, showing limited changes in the scenario when it is implemented.

4.2.2.2 Effects of vegetation on air temperature

We now examine the impacts of the intervention on air temperature. Before considering the effect of the intervention, however, we analyse the effects of climate change on air temperature in Vantaa, considering both January and July months.

Figure 90 and Figure 91 represent temperature maps in future January and future July in Vantaa. We can observe that while in the present climate conditions temperatures were below zero everywhere, in the future January temperatures are above freezing level even far from the mitigating action of sea and from built areas. Similarly, also July temperatures will increase, while the spatial patterns will remain unchanged in both months.

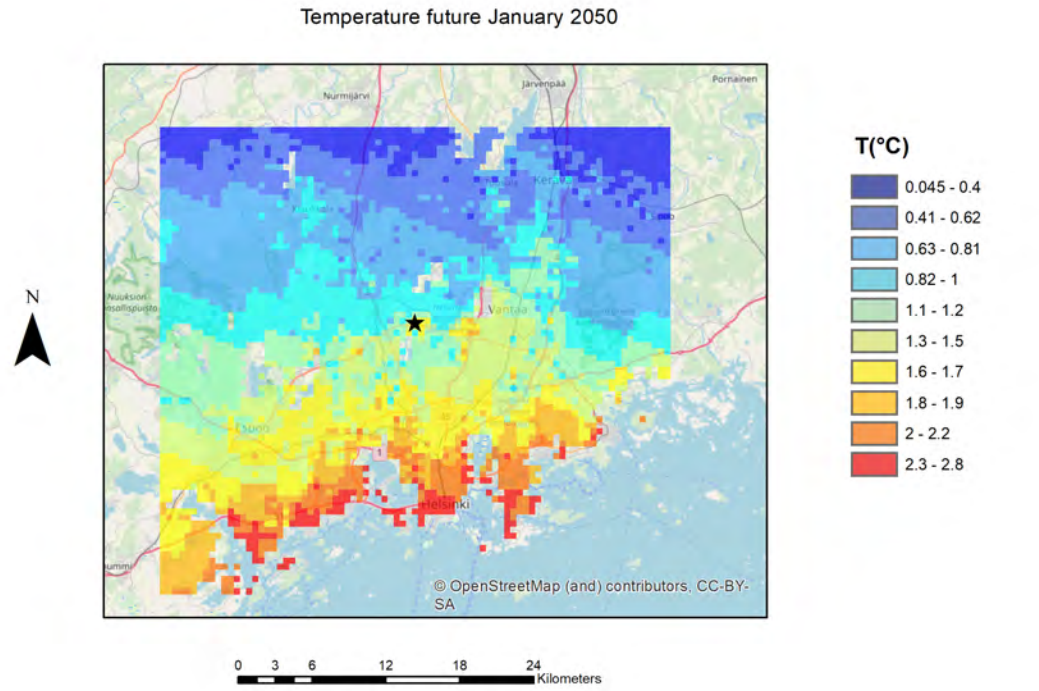

Figure 90. Monthly mean air temperature as simulated by SURFEX in future January, considering the effect of climate changes only. The commercial area of Tikkurila is indicated with the black star.

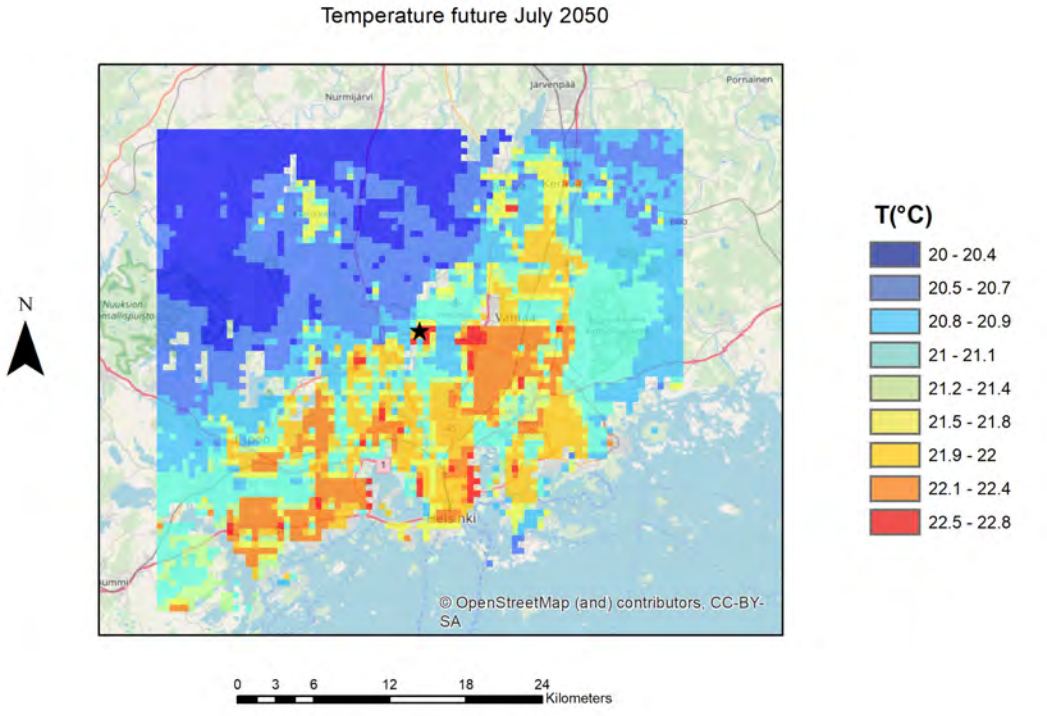

Figure 91. Monthly mean air temperature as simulated by SURFEX in future July, considering the effect of climate changes only. The commercial area of Tikkurila is indicated with the black star.

Differences are examined more closely looking at temperature differences maps (Figure 92 and Figure 93). These maps show that the major temperature increases in air temperatures will be observed in winter, which present increases of 4°C or more over the simulation domain. July differences are instead comprised between 2.7 and 3.3°C. Maps of temperature differences also show a slightly different spatial pattern in the two months, with larger increases located to the N far from the sea in January and more spread over the whole simulation domain during July. This tendency of higher increase away from the city center in parallel with a reduced increase in proximity of built areas seems to indicate a reduction of the UHI (Urban Heat Island) in the future in Vantaa.

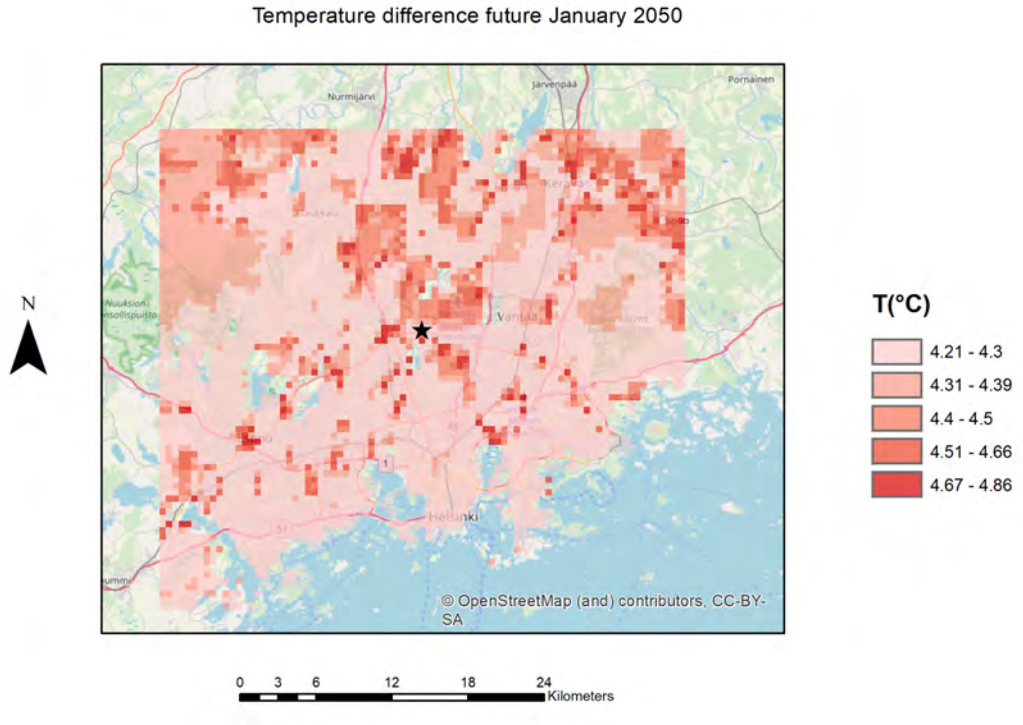

Figure 92. Temperature difference map between the future and the present January. The commercial area of Tikkurila is indicated with the black star.

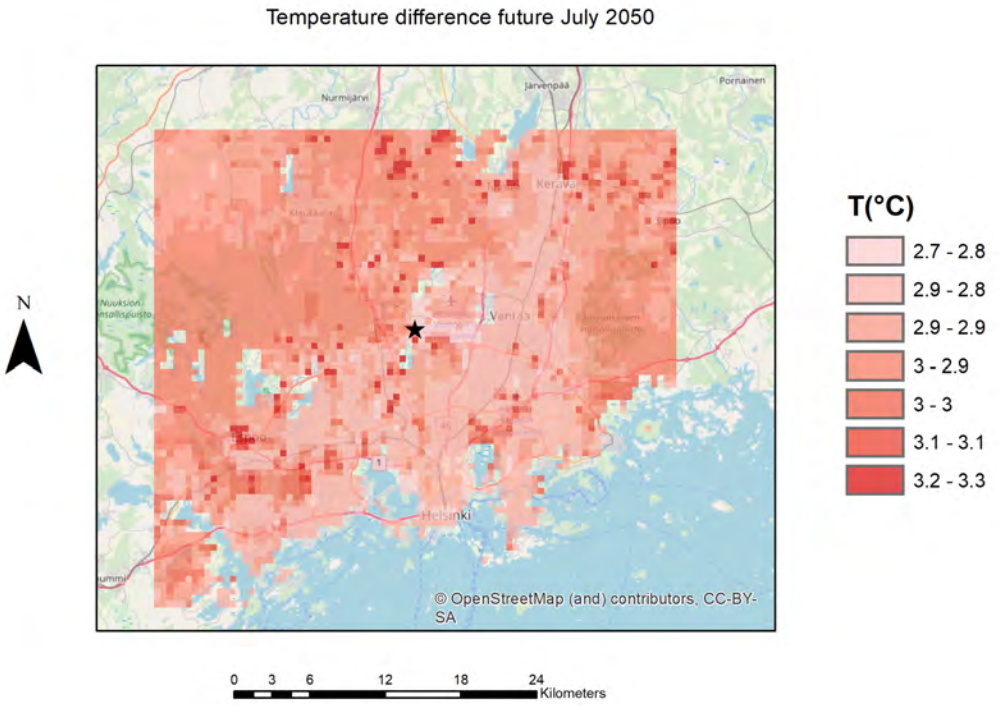

Figure 93. Temperature difference map between the future and the present July. The commercial area of Tikkurila is indicated with the black star.

We then examine the impact of the intervention under future January and July conditions (Figure 94 and Figure 95). As previously resulted in the present conditions, we can observe that the intervention will not significantly alter the spatial distribution of air temperature, and magnitude of temperatures will be only limited impacted by the implementation of the intervention considering an alteration of the urban layout.

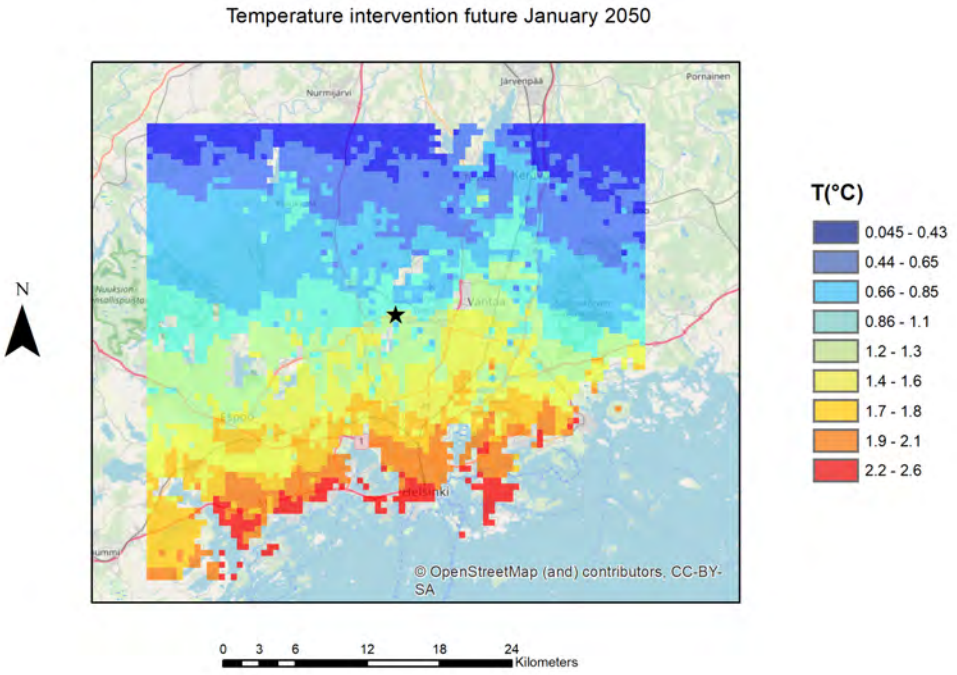

Figure 94. Monthly mean air temperature as simulated by SURFEX in future January, considering the effect of climate changes and the intervention altering the urban layout. The commercial area of Tikkurila is indicated with the black star.

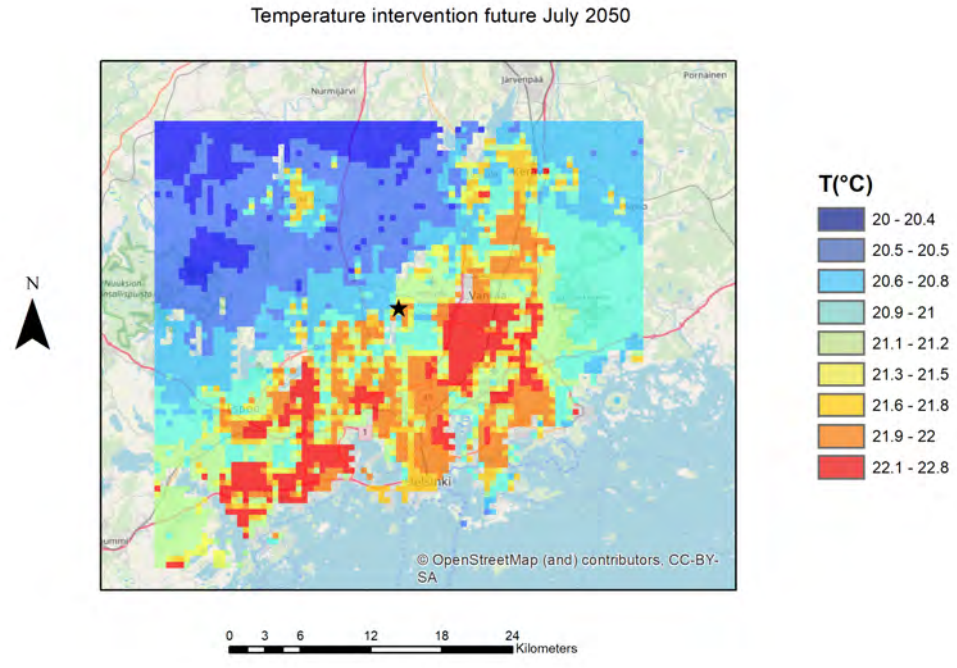

Figure 95. Monthly mean air temperature as simulated by SURFEX in future July, considering the effect of climate changes and the intervention altering the urban layout. The commercial area of Tikkurila is indicated with the black star.

However, when looking at maps of temperature differences between the scenario of implementation of the intervention in the two months (Figure 96 and Figure 97), we can observe that the intervention is capable of mitigating the temperature increases of 0.3°C in January and of 0.7°C in July in some areas of the city center, therefore ameliorating the thermal comfort and reducing the impacts of climate change at least in some neighborhoods.

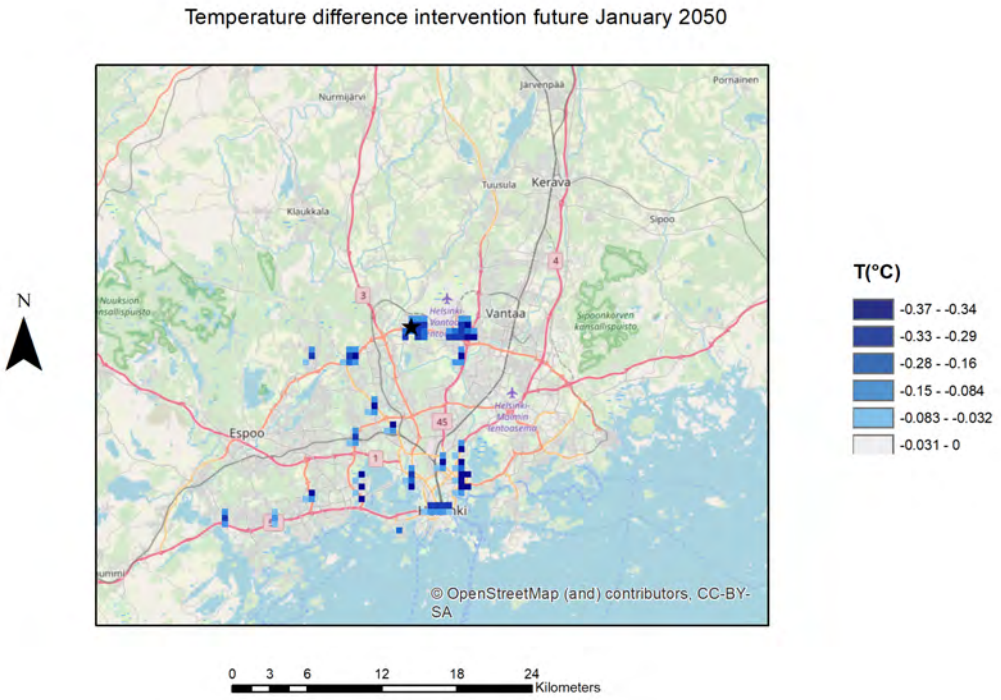

Figure 96. Temperature difference map between the intervention scenario and the scenario considering only the impact of future climate conditions in future January. The commercial area of Tikkurila is indicated with the black star.

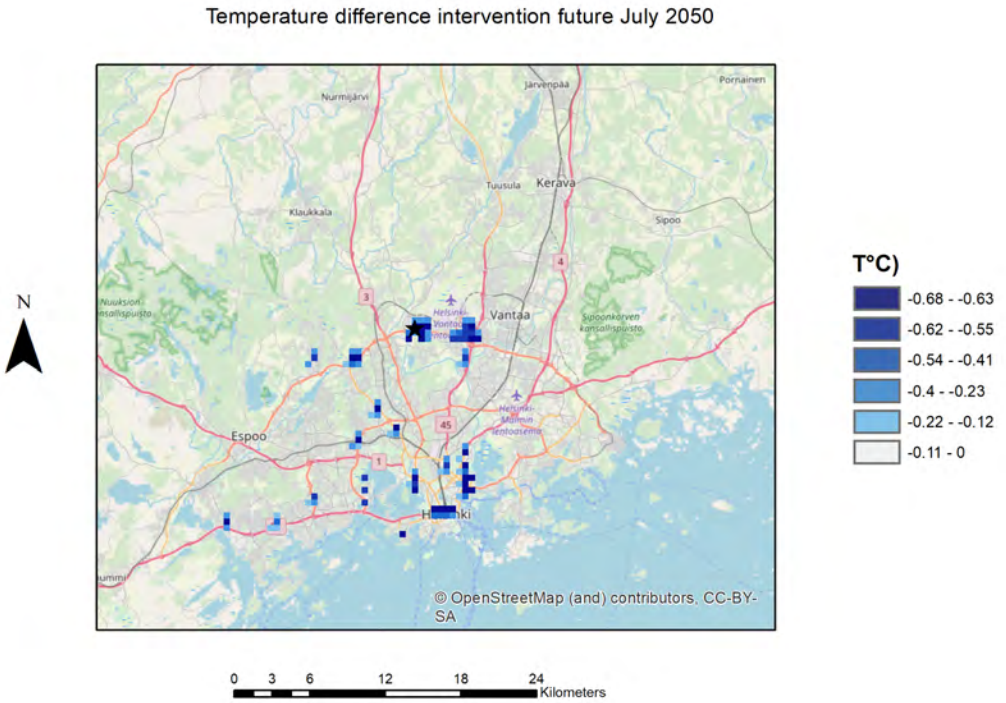

Figure 97. Temperature difference map between the intervention scenario and the scenario considering only the impact of future climate conditions in future July. The commercial area of Tikkurila is indicated with the black star.

4.3 Dublin

This section presents the results obtained for Dublin based on the methodology described in section 3.3.

4.3.1 Present scenario/Baseline period

As mentioned before, two different models were developed to represent the summer and the winter seasons. For the summer period ranging from 20th August, 2018 12AM to 26th August, 2018 12AM, the wind velocity and wind direction at Dublin airport obtained from Met Eireann are shown as wind rose diagram in Figure 98(a). Similarly, Figure 98(b) shows the wind rose diagram for the winter season data ranging from 6th February, 2019 12AM to 12th February, 2019 12AM. The figure indicate that the wind direction changes considerably between summer and winter for Dublin. The observed wind speed for summer and winter season at Dublin airport is provided in Figure 99

The LES based CFD models were developed separately for summer and winter months and were run at an interval of 5 second for the aforementioned time period corresponding to each season, where the observed wind speed and wind direction were considered as the boundary condition and the traffic emission obtained based on COPERT4 for different types of vehicles were considered as the source of $PM_{2.5}$ air pollutant. Two different CFD models, one for summer and another for winter were developed and the average $PM_{2.5}$ concentration at 2 meter height were noted for the duration of the simulation.

The simulated $PM_{2.5}$ concentrations were subsequently averaged at hourly scale and plotted inFigure 100.

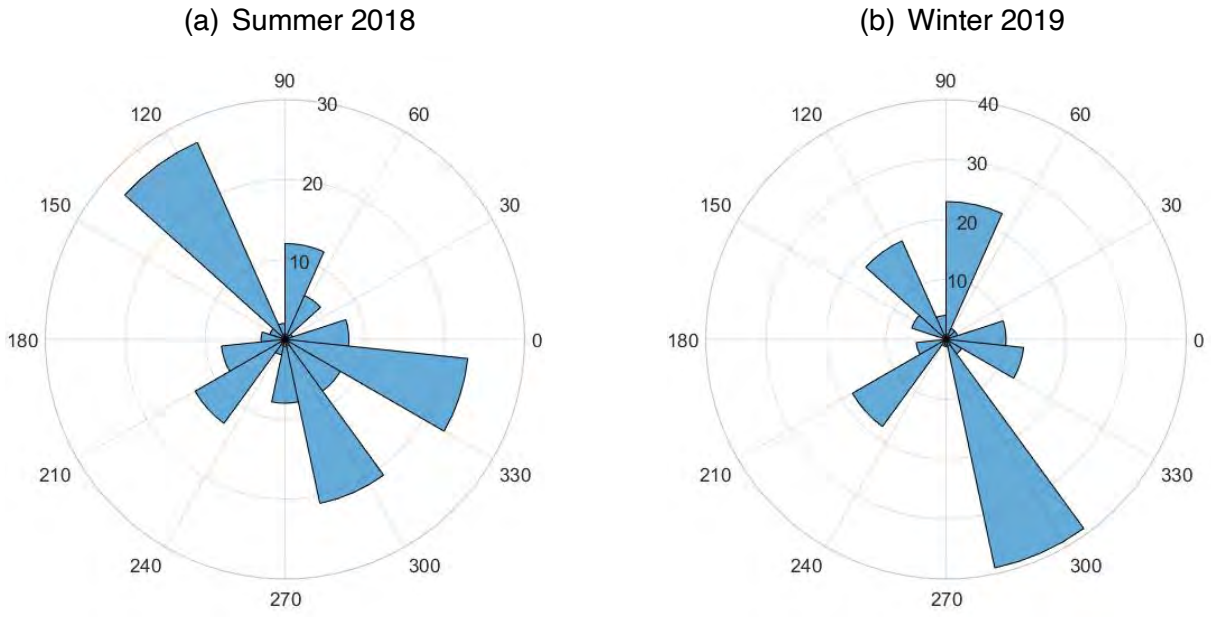

Figure 98. Wind rose for baseline period at Dublin during (a) summer 2018 and (b) winter 2019. Meteorological observations were obtained from Dublin airport Met Eireann meteorological station.

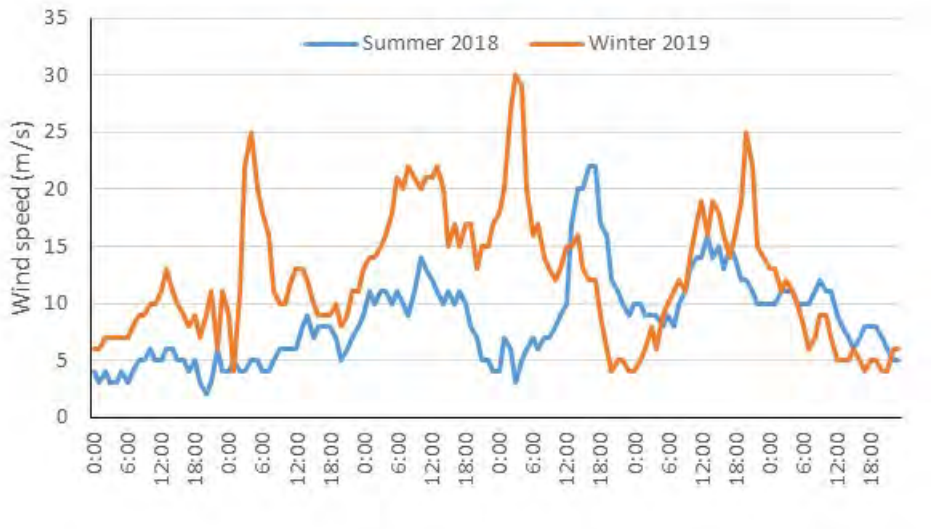

Figure 99. Observed wind speed for (a) summer 2018 and (b) winter 2019 at baseline period.

(a)

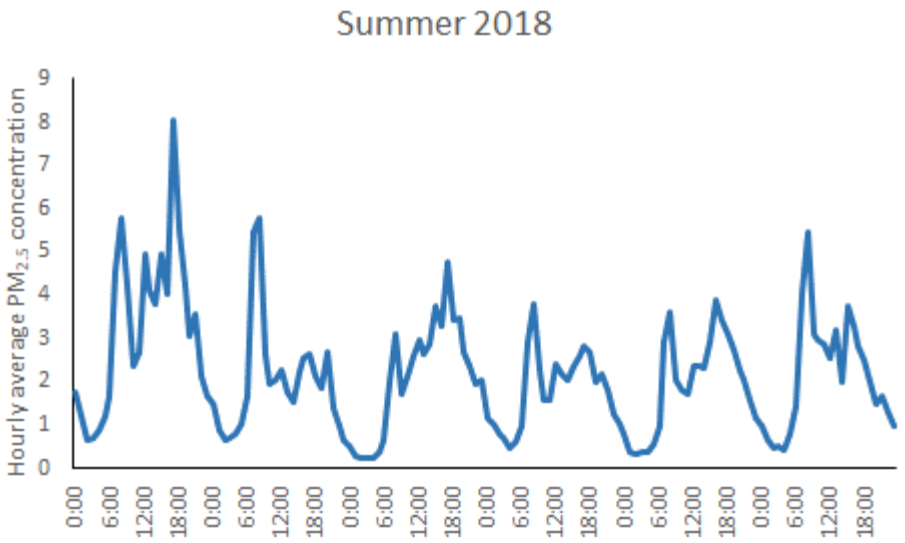

(b)

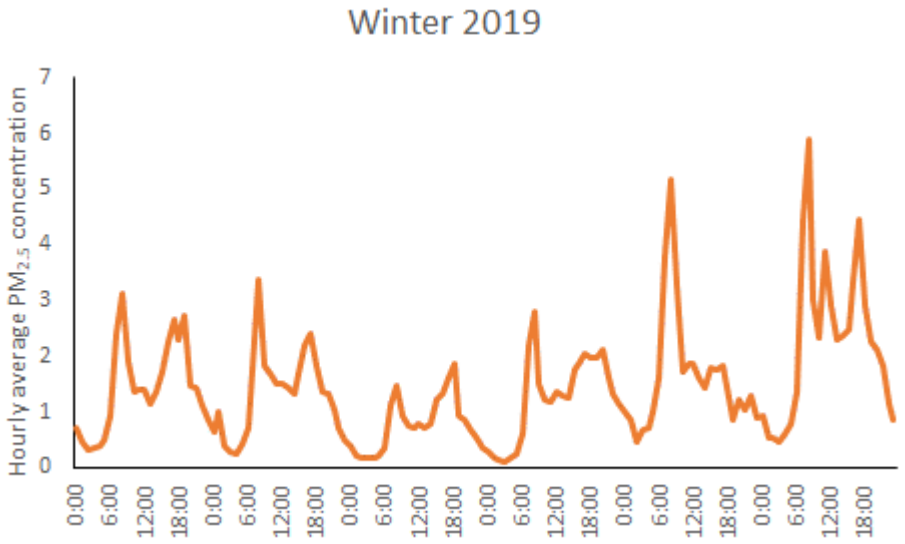

Figure 100. Hourly averaged values of simulated $PM_{2.5}$ concentration for (a) summer 2018 and (b) winter 2019 baseline period estimated at 2 meter height.

The CFD models for summer and winter seasons were rerun after installing the low boundary walls of 1 meter high at each sides of the road. Cross sectional figure showing the locations of the LBWs is provided in Figure 101.

Figure 101. Cross-section of the canyon at Pearse Street showing locations of low boundary walls (LBWs).

Figure 102 shows the simulated hourly average $PM_{2.5}$ concentration after the intervention of LBWs. Differences in average concentration at 2 meter height with and without the LBWs for summer and winter seasons are shown in Figure 103. In this Figure, a positive difference indicates that the average $PM_{2.5}$ concentration has increased due to the presence of the LBW, while a negative value indicates an improvement in air quality due to LBWs. The figures indicate that the insertion of the LBW causes an overall improvement of air quality at both sides of the road. However, the figures further indicate that the presence of LBWs can increase the average pollutant concentrations for a certain period of time depending on the wind velocity and wind direction, in agreement with what previously shown analysing observations gathered in the experimental campaign at Pearse Street in D5.2. It can also be noted from the figure that the pollution is slightly lower during the winter season, which can be attributed to the increase in wind velocity compared to the summer months. The overall improvement in air quality due to intervention of LBWs is higher during summer months than in the winter months. This is due to the low wind velocity typical of the summer months in Dublin, and the effect of LBWs in the overall flow circulation inside the canyon is higher compared to winter.

(a)

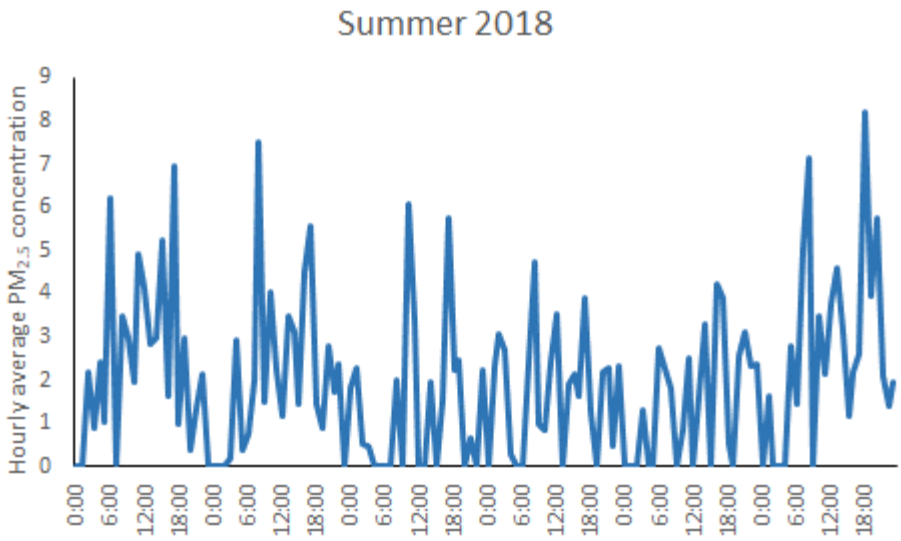

(b)

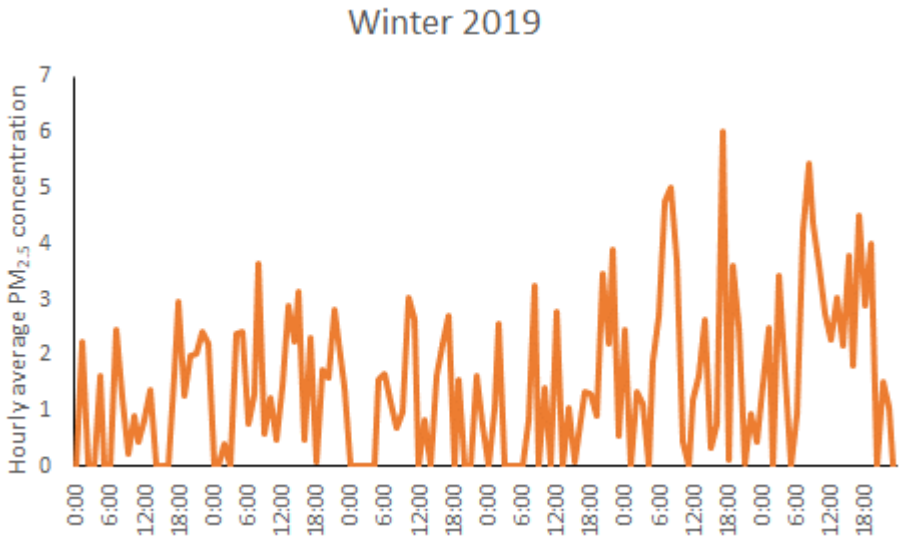

Figure 102. Hourly averaged values of simulated $PM_{2.5}$ concentration for (a) summer 2018 and (b) winter 2019 baseline period estimated at 2 meter height after intervention of LBWs.

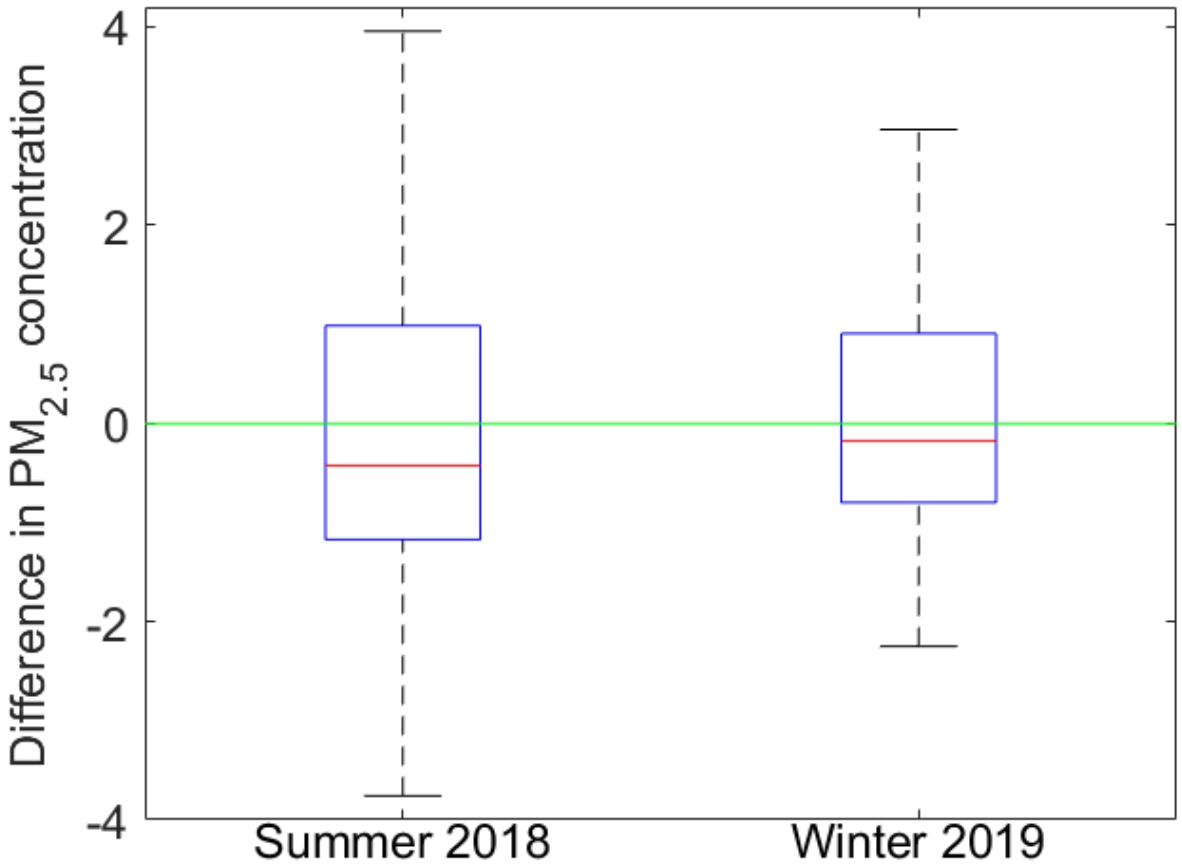

Figure 103. Difference in $PM_{2.5}$ concentration with and without the LBWs for (a) summer 2018 and (b) winter 2019. Negative value indicate decrease in air pollution concentration due to LBWs at 2 meter height.

4.3.2 Future scenario

The change in air pollution in the future climate scenario was obtained based on future projected values of the meteorological variables (wind speed and wind direction) obtained with WRF simulations previously described. The traffic volume and the emissions from the traffic were assumed to remaib the same as that of the baseline period for consistency with the RCP8.5 assumption, as the goal of this section is to investigate the effect of climate change in air pollution. As mentioned before, the wind speed and wind direction were simulated for summer (20-26th August) and winter (6-12th February) for the year 2050. The wind direction and wind speed for the future scenario are provided in Figure 104 and Figure 105 respectively.

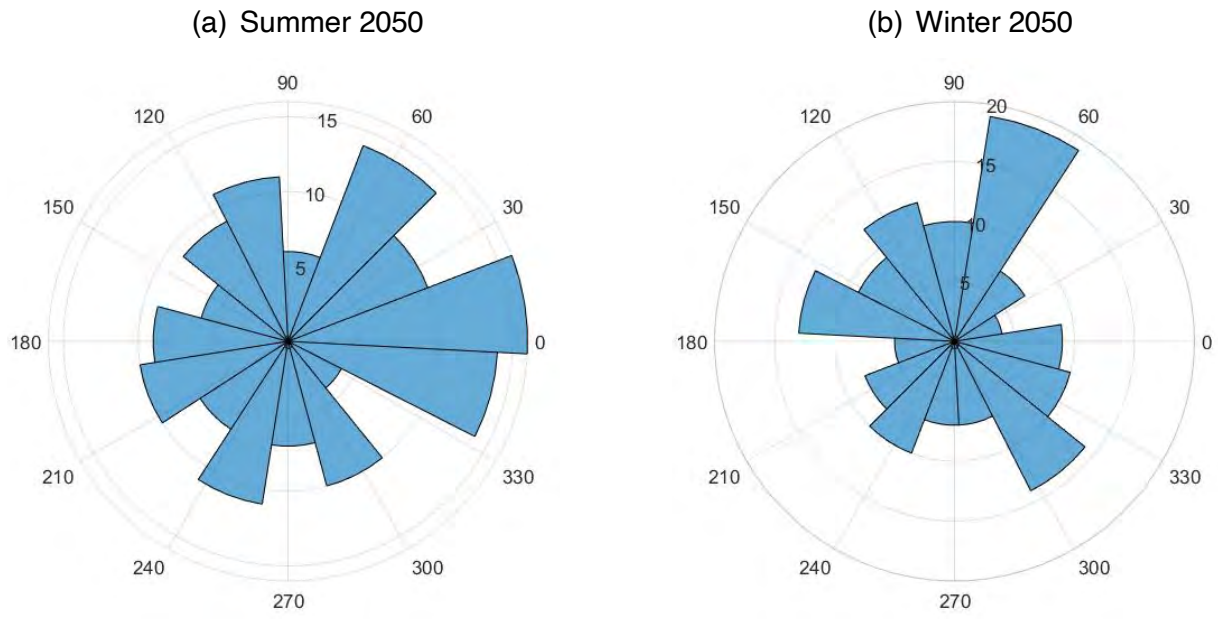

Figure 104. Wind rose for future scenario at Dublin during (a) summer 2050 and (b) winter 2050. The data were simulated using WRF model.

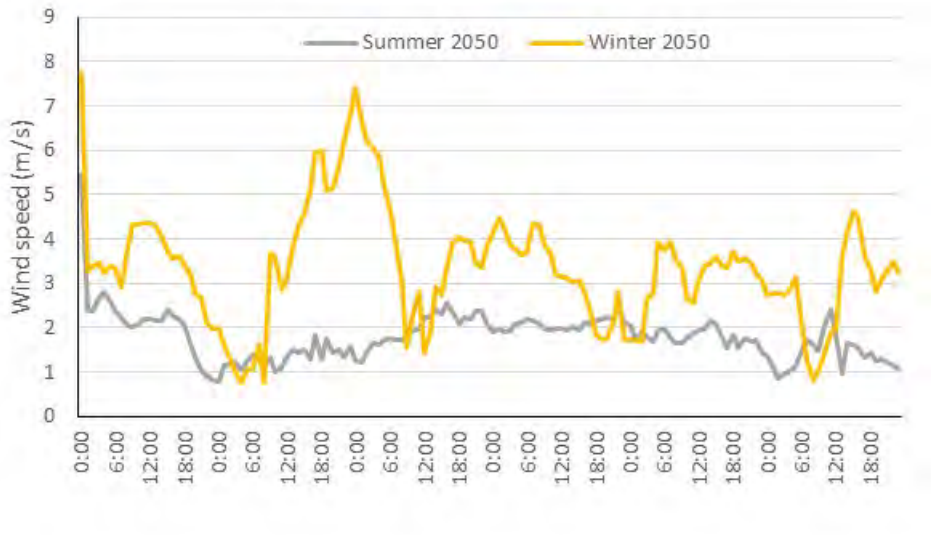

Figure 105. Future projected wind speed for (a) summer 2050 and (b) winter 2050 using WRF simulation.

The figures indicate that the wind direction as well as wind speed is expected to change considerably in the future scenario as per the WRF simulation study. Changes in wind properties is expected to have

a considerable effect in the air pollution. In the following, the average $PM_{2.5}$ concentrations at 2 meter height were estimated with and without the LBWs for the future projected scenario. Figure 106 shows the average $PM_{2.5}$ concentration without the LBWs, while Figure 107 presents the average $PM_{2.5}$ concentration under the future scenario in the presence of LBWs. Figure 108 provides the difference between average $PM_{2.5}$ concentrations in the future scenario with and without LBWs. The figures indicate that the $PM_{2.5}$ pollution concentration is expected to increase considerably in the future scenario for both summer and winter months, if the traffic volume and emissions are kept the same as that of the present/baseline period. Furthermore, the improvement in air quality due to LBWs in the future scenario is found to be higher in the summer months, as noted for the baseline period.

(a)

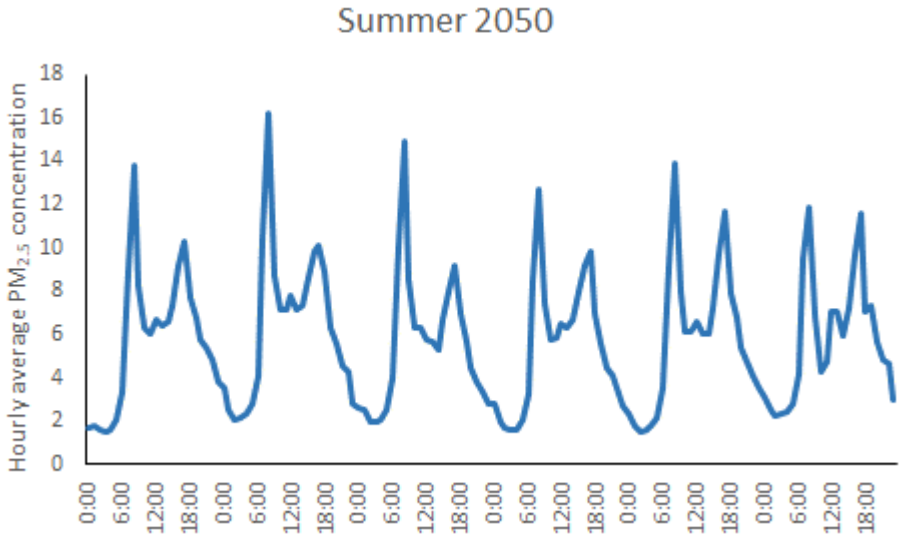

(b)

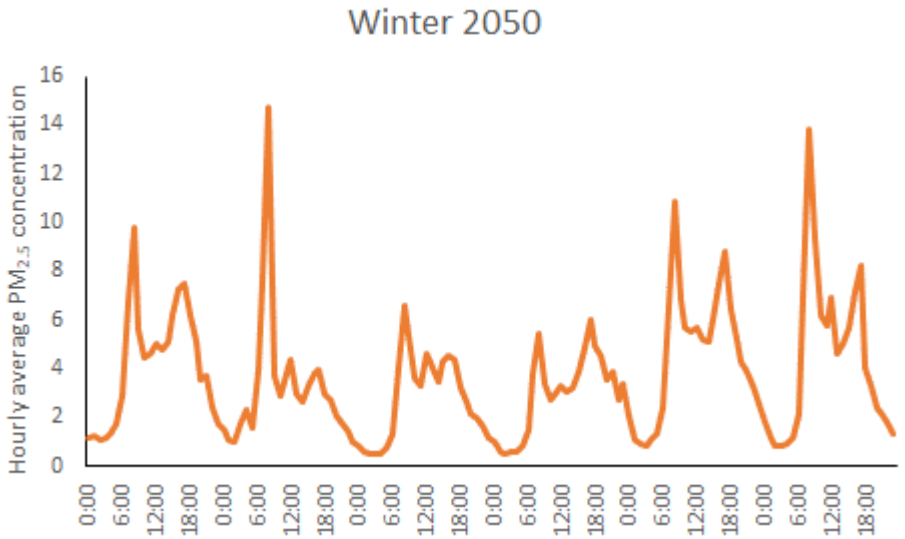

Figure 106. Hourly averaged values of simulated $PM_{2.5}$ concentration for (a) summer 2050 and (b) winter 2050 future estimated at 2 meter height without LBWs.

(a)

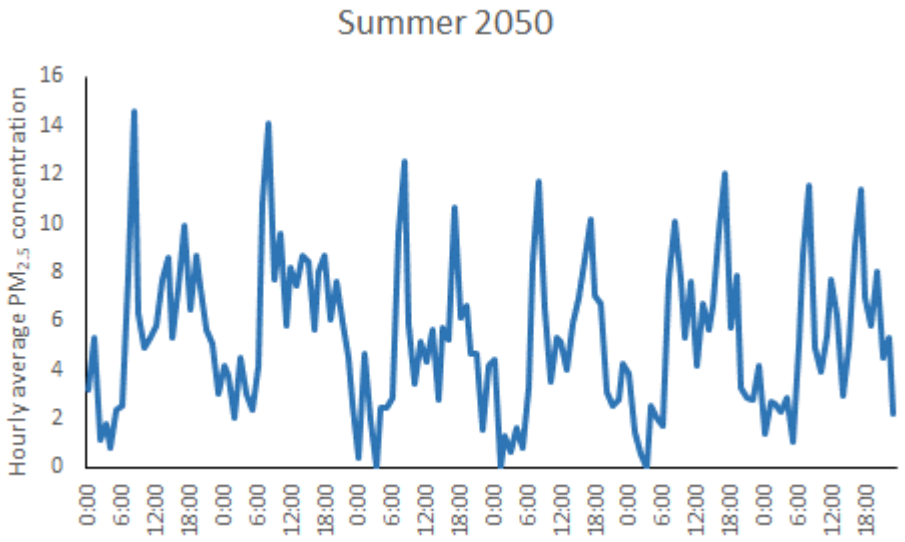

(b)

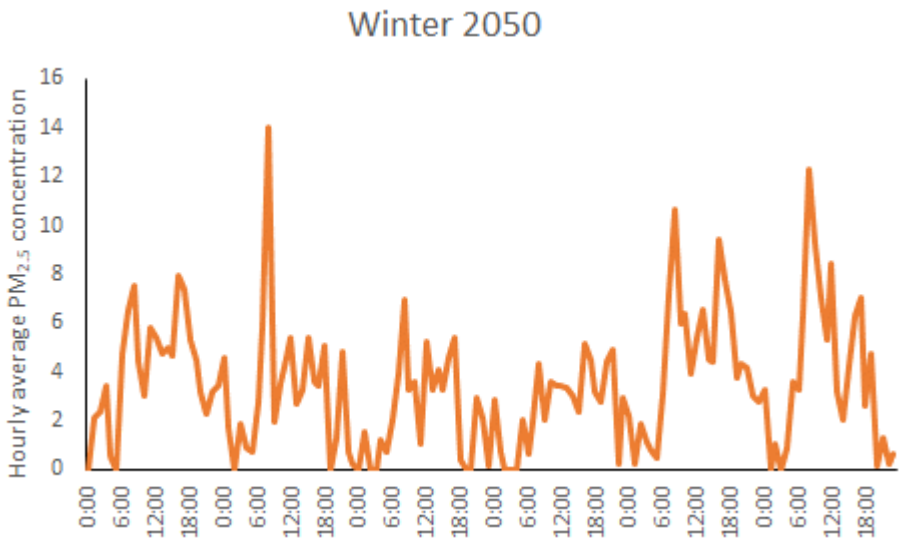

Figure 107. Hourly averaged values of simulated $PM_{2.5}$ concentration for (a) summer 2050 and (b) winter 2050 future estimated at 2 meter height after intervention of LBWs.

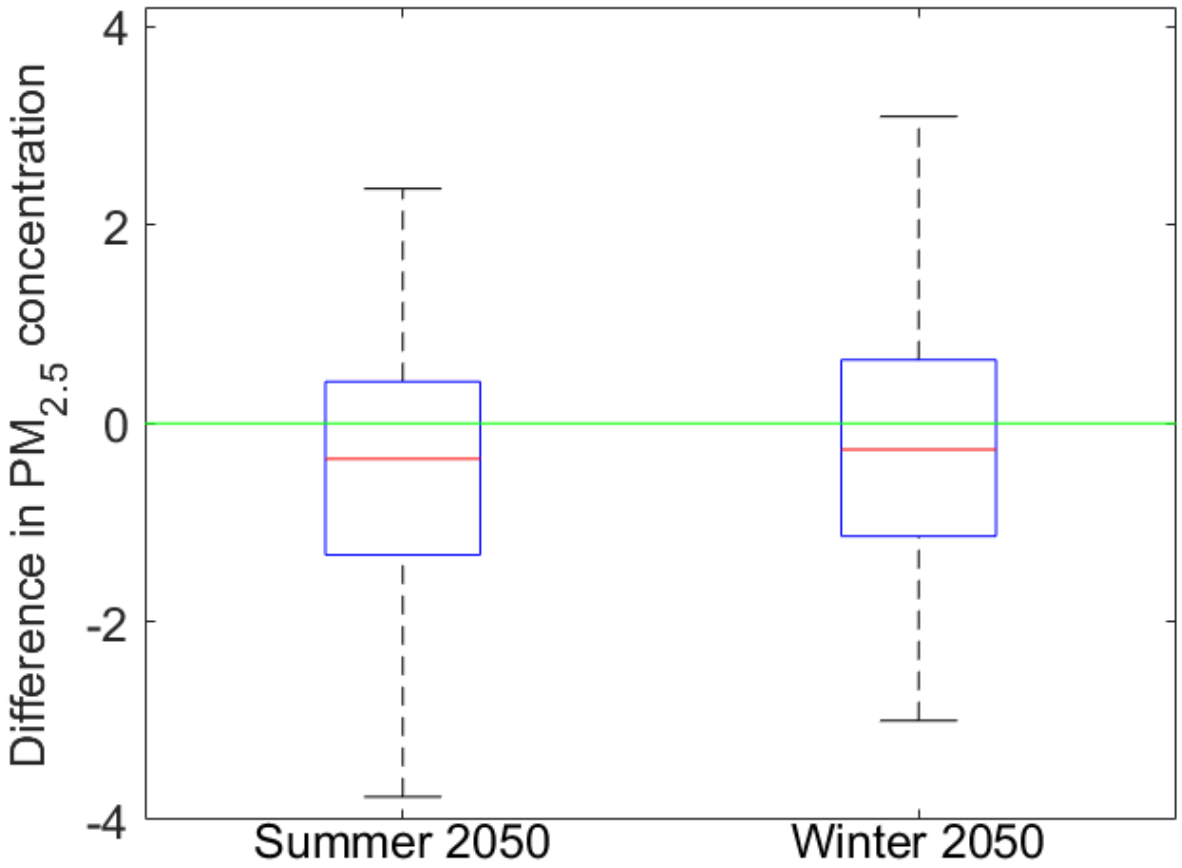

Figure 108. Difference in $PM_{2.5}$ concentration with and without the LBWs for (a) summer 2050 and (b) winter 2050. Negative value indicate decrease in air pollution concentration due to LBWs at 2 meter height.

Overall, it can be noted that the presence of LBWs can reduce the air pollution for baseline as well as the future climate scenarios. Furthermore, it has also been noted that the air pollution is expected to increase in the future if the traffic volume and the traffic emissions remain the same.

5 Conclusions

This report aims to describe and provide results about the effectiveness of PCSs interventions such as vegetated spaces and low boundary walls in improving air quality and urban thermal comfort in present and future scenarios in iSCAPE selected cities. To this aim, pollutant dispersion model simulations and high resolution numerical simulations of air temperature fields were conducted in two selected iSCAPE cities, namely Bologna in Italy and Vantaa in Finland. In addition, high resolution CFD simulations were conducted in two neighborhoods of Bologna and Dublin. The three cities were selected to represent

different latitudinal bands, i.e. southern, central and northern Europe, differently impacted by climate change as reported in a parallel Deliverable of this WP (D6.4). In addition, in both cities of Bologna and Vantaa an emission inventory of the major pollutant emission sources was already developed within the iSCAPE project for the purpose of analysing the effectiveness of behavioral changes related to mobility in contrasting air pollution (D4.5).

In both cities, the setup of the dispersion model simulations developed for D4.5 was adequately modified to be capable of representing the intervention consisting in a modification of the urban layout or the insertion of GI. In particular, in Bologna, the simulations were run in the vicinity of a tree-free street canyon, Marconi St., where two experimental field campaigns were carried out. The setups of dispersion model simulations of both cities were preliminarily verified in two periods, one cold and one warm, representative of present climate conditions with the real configuration (i.e., without alteration of the urban layout or addition of trees) comparing pollutant concentrations against available observations gathered as open data (Vantaa) or from experimental field campaigns conducted within the project (Bologna). In both cities, simulated concentrations in the base case were in good agreement with the observations, indicating a good performance of the setups.

Air pollutant concentrations obtained in a scenario considering the implementation of an intervention were then compared with those obtained in the baseline reference case in the present climate conditions. In Bologna, the intervention consisting in planting deciduous trees in Marconi St. proved to be effective in improving air quality, leading to reductions of NO_x concentrations of 21-39% during the winter period at the receptor sites. The analysis of pollutant concentration maps obtained in the vicinity of Marconi St. highlights the appearance of one region of increase in concentrations and one of decrease in concentrations in the intervention scenario; the two regions are characterized by a similar magnitude but a very different spatial area, with a larger area covered by reductions in concentrations.

Conversely, in Vantaa, the intervention altering the urban layout do not impact much on pollutant concentrations, which remain practically unchanged in the intervention scenario. Similar to what found in D4.5, the low effect of the intervention on pollutant concentrations is likely due to the low pollutant concentrations characterizing Vantaa already in the current configuration. In addition, in D6.4 it was already observed that in Vantaa the intervention did not cause major changes in meteorological variables, which is likely to be mirrored in the limited effects observed on pollutant dispersion.

Scenarios considering the impact of future climate conditions were also analysed for the two cities. For the city of Bologna, the future scenario was constructed considering the outputs of the mesoscale WRF model driven with an appropriate new dataset including global bias-corrected climate model output data for one cold and one warm period. For Vantaa, instead, the outputs of the regional scale surface interaction SURFEX model forced with a morphing adjustment of the recent past weather conditions were used. In both cases, simulations considered the RCP8.5 emission scenario. The scenarios considering the implementation of the interventions in the future indicated similar results to those obtained in the present climate conditions. In fact, while in Bologna the planting of trees leads to reductions of NO_x concentrations in the range 23-25% also in the future, in Vantaa the intervention does not cause major changes in pollutant concentrations, again attributed to the low pollutant concentrations characterizing the city and to the low effect of the intervention on meteorological variables.

The impact of the interventions on air temperature in present and future climate conditions was also analysed. Also for this analysis the methodologies utilized in the two cities were different. In fact, while

in Bologna the outputs of a temperature perturbation model run were analysed, in Vantaa we utilized the outputs of the SURFEX model. In both cities, the results indicate that the PCSs are capable of improving thermal comfort not only in the area of the intervention but also in its vicinity. Climate projections indicate a temperature warming in both cities; however, while in Bologna the highest warming is predicted during the summer season, in Vantaa the largest warming will occur during winter. In Bologna, the intervention planting trees in a tree-free street canyon results in a low, though systematic reduction of air temperature in the street canyon and its vicinity, with a reduction of similar magnitude in present and future climate conditions.

In Vantaa, the modification of the urban layout reduced temperature by 0.4°C in winter and 0.8°C in summer in the present climate in some neighborhoods. The somewhat smaller temperature reductions observed in the future (0.3-0.7°C) might partially the warming caused by climate change, and therefore indicate the potential effectiveness of the intervention even in the future.

Additionally, high resolution CFD simulations of selected neighborhoods under future summer and winter conditions, whose setup was verified in present meteorological conditions comparing the outputs of numerical simulations with the observations gathered within experimental campaigns, are evaluated for Bologna and Dublin. In particular, the outputs of CFD simulations indicate that the effect of climate change will produce higher pollutant concentrations and higher air temperatures (even up to 10°C higher than in the present conditions) in the selected neighborhoods. These increases in pollutant concentrations and air temperatures within urban street canyons can be effectively contrasted by implementing PCSs interventions: in particular, the results obtained for Bologna suggest that a tree planting policy might be effective in mitigating both air pollution and climate change in urban street canyons, while results obtained for Dublin indicate that the addition of LBWs might be effective in mitigating air pollution, especially in the summer months characterized by lower wind speeds with respect to the colder season .

On the basis of these results, it can be concluded that the PCSs interventions are effective in improving thermal comfort and contrasting climate change in urban areas. In addition, our results indicate that the effect on air quality and air temperature caused by a PCSs intervention in the future is similar to that observed in the present climate condition, so that, once a PCSs intervention proved to be effective in contrasting air pollution in the present, it will likely present a similar effectiveness also in future climatic scenarios.

These results, taken together with those previously obtained in this WP regarding the effect of PCSs at neighborhood and urban scales establish the basis for WP7 to provide generalized solutions for urban infrastructure and related decision-makers. The close link of this work with that carried out under WP4 related to simulations of CC and of interventions related to behavioral changes gives the possibility to widen the horizon for an appropriate urban planning strategy including different kind of measures (infrastructural, behavioral, etc…) adequately setup in the reference situation but also over a CC perspective.

6 References / Bibliography

ADMS-Urban Temperature and Humidity, A supplement to the ADMS-Urban User Guide, 2018, CERC, 3 King's Parade, Cambridge, http://www.cerc.co.uk/environmental-software/assets/data/doc_userguides/CERC_ADMS-Urban_Temperature_and_Humidity_User_Guide.pdf, last accessed 9 June 2019

Bengtsson, L., Andrae, U., Aspelien, T., Batrak, Y., Calvo, J., de Rooy, W., Gleeson, E., Hansen-Sass, B., Hormleid, M., Hortal, M., Ivarsson, K.-I., Lenderink, G., Niemelä, S., Nielsen, K.-P., Onvlee J., Rontu, L., Samuelsson, P., Muñoz, D.S., Subias, A., Tijim, S., Toll, V., Yang, X., & Køltzow, M.Ø., 2017. The HARMONIE-AROME model configuration in the ALADIN-HIRLAM NWP system. Monthly Weather Reviews, 145, 1919-1935.

Belcher, S.E., Hacker, N.J., Powell, D.S., 2005. Constructing design weather data for future climates. Building Services Engineering Research and Technology, 26, 49–61.

Breuer, L., Eckhardt, K., Frede, G., 2003. Plant parameter values for models in temperate climates. Ecological Modelling 169, 237–293

Cambridge Environmental Research Consultants Ltd, 2018: ADMS-Urban Temperature and Humidity, A supplement to the ADMS-Urban User Guide, Version 4.1 CERC, 3 King's Parade, Cambridge. Online available: http://www.cerc.co.uk/environmental-software/assets/data/doc_userguides/CERC_ADMS-Urban_Temperature_and_Humidity_User_Guide.pdf (access 14.12.2018)

Carruthers, D.J., Edmunds, H.A., Lester, A.E., McHugh, C.A., & Singles, R.J., 2000. Use and validation of ADMS-Urban in contrasting urban and industrial locations. International Journal of Environment and Pollution, 14, 363-374

CERC, 2011. ADMS-Urban User Guide. Version 3.1. Cambridge, UK, 324 pp., http://www.cerc.co.uk/environmental-software/assets/data/doc_userguides/CERC_ADMS-Urban4.1.1_User_Guide.pdf. *Accessed 30 May 2019*

CERC, 2015. EMIT Atmospheric Emissions Inventory Toolkit User Guide Version 3.4, Cambridge, UK, 390 pp, https://www.cerc.co.uk/environmental-software/assets/data/doc_userguides/CERC_EMIT3.4_User%20Guide.pdf Accessed 30 May 2019

Chang, J.C., & Hanna, S.R., 2004. Air quality model performance evaluation. Meteorology and Atmospheric Physics, 87, 167-196.

City of Vantaa, Centre for Environmental Affairs, 2012. State of the environment in Vantaa. Summary August 2012. Vantaan kaupungin paino, ISBN 978-952-443-392-1, 23 pp.

Di Sabatino, S., Buccolieri, R., Pulvirenti, B., & Britter, R.E., 2008. Flow and pollutant dispersion in street canyons using FLUENT and ADMS-Urban. Environmental Modeling and Assessment, 13(3),369-381.

Duffy, P.; Hanley, E.; Black, K.; O'Brien, P.; Hyde, B.; Ponzi, J.; Alam, S. Ireland's National Inventory Report; Environmental Protection Agency: Washington, DC, USA, 2015.

Hagenbjörk, A., Malmqvist, E., Mattisson, K., Sommar, N.J., & Modig, L., 2017. The spatial variation of O_3, NO, NO_2 and NO_x and the relation between them in two Swedish cities. Environmental Monitoring Assessment, 189, 4, 161.

Hanna, S.R., 1993. Uncertainties in air quality model predictions. Boundary-Layer Meteorology, 62, 3-20.

Hogstrom, U., 1996. Review of some basic characteristics of the atmospheric surface layer. Boundary-Layer Meteorol. 28, 215–246.

Jylhä, K., Jokisalo, J., Ruosteenoja, K., Pilli-Sihvola, K., Kalamees, T., Seitola, T., Mäkelä, H.M., Hyvönen, R., Laapas, M., & Drebs, A., 2015a. Energy demand for the heating and cooling of residential houses in Finland in a changing climate. Energy and Buildings, 99, 104-116

Jylhä, K, Ruosteenoja, K., Jokisalo, J., Pilli-Sihvola, K., Kalamees, T., Mäkelä, H.M., Hyvönen, R., & Saku, S., 2015b. Hourly test reference weather data in the changing climate of Finland for building energy simulations. Data Brief, 4, 162–169.

Kakosimos, K.E.; Hertel, O.; Ketzel, M.; Berkowicz, R. Operational Street Pollution Model (OSPM)—A review of performed application and validation studies, and future prospects. Environ. Chem. 2010, 7, 485.

Katsis, P., Ntziachristios, L., & Mellios, G., 2012. Description of new elements in COPERT 4 v10.0, EMISIA SA Report No.12.RE.012.V1

Kent, C. W., Grimmond, S., Gatey, D., 2017. Aerodynamic roughness parameters in cities: Inclusion of vegetation. Journal of Wind Engineering & Industrial Aerodynamics 169, 168-176.

Kinney, P.L., 2018. Interactions of climate change, air pollution and human health. Current Environmental Health Reports, 5(1), 179-186

Lehtonen, I., Ruosteenoja, K., Venäläainen, A, & Gregow, H., 2014. The projected 21st century forest-fire risk in Finland under different greenhouse gas scenarios. Boreal Environmental Research, 19, 127-139.

Masson, V., Le Moigne, P., Martin, E., Faroux, S., Alias, A., Alkama, R., Belamari, S., Barbu, A., Boone, A., Bouyssel, F., Brousseau, P., Brun, E., Calvet, J.C., Carrer, D., Decharme, B., Delire, C., Donier, S., Essaouini, K., Gibelin, A.L., Giordani, H., Habets, F., Jidane, M., Kerdraon, G., Kourzeneva, E., Lafaysse, M., Lafont, S., Lebeaupn, Brossier, C., Lemonsu, A., Mahmouf, J.F., Marguinaud, P., Mokhtari, M., Morin, S., Pigeon,G., Salgado, R., Seity, Y., Taillefer, F., Tanguy, G., Tulet, P., Vincendon, B., Vionnet, V., & Voldoire, A., 2013. The SURFEXv7.2 land and ocean surface platform for coupled or offline simulation of earth surface variables and fluxes. Geoscientific Model Development, 6, 929-960.

McDonald, R.W., Griffith, R.F., Hall, D.J., 1998. An improved method for the estimation of surface roughness of obstacle arrays, Atmospheric Environment, 32(11), 1857-1864.

Monaghan, A. J., D. F. Steinhoff, C. L. Bruyere, and D. Yates. 2014. NCAR CESM Global Bias-Corrected CMIP5 Output to Support WRF/MPAS Research. Research Data Archive at the National

Center for Atmospheric Research, Computational and Information Systems Laboratory. https://doi.org/10.5065/D6DJ5CN4. Last accessed 06/07/2019.

Oke, T.R., 1987. Boundary-layer climates. Second Edition, Methuen.

Pakkanen, T.A., Mäkelä, T., Hillamo, R.E., Virtanen, A., Rönkkö, T., Keskinen, J., Pirjola, L., Parviainen, H., Hussein, T., & Hämeri, K., 2006. Monitoring of black carbon and size-segregated particle number concentrations at 9-m and 65-m distances from major road in Helsinki. Boreal Environment Research, 11, 295-309.

Ramírez, A.Z., & Muñoz, C.B., 2012. Albedo effect and energy efficiency of cities. In: Sustainable development-Energy, engineering and technologies-Manufacturing and environment, doi:10.5772/29536

Smith, S.E., Stocker, J., Seaton, M., & Carruthers, D., 2017. Model inter-comparison and validation study of ADMS plume chemistry schemes. International Journal of Environment and Pollution, 62, 395-406.

Soares J., Kousa A., Kukkonen J., Matilainen L., Kangas L., Kauhaniemi M., Riikonen K., Jalkanen J.-P., Rasila T., Hänninen O., Koskentalo T. & Karppinen A., 2014. Refinement of a model for evaluating the population exposure in an urban area. Geoscientific Model Development, 7, 1855–1872.

Stewart, I.D., and Oke, T.R., 2012. Local Climate Zones for urban temperature studies, Bulletin of the Americal Meteorological Society, 93(12), 1879-1900.

Stocker, J., Hood, C., Carruthers, D., & McHugh, C., 2012. ADMS-Urban: developments in modelling dispersion from the city scale to the local scale. International Journal of Environment and Pollution, 50, 308-316.

Vantaan kaupunki, 2012. Vantaan kaupungin tilastollinen vuosikirja 2011 (Statistical yearbook of the city of Vantaa 2011). Vantaan kaupunki, Tietopalveluysikkö, 130 pp.

Yuan, C., Norford, L., Ng, E., 2017. A semi-empirical model for the effect of trees on the urban wind environment. Landscape and Urban Planning 168, 84–93